

We are committed to providing [accessible customer service](#).

If you need accessible formats or communications supports, please [contact us](#).

Nous tenons à améliorer [l'accessibilité des services à la clientèle](#).

Si vous avez besoin de formats accessibles ou d'aide à la communication, veuillez [nous contacter](#).

REPORT ON A HELICOPTER-BORNE VERSATILE TIME
DOMAIN ELECTROMAGNETIC (VTEM™ PLUS) AND
HORIZONTAL MAGNETIC GRADIOMETER SURVEY
MIDLOTHIAN PROJECT,
MIDLOTHIAN TOWNSHIP, ONTARIO, NTS 41P14 & 41P15



Project Name: Midlothian

Client:  **CANADA NICKEL
COMPANY**

Contractor:  **GEOTECH**

Report Prepared by:

**Edwin Escarraga,
P.Ge**

Date: December 21, 2022

TABLE OF CONTENTS

EXECUTIVE SUMMARY	4
1.0 INTRODUCTION.....	5
2.0 SURVEY AREA.....	5
2.1 LOCATION	5
2.2 CLIMATE AND PHYSYOGRAPHY.....	7
2.3 MINING CLAIMS.....	7
2.4 FLIGHT SPECIFICATIONS AND TIE LINES.....	7
2.5 DATUM AND PROJECTION	8
2.6 SURVEY OPERATIONS	8
2.7 AIRCRAFT AND EQUIPMENT	8
2.7.1 <i>Electromagnetic System</i>	9
2.7.2 <i>Full Waveform VTEM™ Sensor Calibration</i>	11
2.7.3 <i>Horizontal Magnetic Gradiometer</i>	11
2.7.4 <i>Radar Altimeter</i>	12
2.7.5 <i>GPS Navigation System</i>	12
2.7.6 <i>Digital Acquisition System</i>	12
2.8 BASE STATION	12
2.9 PERSONNEL	12
3.0 EXPLORATION HISTORY	13
4.0 GEOLOGY	15
4.1 REGIONAL GEOLOGY	15
4.2 PROPERTY GEOLOGY	16
4.3 DEPOSIT GEOLOGY	16
5.0 DATA PROCESSING AND PRESENTATION.....	18
DATA COMPILATION AND PROCESSING WERE CARRIED OUT BY THE APPLICATION OF GEOSOFT OASIS MONTAJ AND PROGRAMS PROPRIETARY TO GEOTECH LTD.	18
5.1 ELECTROMAGNETIC DATA.....	18
5.2 HORIZONTAL MAGNETIC GRADIOMETER DATA	19
5.3 TAU PARAMETER AND CVG	20
6.0 VTEM SURVEY RESULTS AND DELIVERABLES	20
6.1 SURVEY REPORT	20
6.2 MAPS.....	20
6.3 DIGITAL DATA	21
7.0 INTERPRETATION AND CONCLUSIONS	25
8.0 REFERENCES.....	27
9.0 CERTIFICATE OF QUALIFICATIONS	28
STATEMENT OF QUALIFICATIONS	28
APPENDIX A – MINING CLAIMS DATA	30

APPENDIX B – GEOPHYSICAL MAPS	44
APPENDIX C. GENERALIZED MODELING OF THE VTEM SYSTEM	55

FIGURES

Figure 1: Midlothian Project map showing location of geophysical survey area (pink) and property boundary (blue).....	6
Figure 2. Flight path	8
Figure 3. VTEM Transmitter Current Waveform	9
Figure 4. VTEM™ Plus System Configuration	11
Figure 5: Midlothian Project bedrock geology map from: OGS report MRD 126 REV-1 1:250,000 Scale Bedrock Geology of Ontario.	17
Figure 6. Z, X and Fraser filtered X (FFx) components for "thin" target	19

TABLES

Table 1: Geophysical Survey Specifications	7
Table 2. Survey Schedule	8
Table 3. VTEM™ System Specifications.....	9
Table 4. Off-Time Decay Sampling Scheme. Z comp: 4-46 time gates; X comp: 20-46 gates	9
Table 5. Acquisition Sampling Rates	12
Table 6: Ontario Assessment File Database (OAFD) Historical Exploration Work Completed at the Midlothian Project.....	13
Table 7. Geosoft GDB Data Format	21
Table 8. Geosoft Resistivity Depth Image GDB Data Format	24

EXECUTIVE SUMMARY

Geotech was approached by Canada Nickel (the client) with the objective of conducting an airborne VTEM survey to gain information needed for detailed property scale targeting, with the goal of creating drill ready locations.

This report details the survey conducted using a versatile time domain electromagnetic (VTEM™ Plus) system and a horizontal magnetic gradiometer with two caesium sensors, between June 3rd and June 9th, over the Midlothian Project located 23km WSW of Matachewan, Ontario.

The property consists of 272 contiguous mining claims centered around a potential bulk-tonnage magmatic nickel sulphide deposit. These Type II disseminated nickel sulphide deposits have unique geophysical characteristics due to the serpentinization process which liberates nickel from the mafic minerals, chiefly olivine found within ultramafic peridotite and dunite. This alteration process produces magnetite and an associated decrease in density which produces overlapping gravity lows with magnetic highs.

This survey was flown using the WGS-84 Datum. The projection is UTM, Zone 17 N. The survey successfully produced the following maps:

- Electromagnetic stacked profiles of the B-field Z Component
- Electromagnetic stacked profiles of dB/dt Z Component
- B-Field Z Component Channel grid
- dB/dt Z Component Channel grid
- Fraser Filtered X Component Channel grid
- Total Magnetic Intensity (TMI)
- Calculated Time Constant (Tau) with Calculated Vertical Derivative of TMI contours
- Calculated Vertical Derivative of TMI (CVG)
- Magnetic Total Horizontal Gradient (TotHG)
- Magnetic Tilt-Angle Derivative (TiltDrv)
- Resistivity Depth Imaging (RDI) sections and depth-slices are presented.

The next steps for evaluating this target include but are not limited to a 10-hole ~4,000m diamond drill program with widely spaced holes, and minor surface prospecting activities.

1.0 INTRODUCTION

Geotech Ltd. performed a helicopter-borne geophysical survey over the Midlothian Block near Matachewan, ON (Figure 1). Steve Balch and Edwin Escarraga represented Canada Nickel Company (“the Company”), having its head office at 130 King Street West, Toronto, Ontario, Canada, M5X 1E3.

The objective of this survey is to delineate and aid in the evaluation of ultramafic intrusions located on the property using the combination of products delivered by the VTEM system.

The geophysical surveys consisted of helicopter borne EM using the versatile time-domain electromagnetic (VTEM™) plus system with Full-Waveform processing. Measurements consisted of Vertical (Z) and In-line Horizontal (X) components of the EM fields using an induction coil, and a horizontal magnetic gradiometer using two caesium magnetometers. A total of 624 line-km of geophysical data were acquired during the survey

The crew was based out of Gowganda, ON for the acquisition phase of the survey. Survey flying started on June 3rd and was completed on June 8th, 2022.

Data quality control and quality assurance, and preliminary data processing were carried out daily during the acquisition phase of the project. Final data processing followed immediately after the end of the survey. Final reporting, data presentation and archiving were completed in December 2022.

2.0 SURVEY AREA

2.1 LOCATION

The survey area centered at approximately 499750E, 5302990N (UTM Z 17N) contained within the NTS topographic sheet 041P, covered a 106 km² area approximately 23 km WSW of Matachewan, Ontario.

The property is accessible from Matachewan, Ontario by a series of logging roads. Follow Highway 566 west for 23 km’s then take a left (south) onto Wilson Lumber road. Follow Wilson for 14 km south until you reach the Asbestos Mine road, make a right and head west for 7 km until reaching the site.

Within the survey block there are few minor dirt roads and an abandoned open pit mine site at the approximate west-central portion of the survey area.

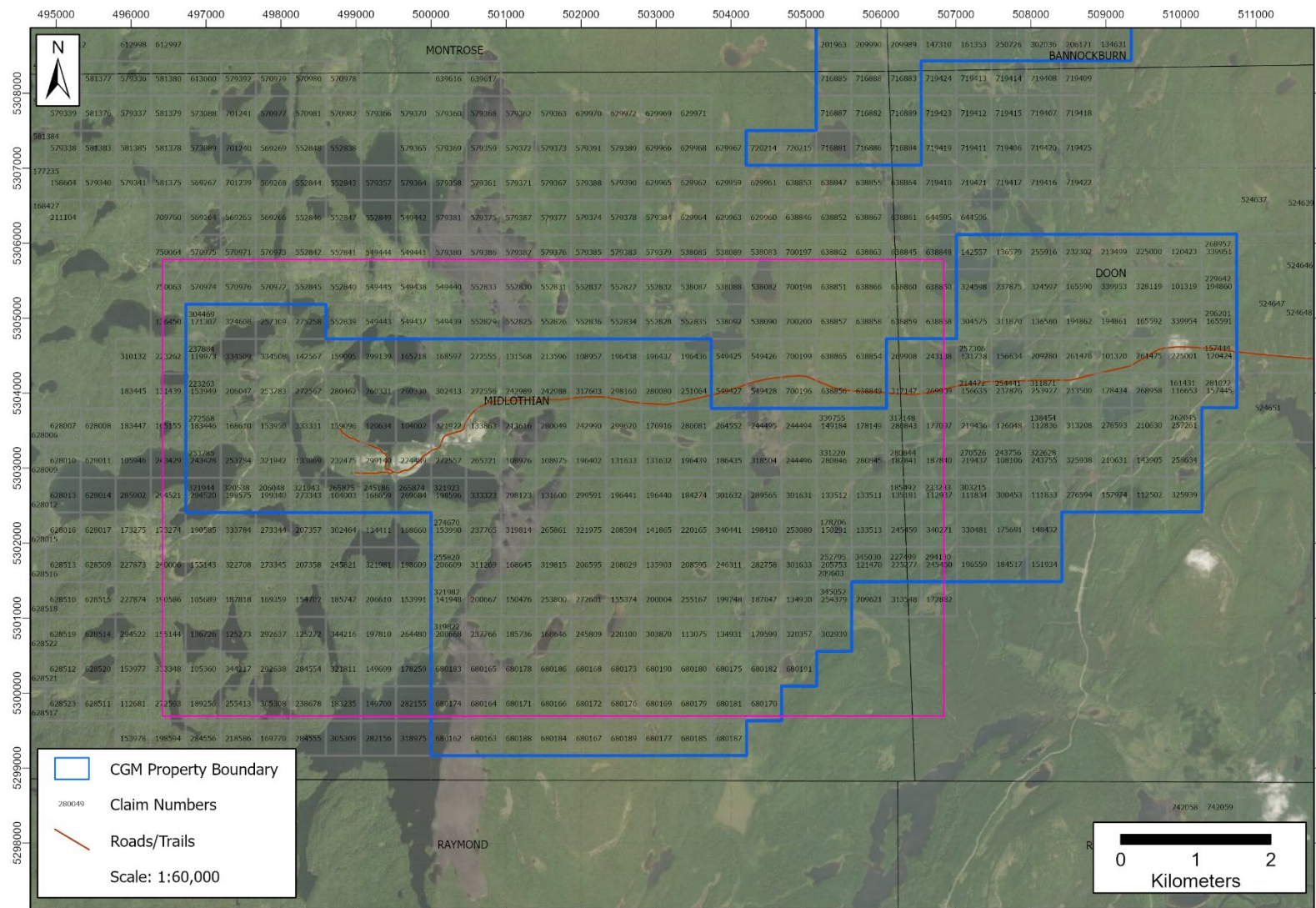


Figure 1: Midlothian Project map showing location of geophysical survey area (pink) and property boundary (blue).

2.2 CLIMATE AND PHYSIOGRAPHY

The average daily temperature varies from a high of +24°C during July to a low of -10°C during January. Annual snowfall is approximately 41 cm and annual rainfall is 6 cm. The survey area physiography consists of rolling hills with some outcrop and a few lakes. Total topographic variation is ~162 m ranging from 336 m to 498 m for the ~106 square kilometer survey area.

2.3 MINING CLAIMS

The property consists of 272 single cell mining claims (see Figure 1, Appendix A) optioned from Canadian Gold Miner Corp. (70% interest) and Laurion Mineral Exploration Inc. (30%) interest) to Canada Nickel Company (see CNC press release dated November 22, 2021).

2.4 FLIGHT SPECIFICATIONS AND TIE LINES

The survey area was flown in a north to south (N 0° E azimuth) direction with traverse line spacings of 100 metres, as depicted in Figure 2. Tie lines were flown perpendicular to the traverse lines at 5000 metre line spacing. For more detailed information on the flight spacings and directions, see Table 1.

During the survey the helicopter was maintained at a mean altitude of 93 metres above the ground with an average survey speed of 83 km/hour. This allowed for an average Transmitter-receiver loop terrain clearance of 57 metres and a magnetic sensor clearance of 67 metres.

The on-board operator was responsible for monitoring the system integrity. He also maintained a detailed flight log during the survey, tracking the times of the flight as well as any unusual geophysical or topographic features.

On return of the aircrew to the base camp the survey data was transferred from a compact flash card (PCMCIA) to the data processing computer. The data were then uploaded via ftp to the Geotech office in Aurora for daily quality assurance and quality control by qualified personnel

Table 1: Geophysical Survey Specifications

Line Spacing (m)	Area (km ²)	Planned line-km	Actual line-km	Flight direction
Traverse: 100 Tie: 5,000	61	613	624	N/S E/W

Figure 2. Flight path



2.5 DATUM AND PROJECTION

The survey was flown using the WGS-84 Datum. The Datum used to produce this report as well as the map products, grids and database is WGS-84. The projection is UTM, ZONE 17 N.

2.6 SURVEY OPERATIONS

The survey was based out of Gowganda, Ontario. Table 2 shows the timing of the flying.

Table 2. Survey Schedule

Date	Comments
03-Jun	Mobilization, recon flight, and base setup completed
04-Jun	Weather day
05-Jun	Production Flight – 376 km flown
06-Jun	Production Flight – 125 km flown
07-Jun	Weather day
08-Jun	Production Flight – 117 km flown
09-Jun	Demobilization

2.7 AIRCRAFT AND EQUIPMENT

The survey was flown using a Eurocopter Aerospatiale (A-Star) 350 B3 helicopter, registration C-GEOQ. The helicopter is owned and operated by Geotech Aviation Ltd. Installation of the geophysical and ancillary equipment was carried out by a Geotech Ltd. crew.

2.7.1 Electromagnetic System

The electromagnetic system was a Geotech Time Domain EM (VTEM™ Plus) full receiver-waveform streamed data recorded system. The “full waveform VTEM system” uses the streamed half-cycle recording of transmitter and receiver waveforms to obtain a complete system response calibration throughout the entire survey flight. VTEM with the serial number 15 had been used for the survey. The VTEM™ transmitter current waveform is shown diagrammatically in Figure 3 and the VTEM specifications in Table 3.

The VTEM™ Receiver and transmitter coils were in concentric-coplanar and Z-direction oriented configuration. The receiver system for the project also included coincident-coaxial X-direction coil to measure the in-line dB/dt and calculate B-Field responses. The Transmitter-receiver loop was towed at a mean distance of 36 metres below the aircraft as shown in Figure 4.

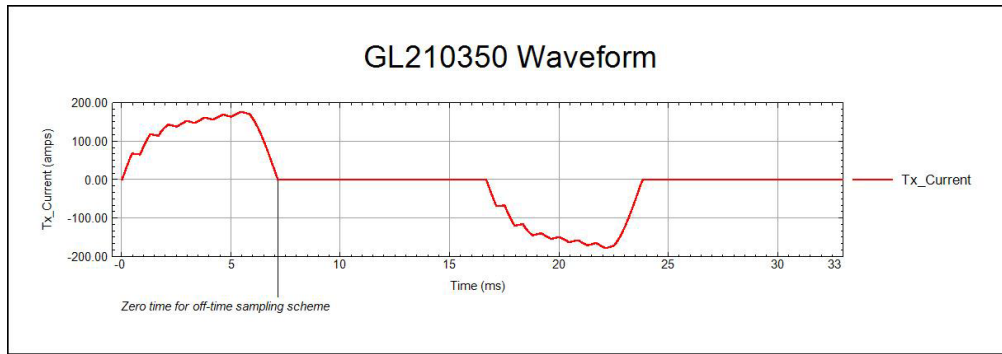


Figure 3. VTEM Transmitter Current Waveform

The VTEM™ decay sampling scheme is shown in Table 4 below. Forty-three time measurement gates were used for the final data processing in the range from 0.021 to 8.083 msec. Zero time for the off-time sampling scheme is equal to the current pulse width and is defined as the time near the end of the turn-off ramp where the dI/dt waveform falls to 1/2 of its peak value.

Table 3. VTEM™ System Specifications

Transmitter		Receiver	
• Transmitter loop diameter: 26 m		• X -Coil diameter: 0.32 m	
• Number of turns: 4		• Number of turns: 245	
• Effective Transmitter loop area: 2123.71 m ²		• Effective coil area: 19.69 m ²	
• Transmitter base frequency: 30 Hz			
• Peak current: 177.6 A		• Z-Coil diameter: 1.2 m	
• Pulse width: 7.14 ms		• Number of turns: 100	
• Waveform shape: Bi-polar trapezoid		• Effective coil area: 113.04 m ²	
• Peak dipole moment: 377171.76 nIA			
• Average transmitter-receiver clearance: 57 m			

Table 4. Off-Time Decay Sampling Scheme. Z comp: 4-46 time gates; X comp: 20-46 gates

Index	Start (ms)	End (ms)	Middle (ms)	Width (ms)
4	0.018	0.023	0.021	0.005
5	0.023	0.029	0.026	0.005
6	0.029	0.034	0.031	0.005

7	0.034	0.039	0.036	0.005
8	0.039	0.045	0.042	0.006
9	0.045	0.051	0.048	0.007
10	0.051	0.059	0.055	0.008
11	0.059	0.068	0.063	0.009
12	0.068	0.078	0.073	0.010
13	0.078	0.090	0.083	0.012
14	0.090	0.103	0.096	0.013
15	0.103	0.118	0.110	0.015
16	0.118	0.136	0.126	0.018
17	0.136	0.156	0.145	0.020
18	0.156	0.179	0.167	0.023
19	0.179	0.206	0.192	0.027
20	0.206	0.236	0.220	0.030
21	0.236	0.271	0.253	0.035
22	0.271	0.312	0.290	0.040
23	0.312	0.358	0.333	0.046
24	0.358	0.411	0.383	0.053
25	0.411	0.472	0.440	0.061
26	0.472	0.543	0.505	0.070
27	0.543	0.623	0.580	0.081
28	0.623	0.716	0.667	0.093
29	0.716	0.823	0.766	0.107
30	0.823	0.945	0.880	0.122
31	0.945	1.086	1.010	0.141
32	1.086	1.247	1.161	0.161
33	1.247	1.432	1.333	0.185
34	1.432	1.646	1.531	0.214
35	1.646	1.891	1.760	0.245
36	1.891	2.172	2.021	0.281
37	2.172	2.495	2.323	0.323
38	2.495	2.865	2.667	0.370
39	2.865	3.292	3.063	0.427
40	3.292	3.781	3.521	0.490
41	3.781	4.341	4.042	0.560
42	4.341	4.987	4.641	0.646
43	4.987	5.729	5.333	0.742
44	5.729	6.581	6.125	0.852
45	6.581	7.560	7.036	0.979
46	7.560	8.685	8.083	1.125

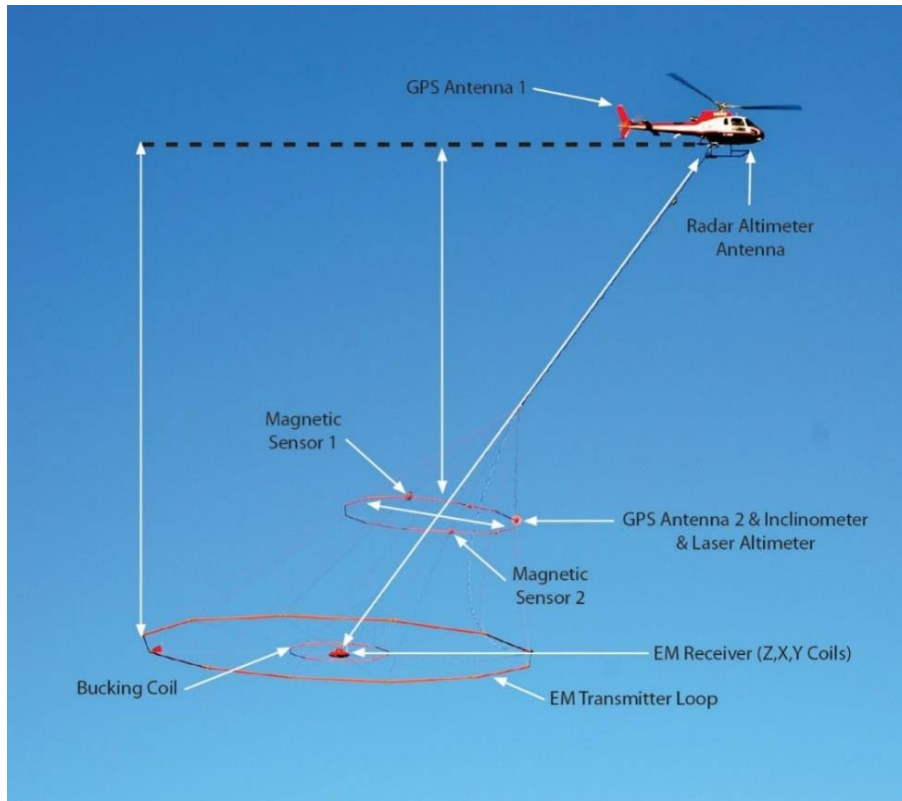


Figure 4. VTEM™ Plus System Configuration

2.7.2 Full Waveform VTEM™ Sensor Calibration

The calibration is performed on the complete VTEM™ system installed in and connected to the helicopter, using special calibration equipment. This calibration takes place on the ground at the start of the project prior to surveying.

The procedure takes half-cycle files acquired and calculates a calibration file consisting of a single stacked half-cycle waveform. The purpose of the stacking is to attenuate natural and man-made magnetic signals, leaving only the response to the calibration signal.

This calibration allows the transfer function between the EM receiver and data acquisition system and the transfer function between the current monitor and data acquisition system to be determined. These calibration results are then used in VTEM full waveform processing

2.7.3 Horizontal Magnetic Gradiometer

The horizontal magnetic gradiometer consists of two Geometrics split-beam field magnetic sensors with a sampling interval of 0.1 seconds. These sensors are mounted 12.5 metres apart on a separate loop, 10 metres above the Transmitter-receiver loop. A GPS antenna and Gyro Inclinator is installed on the separate loop to accurately record the tilt and position of the magnetic gradiometer sensors.

2.7.4 Radar Altimeter

A Terra TRA 3000/TRI 40 radar altimeter was used to record terrain clearance. The antenna was mounted beneath the bubble of the helicopter cockpit (Figure 4).

2.7.5 GPS Navigation System

The navigation system used was a Geotech PC104 based navigation system utilizing a NovAtel WAAS (Wide Area Augmentation System) enabled GPS receiver, Geotech navigate software, a full screen display with controls in front of the pilot to direct the flight and a NovAtel GPS antenna mounted on the helicopter tail (Figure 4). As many as 11 GPS and two WAAS satellites may be monitored at any one time. The positional accuracy or circular error probability (CEP) is 1.8 m, with WAAS active, it is 1.0 m. The coordinates of the survey area were set-up prior to the survey and the information was fed into the airborne navigation system. The second GPS antenna is installed on the additional magnetic loop together with Gyro Inclinometer.

2.7.6 Digital Acquisition System

A Geotech data acquisition system recorded the digital survey data on an internal compact flash card. Data is displayed on an LCD screen as traces to allow the operator to monitor the integrity of the system. The data type and sampling interval as provided in Table 5.

Table 5. Acquisition Sampling Rates

Data Type	Sampling
TDEM	0.1 sec
Magnetometer	0.1 sec
GPS Position	0.2 sec
Radar Altimeter	0.2 sec
Inclinometer	0.1 sec

2.8 BASE STATION

A combined magnetometer/GPS base station was utilized on this project. A Geometrics Caesium vapour magnetometer was used as a magnetic sensor with a sensitivity of 0.001 nT. The base station was recording the magnetic field together with the GPS time at 1 Hz on a base station computer.

The base station magnetometer sensor was installed in a secured location away from electric transmission lines and moving ferrous objects such as motor vehicles. The base station data were backed-up to the data processing computer at the end of each survey day.

2.9 PERSONNEL

The following Geotech Ltd. personnel were involved in the project.

FIELD:

Project Manager: Tristan Rice

Data QC: Nick Venter

Crew chief: Paul Taylor

Operator: Fred Gosse

The survey pilot and the mechanical engineer were employed directly by the helicopter operator – Geotech Aviation Ltd.

Pilot: Bill Hofstede

Mechanical Engineer: Alex Carniello

OFFICE:

Preliminary Data Processing: Nick Venter

Final Data Processing: Shuang Wang

Data QA/QC: Taichyi Shei

Jean Legault

Reporting/Mapping: Moyosore Lanisa

Processing and Interpretation phases were carried out under the supervision of Jean M. Legault, Chief Geophysicist. The customer relations were looked after by Paolo Berardelli.

3.0 EXPLORATION HISTORY

Historical exploration activities completed at the Midlothian Project area are summarized in Table 6 below. The most recent exploration work was completed by Transition Metals Corp on behalf of Canadian Gold Miner (CGM) in 2017. The goal of this program was to test for the ‘Bjorkman Showing’ a precious metals occurrence near the northern contact of the main ultramafic body. Multiple short diamond drill holes were completed to test this mineral occurrence, and in the process, a better understanding of the property geology was gained. Refer to Table 6 for a summarized property exploration history acquired from the Ontario Assessment File Database (OAFD).

Table 6: Ontario Assessment File Database (OAFD) Historical Exploration Work Completed at the Midlothian Project.

Company	Year	File ID	Value of Work	Work Description
Transition Metals Corp	2017	20000015247	\$ 61,338.00	Diamond Drilling
Transition Metals Corp	2016	20000014020	\$ 85,836.00	Geological Survey / Mapping, Microscopic Studies, Overburden

				Stripping, Prospecting By Licence Holder, Rock Sampling
Kiska Metals Co.	2015	20000014242	\$ 52,924.00	Assaying and Analyses, Geochemical, Prospecting By Licence Holder
Laurion Mineral Exploration Inc	2014	20000008134	\$ 36,218.00	Assaying and Analyses, Prospecting By Licence Holder
Laurion Mineral Exploration Inc	2014	20000008134	\$ 36,218.00	Assaying and Analyses, Prospecting By Licence Holder
Laurion Mineral Exploration Inc	2009	20000003973	\$ 272,297.00	Assaying and Analyses, Diamond Drilling
Geoinformatics Expl Can Ltd, Laurion Mineral Expl Inc	2008	20000003994	\$ 72,833.00	Airborne Electromagnetic, Airborne Magnetometer
Falconbridge Ltd	2005	20000001787	\$ 30,764.00	Assaying and Analyses, Diamond Drilling
Falconbridge Ltd	2005	20000000908	\$ 7,600.00	Electromagnetic, Line cutting, Magnetic / Magnetometer Survey
Mustang Minerals Corp	2004	20000000463	\$ 50,406.00	Airborne Electromagnetic, Airborne Magnetometer
David V Mullen	1997	41P15NW2003	\$ 9,511.00	Electromagnetic Very Low Frequency, Geochemical
D R Pyke	1997	41P15NW0011	\$ 19,920.00	Assaying and Analyses, Geological Survey / Mapping, Microscopic Studies, Open Cutting, Other
D R Pyke	1997	41P15NW2006	\$ 7,352.00	Induced Polarization, Magnetic / Magnetometer Survey
United Asbestos Inc	1981	41P14SE8412	-	Geological Survey / Mapping
Scintrex Ltd	1981	41P14SE0001	-	Airborne Electromagnetic, Airborne Magnetometer
United Asbestos Inc	1981	41P14SE0002	-	Geological Survey / Mapping
Intl Trust Co	1976	41P14NE0112	-	Diamond Drilling
Intl Trust Co	1975	41P14NE0024	-	Compilation and Interpretation - Diamond Drilling, Magnetic / Magnetometer Survey
Intl Trust Co	1975	41P14NE0024	-	Compilation and Interpretation - Diamond Drilling, Magnetic / Magnetometer Survey
Northim Mines Inc	1975	41P14SE0013	-	Diamond Drilling
Northim Mines Inc	1975	41P14SE0003	-	Diamond Drilling
Northim Mines Inc	1975	41P14NE0115	-	Miscellaneous Compilation and Interpretation, Other
Hanna Mining Co Ltd	1974	41P14NE0027	-	Electromagnetic, Geological Survey / Mapping, Magnetic / Magnetometer Survey

Northim Mines Inc	1974	41P14SE0010	-	Compilation and Interpretation - Geology, Electromagnetic, Magnetic / Magnetometer Survey
Northim Mines Inc	1974	41P14SE0004	-	Electromagnetic, Geological Survey / Mapping
Hanna Mining Co Ltd	1973	41P14NE0026	-	Electromagnetic, Geological Survey / Mapping, Magnetic / Magnetometer Survey
Allied Mining Corp Ltd	1972	41P14SE0014	-	Diamond Drilling
Allied Mining Corp Ltd	1972	41P14SE0017	-	Diamond Drilling
J Hogan	1971	41P14SE0012	-	Diamond Drilling
J Hogan	1971	41P14SE0015	-	Diamond Drilling
Cdn Johns-Manville Co Ltd	1970	41P14SE0016	-	Diamond Drilling
Cdn Johns-Manville Co Ltd	1969	41P14NE0113	-	Airborne Magnetometer
Timiskaming Nickel Ltd	1968	41P14SE0018	-	Diamond Drilling
Timiskaming Nickel Ltd	1968	41P14NE0035	-	Airborne Electromagnetic, Airborne Magnetometer
Dominion Gulf Co	1956	41P14NE0038	-	Geological Survey / Mapping, Magnetic / Magnetometer Survey, Overburden Stripping, Prospecting By Licence Holder

4.0 GEOLOGY

The following descriptions of both regional and property geology are based on the key papers of (Ayer et al., 2002, 2005; BRIGHT EG, 1970; Houlé & Leshar, 2019; Monecke et al., 2017, 2019; Thurston et al., 2008). Deposit geology is based on the synthesis of historical exploration data by CNC staff geologists (see CNC press release dated November 22, 2021), key papers by (Ausenco Engineering Canada Inc., 2021; Sciortino et al., 2015) which includes the Preliminary Economic Assessment completed on the Crawford Project a possible analogue for the Midlothian Project.

4.1 REGIONAL GEOLOGY

The Midlothian Project is situated on the southern Abitibi Greenstone Belt ('AGB'), a Precambrian aged volcano-sedimentary belt cored by intervening domes of synvolcanic to syntectonic felsic plutonic rocks. Mafic to ultramafic sills and flows intrude volcanic stratigraphy, particularly around the flanks of regional volcanic domes. Younger Archean ultrabasic lamprophyre and minor carbonatite dikes variably cut

stratigraphy. Regional east-west trending strike-slip faults such as the Porcupine-Destor and Cadillac-Larder deformation zones cross the AGB. These deformation zones are interpreted as Archean rifts, filled with clastic sediments, and later reactivated as strike-slip faults by compressional shortening that has tilted regional stratigraphy to near vertical dips. Multiple diabase dike swarms generally trending north-south occupy regional faults/structures in the AGB.

4.2 PROPERTY GEOLOGY

The property flanks the 'Holiday Dome' a major volcanic domal structure that is generally comprised of tuffs, breccias, volcanoclastics, and massive flows. A large east-west trending ultramafic sill consisting primarily of serpentinized cumulate dunite/peridotite occurs in the center of the study area (Figure 5). The southeast portion of the study area is covered by Proterozoic Huronian Supergroup metasediments consisting primarily of wackes capped by conglomerates.

4.3 DEPOSIT GEOLOGY

Based on historic diamond drill logs, the interpreted overall structure of the main ultramafic unit from bottom-up is, a relatively sharp basal contact with a thick cumulate, variably serpentinized dunitic core grading into a layered peridotite-pyroxenite-gabbro sequence with possible waning rhythmic layering to the top. These magmatic intrusions may contain disseminated primary blebs of predominantly pentlandite and nickeliferous pyrrhotite. Secondary greenschist alteration then liberates the Ni from the silicate olivine structure through the serpentinization process, effectively adding to, and upgrading existing sulphides to the more nickeliferous heazewoodite. Magnetite is produced as a byproduct of the serpentinization process causing the deposits to have strong magnetic signatures. Additionally, during the serpentinization process, the density of the dunite decreases from $\sim 3.2 \text{ g/cm}^3$ to $\sim 2.5\text{-}2.6 \text{ g/cm}^3$ producing a gravity low due to the contrast with surrounding volcanic sequences. The combined geophysical signatures of strong magnetic responses with overlapping low gravity anomalies are what is being targeted with this survey.

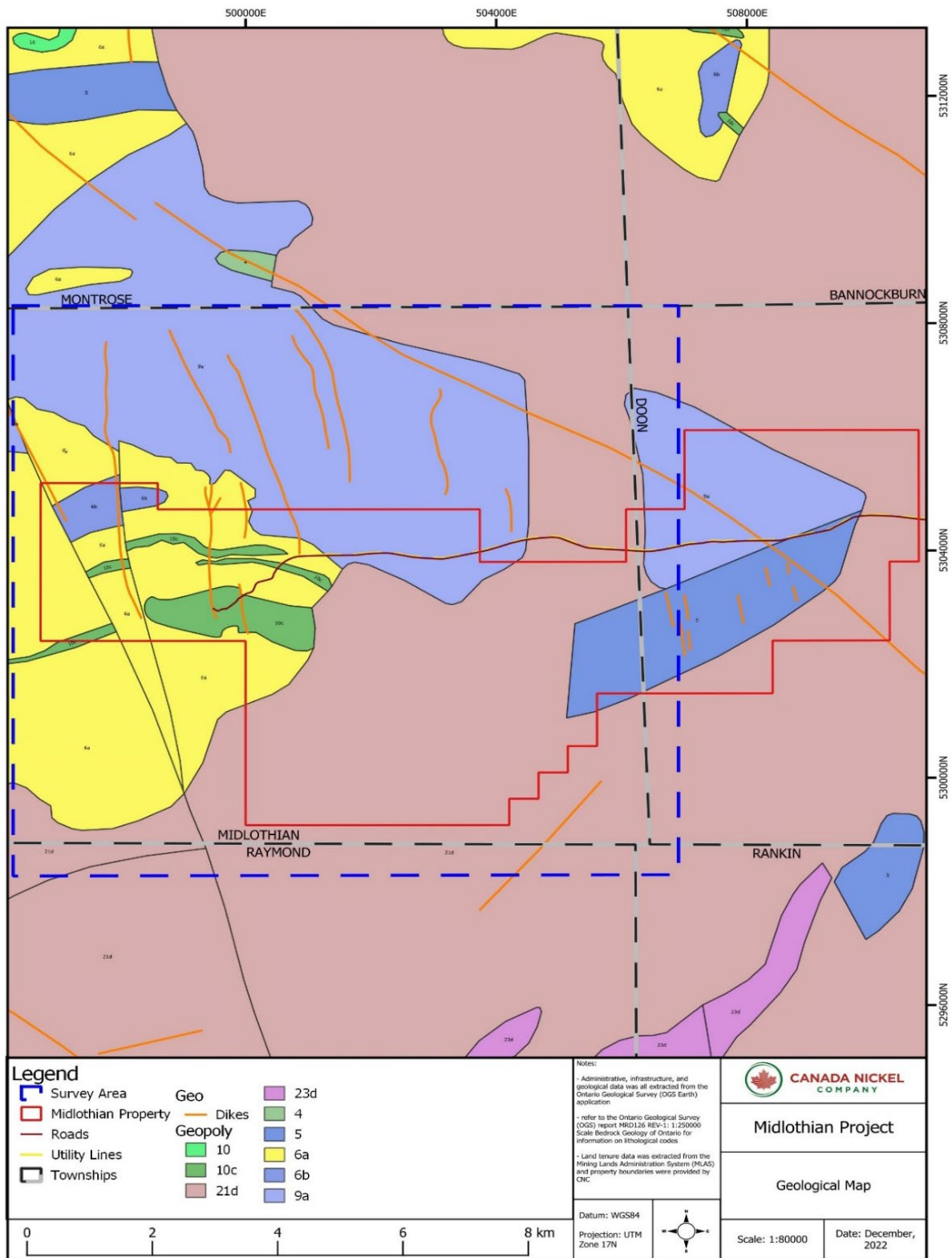


Figure 5: Midlothian Project bedrock geology map from: OGS report MRD 126 REV-1 1:250,000 Scale Bedrock Geology of Ontario.

5.0 DATA PROCESSING AND PRESENTATION

Data compilation and processing were carried out by the application of Geosoft OASIS Montaj and programs proprietary to Geotech Ltd.

5.1 ELECTROMAGNETIC DATA

The Full Waveform EM specific data processing operations included:

- Half cycle stacking (performed at time of acquisition).
- System response correction.
- Parasitic and drift removal.

A three-stage digital filtering process was used to reject major spheric events and to reduce noise levels. Local spheric activity can produce sharp, large amplitude events that cannot be removed by conventional filtering procedures. Smoothing or stacking will reduce their amplitude but leave a broader residual response that can be confused with geological phenomena. To avoid this possibility, a computer algorithm searches out and rejects the major spheric events.

The signal to noise ratio was further improved by the application of a low pass linear digital filter. This filter has zero phase shift which prevents any lag or peak displacement from occurring, and it suppresses only variations with a wavelength less than about 1 second or 15 metres. This filter is a symmetrical 1 sec linear filter.

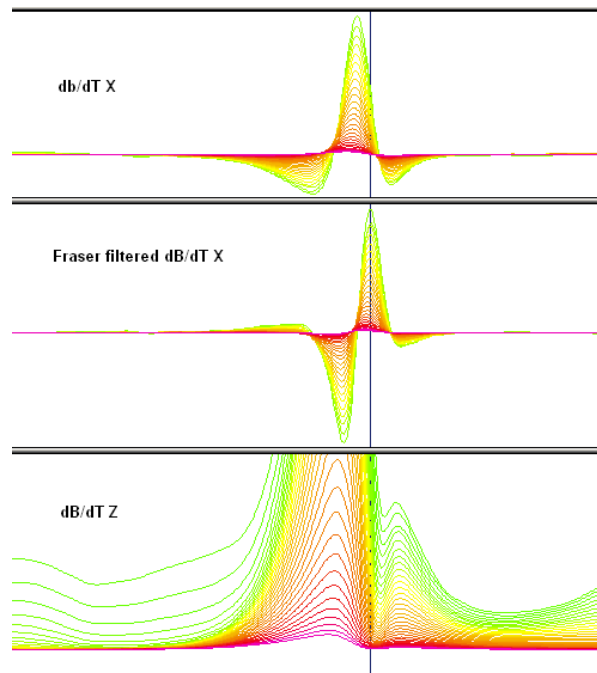
The results are presented as stacked profiles of EM voltages for the time gates, in linear - logarithmic scale for the B-field Z component and dB/dt responses in the Z and X components. B-field Z component time channels recorded at 0.880 milliseconds after the termination of the impulse is also presented as a colour image. Calculated Time Constant (TAU) with Calculated Vertical Derivative contours is presented in Appendix B.

VTEM™ has three receiver coil orientations. Z-axis coil is oriented parallel to the transmitter coil axis, and both are horizontal to the ground. The X-axis coil is oriented parallel to the ground and along the line-of-flight. The Y-axis coil is oriented parallel to the ground and across the line-of-flight. The combination of the X, Y, and Z coils configuration provides information on the position, depth, dip, and thickness of a conductor.

In general X-component data produce cross-over type anomalies: from “+ to -” in flight direction of flight for “thin” sub vertical targets and from “- to +” in direction of flight for “thick” targets. Z component data produce double peak type anomalies for “thin” sub vertical targets and single peak for “thick” targets. The limits and change-over of “thin-thick” depends on dimensions of a TEM system.

Because of X component polarity is under line-of-flight, convolution Fraser Filter (Figure 6) is applied to X component data to represent axes of conductors in the form of grid map. In this case positive FF anomalies always correspond to “plus-to-minus” X data crossovers independent of the flight direction.

Figure 6. Z, X and Fraser filtered X (FFx) components for "thin" target



5.2 HORIZONTAL MAGNETIC GRADIOMETER DATA

The horizontal gradients data from the VTEM™ Plus are measured by two magnetometers 12.5 m apart on an independent bird mounted 10m above the VTEM™ loop. A GPS and a Gyro Inclinometer help to determine the positions and orientations of the magnetometers. The data from the two magnetometers are corrected for position and orientation variations, as well as for the diurnal variations using the base station data.

The position of the centre of the horizontal magnetic gradiometer bird is calculated from the GPS utilizing in-house processing tool in Geosoft. Following that total magnetic intensity is calculated at the center of the bird by calculating the mean values from both sensors. In addition to the total intensity advanced processing is done to calculate the in-line and crossline (or lateral) horizontal gradient which enhance the understanding of magnetic targets. The in-line (longitudinal) horizontal gradient is calculated from the difference of two consecutive total magnetic field readings divided by the distance along the flight line direction, while the crossline (lateral) horizontal magnetic gradient is calculated from the difference in the magnetic readings from both magnetic sensors divided by their horizontal separation.

Two advanced magnetic derivative products, the total horizontal derivative (THDR), and tilt angle derivative and are also created. The total horizontal derivative or gradient is defined as:

THDR = $\sqrt{H_x^2 + H_y^2}$, where H_x and H_y are crossline and in-line horizontal gradients.

The tilt angle derivative (TDR) is defined as:

TDR = $\arctan(V_z / \text{THDR})$, where THDR is the total horizontal derivative, and V_z is the vertical derivative.

Measured crossline gradients can help to enhance crossline linear features during gridding.

5.3 TAU PARAMETER AND CVG

The processed VTEM survey results are presented as a calculated dB/dt time constant (Tau), which is an indicator of geological unit's electrical conductance.

The TAU dB/dt map is presented in Appendix B. The map is accompanied by an overlay of the calculated vertical gradient of TMI anomaly contours for tracing possible EM-MAG anomaly correlations.

The CVG contour layer, on the top of TAU color grid, is generally more representative of the smaller scale and shallower magnetic sources in comparison with the TMI. The calculated vertical derivative (CVG) is designed to emphasize structures and lithological units that may not otherwise be seen on the TMI due to the nearby presence of stronger magnetic responses, showing a high resolution in terms of individual structures.

6.0 VTEM SURVEY RESULTS AND DELIVERABLES

6.1 SURVEY REPORT

The survey report describes the data acquisition, processing, and final presentation of the survey results. The information from the survey report provided, was re-organized and is presented here in this assessment report.

6.2 MAPS

Final maps were produced at scales of 1:10,000 for best representation of the survey size and line spacing. The coordinate/projection system used was WGS84 Datum, UTM Zone 17N. All maps showed the flight path trace and topographic data, latitude and longitude.

The results of the survey were presented as EM profiles, a late-time gate gridded EM channel, and a colour magnetic TMI contour map.

• Maps at 1:10,000 in Geosoft MAP format, as follows:

GL210350_**_dBdt: dB/dt profiles Z Component, Time Gates 0.220 – 7.036 ms in linear – logarithmic scale.

GL210350_**_BField: B-field profiles Z Component, Time Gates 0.220 – 7.036 ms in linear – logarithmic scale.

GL210350_**_BFz25: B-field Z Component Channel 25, Time Gate 0.440 ms colour image.

GL210350_**_SFz25: VTEM dB/dt Z Component Channel 25, Time Gate 0.440 ms colour image

GL210350_**_SFxFF30: Fraser Filtered dB/dt X Component Channel 30, Time Gate 0.880 ms colour image.

GL210350_**_TMI: Total Magnetic Intensity (TMI) colour image and contours.

GL210350_**_CVG: Calculated Vertical Derivative (CVG) of TMI colour image.

GL210350_**_TauSF: dB/dt Calculated Time Constant (Tau) with Calculated Vertical Derivative contours.

GL210350_**_TotHG: Magnetic Total Horizontal Gradient colour image

GL210350_**_TiltDrv: Magnetic Tilt Angle Derivative colour image

Where ** represents company name and map scale. Eg. *GL210350_CanadaNickel_10k_Bfield.map*

- Maps were also presented in PDF format.
- The topographic data base was derived from 1:250,000 CANVEC data. Background shading is from ASTER GDEM (<https://gdex.cr.usgs.gov/gdex>). Inset data derived from the Geocommunities (www.geocomm.com).
- A Google Earth files *GL210350_CanadaNickel.kmz* showing the flight path of the blocks is included. Free versions of Google Earth software from: <http://earth.google.com/download-earth.html>

6.3 DIGITAL DATA

Data and maps were received accompanying the report. Digital files of the line data are in GDB Geosoft Montaj format, as well as the maps in Geosoft Montaj Map and PDF format. Databases in Geosoft GDB format, containing the channels listed in Table 7.

Table 7. Geosoft GDB Data Format

Channel name	Units	Description
X	metres	Easting WGS84 Zone 17N
Y	metres	Northing WGS84 Zone 17N
Longitude	Decimal Degrees	WGS84 Longitude data
Latitude	Decimal Degrees	WGS84 Latitude data
Z	metres	GPS antenna elevation
Zb	metres	EM bird elevation
Radar	metres	Helicopter terrain clearance from radar altimeter
Radarb	metres	Calculated EM transmitter-receiver loop terrain clearance from radar altimeter
DEM	metres	Digital Elevation Model
Gtime	Seconds of the day	GPS time
Mag1L	nT	Measured Total Magnetic field data (left sensor)
Mag1R	nT	Measured Total Magnetic field data (right sensor)
Basemag	nT	Magnetic diurnal variation data
Mag2LZ	nT	Z corrected (w.r.t. loop center) and diurnal corrected magnetic field left mag
Mag2RZ	nT	Z corrected (w.r.t. loop center) and diurnal corrected magnetic field right mag
TMI2	nT	Calculated from diurnal corrected total magnetic field intensity of the centre of the loop

TMI3	nT	Microleveled total magnetic field intensity of the centre of the loop
Hginline		Calculated in-line gradient
Hgcxline		Measured cross-line gradient
CVG	nT/m	Calculated Magnetic Vertical Gradient of TMI
SFz[4]	$pV/(A * m^4)$	Z dB/dt 0.021 millisecond time channel
SFz[5]	$pV/(A * m^4)$	Z dB/dt 0.026 millisecond time channel
SFz[6]	$pV/(A * m^4)$	Z dB/dt 0.031 millisecond time channel
SFz[7]	$pV/(A * m^4)$	Z dB/dt 0.036 millisecond time channel
SFz[8]	$pV/(A * m^4)$	Z dB/dt 0.042 millisecond time channel
SFz[9]	$pV/(A * m^4)$	Z dB/dt 0.048 millisecond time channel
SFz[10]	$pV/(A * m^4)$	Z dB/dt 0.055 millisecond time channel
SFz[11]	$pV/(A * m^4)$	Z dB/dt 0.063 millisecond time channel
SFz[12]	$pV/(A * m^4)$	Z dB/dt 0.073 millisecond time channel
SFz[13]	$pV/(A * m^4)$	Z dB/dt 0.083 millisecond time channel
SFz[14]	$pV/(A * m^4)$	Z dB/dt 0.096 millisecond time channel
SFz[15]	$pV/(A * m^4)$	Z dB/dt 0.110 millisecond time channel
SFz[16]	$pV/(A * m^4)$	Z dB/dt 0.126 millisecond time channel
SFz[17]	$pV/(A * m^4)$	Z dB/dt 0.145 millisecond time channel
SFz[18]	$pV/(A * m^4)$	Z dB/dt 0.167 millisecond time channel
SFz[19]	$pV/(A * m^4)$	Z dB/dt 0.192 millisecond time channel
SFz[20]	$pV/(A * m^4)$	Z dB/dt 0.220 millisecond time channel
SFz[21]	$pV/(A * m^4)$	Z dB/dt 0.253 millisecond time channel
SFz[22]	$pV/(A * m^4)$	Z dB/dt 0.290 millisecond time channel
SFz[23]	$pV/(A * m^4)$	Z dB/dt 0.333 millisecond time channel
SFz[24]	$pV/(A * m^4)$	Z dB/dt 0.383 millisecond time channel
SFz[25]	$pV/(A * m^4)$	Z dB/dt 0.440 millisecond time channel
SFz[26]	$pV/(A * m^4)$	Z dB/dt 0.505 millisecond time channel
SFz[27]	$pV/(A * m^4)$	Z dB/dt 0.580 millisecond time channel
SFz[28]	$pV/(A * m^4)$	Z dB/dt 0.667 millisecond time channel
SFz[29]	$pV/(A * m^4)$	Z dB/dt 0.766 millisecond time channel
SFz[30]	$pV/(A * m^4)$	Z dB/dt 0.880 millisecond time channel
SFz[31]	$pV/(A * m^4)$	Z dB/dt 1.010 millisecond time channel
SFz[32]	$pV/(A * m^4)$	Z dB/dt 1.161 millisecond time channel
SFz[33]	$pV/(A * m^4)$	Z dB/dt 1.333 millisecond time channel
SFz[34]	$pV/(A * m^4)$	Z dB/dt 1.531 millisecond time channel
SFz[35]	$pV/(A * m^4)$	Z dB/dt 1.760 millisecond time channel
SFz[36]	$pV/(A * m^4)$	Z dB/dt 2.021 millisecond time channel
SFz[37]	$pV/(A * m^4)$	Z dB/dt 2.323 millisecond time channel
SFz[38]	$pV/(A * m^4)$	Z dB/dt 2.667 millisecond time channel
SFz[39]	$pV/(A * m^4)$	Z dB/dt 3.063 millisecond time channel
SFz[40]	$pV/(A * m^4)$	Z dB/dt 3.521 millisecond time channel
SFz[41]	$pV/(A * m^4)$	Z dB/dt 4.042 millisecond time channel
SFz[42]	$pV/(A * m^4)$	Z dB/dt 4.641 millisecond time channel
SFz[43]	$pV/(A * m^4)$	Z dB/dt 5.333 millisecond time channel
SFz[44]	$pV/(A * m^4)$	Z dB/dt 6.125 millisecond time channel
SFz[45]	$pV/(A * m^4)$	Z dB/dt 7.036 millisecond time channel
SFz[46]	$pV/(A * m^4)$	Z dB/dt 8.083 millisecond time channel
SFx[20]	$pV/(A * m^4)$	X dB/dt 0.220 millisecond time channel
SFx[21]	$pV/(A * m^4)$	X dB/dt 0.253 millisecond time channel
SFx[22]	$pV/(A * m^4)$	X dB/dt 0.290 millisecond time channel

SFx[23]	$pV/(A*m4)$	X dB/dt 0.333 millisecond time channel
SFx[24]	$pV/(A*m4)$	X dB/dt 0.383 millisecond time channel
SFx[25]	$pV/(A*m4)$	X dB/dt 0.440 millisecond time channel
SFx[26]	$pV/(A*m4)$	X dB/dt 0.505 millisecond time channel
SFx[27]	$pV/(A*m4)$	X dB/dt 0.580 millisecond time channel
SFx[28]	$pV/(A*m4)$	X dB/dt 0.667 millisecond time channel
SFx[29]	$pV/(A*m4)$	X dB/dt 0.766 millisecond time channel
SFx[30]	$pV/(A*m4)$	X dB/dt 0.880 millisecond time channel
SFx[31]	$pV/(A*m4)$	X dB/dt 1.010 millisecond time channel
SFx[32]	$pV/(A*m4)$	X dB/dt 1.161 millisecond time channel
SFx[33]	$pV/(A*m4)$	X dB/dt 1.333 millisecond time channel
SFx[34]	$pV/(A*m4)$	X dB/dt 1.531 millisecond time channel
SFx[35]	$pV/(A*m4)$	X dB/dt 1.760 millisecond time channel
SFx[36]	$pV/(A*m4)$	X dB/dt 2.021 millisecond time channel
SFx[37]	$pV/(A*m4)$	X dB/dt 2.323 millisecond time channel
SFx[38]	$pV/(A*m4)$	X dB/dt 2.667 millisecond time channel
SFx[39]	$pV/(A*m4)$	X dB/dt 3.063 millisecond time channel
SFx[40]	$pV/(A*m4)$	X dB/dt 3.521 millisecond time channel
SFx[41]	$pV/(A*m4)$	X dB/dt 4.042 millisecond time channel
SFx[42]	$pV/(A*m4)$	X dB/dt 4.641 millisecond time channel
SFx[43]	$pV/(A*m4)$	X dB/dt 5.333 millisecond time channel
SFx[44]	$pV/(A*m4)$	X dB/dt 6.125 millisecond time channel
SFx[45]	$pV/(A*m4)$	X dB/dt 7.036 millisecond time channel
SFx[46]	$pV/(A*m4)$	X dB/dt 8.083 millisecond time channel
BFz	$(pV*ms)/(A*m4)$	Z B-Field data for time channels 4 to 46
BFx	$(pV*ms)/(A*m4)$	X B-Field data for time channels 20 to 46
SFxFF	$pV/(A*m4)$	Fraser Filtered X dB/dt
NchanBF		Latest time channels of TAU calculation
TauBF	ms	Time constant B-Field
NchanSF		Latest time channels of TAU calculation
TauSF	ms	Time constant dB/dt
PLM		60 Hz power line monitor

Electromagnetic B-field and dB/dt Z component data is found in array channel format between indexes 4 – 46, and X data from 20 – 46, as described above.

Database of the Resistivity Depth Images in Geosoft GDB format, containing the following channels in Table 8.

Table 8. Geosoft Resistivity Depth Image GDB Data Format

Channel name	Units	Description
Xg	metres	Easting WGS84 Zone 17N
Yg	metres	Northing WGS84 Zone 17N
Dist	metres	Distance from the beginning of the line
Depth	metres	array channel, depth from the surface
Z	metres	array channel, depth
AppRes	Ohm-m	array channel, Apparent Resistivity
TR	metres	EM system height
Topo	metres	digital elevation model
Radarb	metres	Calculated EM transmitter-receiver loop terrain clearance from radar altimeter
SF	$\rho V / (A \cdot m^4)$	array channel, Z dB/dT
MAG	nT	TMI data
CVG	nT/m	CVG data
DOI	metres	Depth of Investigation: a measure of VTEM depth effectiveness
PLM		60 Hz Power Line Monitor

- Geosoft Resistivity Depth Image Products:

Sections: Apparent resistivity sections along each line in .GRD and .PDF format

Slices: Apparent resistivity slices at selected depths from 25m to depth of investigation, at an increment of 25m in .GRD and .PDF format

Voxel: 3D Voxel imaging of apparent resistivity data clipped by digital elevation and depth of investigation

- Grids in Geosoft GRD and GeoTIFF format, as follows:

GL210350_**_BFz25: B-Field Z Component Channel 25 (Time Gate 0.440 ms)

GL210350_**_SFxFF30: Fraser Filtered dB/dt X Component Channel 30 (Time Gate 0.880ms)

GL210350_**_SFz10: dB/dt Z Component Channel 10 (Time Gate 0.055 ms)

GL210350_**_SFz25: dB/dt Z Component Channel 25 (Time Gate 0.440 ms)

GL210350_**_SFz40: dB/dt Z Component Channel 40 (Time Gate 3.521 ms)

GL210350_**_TauBF: B-Field Z Component, Calculated Time Constant (ms)

GL210350_**_TauSF: dB/dt Z Component, Calculated Time Constant (ms)

GL210350_**_TMI: Total Magnetic Intensity (nT)

GL210350_**_CVG: Calculated Vertical Derivative(nT/m)

GL210350_**_Hgexline: Measured Cross-Line Gradient (nT/m)

GL210350_**_Hginline: Measured In-Line Gradient (nT/m)

GL210350_**_TotHG: Magnetic Total Horizontal Gradient (nT/m)

GL210350_**_TiltDrv: Magnetic Tilt derivative (radians)

GL210350_**_DEM: Digital Elevation Model (m)

GL210350_**_PLM: 60Hz Power Line Monitor

Where ** denotes company and block name. E.g., *GL210350_CanadaNickel_Midlothian_BFz25.grd*

A Geosoft .GRD file has a .GI metadata file associated with it, containing grid projection information. A grid cell size of 25 metres was used.

7.0 INTERPRETATION AND CONCLUSIONS

The following recommendations and conclusions are taken from Geotech's final report, with the addition of comments from the writers of this report.

The goal of this survey was to identify bulk-tonnage (Type II) disseminated magmatic nickel sulphide deposits. Geophysical signatures associated with the alteration and further endowment of these potentially substantial deposits produce overlapping low gravity anomalies with strong magnetic signatures.

The total area coverage is 61 km² and the total survey line coverage is 624 line-kilometres over one (1) block. The principal sensors included a Time Domain EM system, and a horizontal magnetic gradiometer system with two caesium magnetometers. Results have been presented as stacked profiles, and contour colour images at a scale of 1:10,000. There is no formal interpretation included in this study, however RDI resistivity-depth imaging has been performed in support of the VTEM data.

Based on the geophysical results obtained, several geophysical anomalies of interest have been identified across the survey areas. Magnetically, the Midlothian project is very active, with a measured range of >9,000 nT (TMI = 53,995-63,443 nT). The total magnetic intensity (TMI) and related derivatives (CVG, TiltDrv, TotHG) all highlight a large (>3x6 km), EW elongate, intrusion like magnetic feature in the centre of the block, as well as several subparallel, dyke-like magnetic high and low lineaments on its northern and southern flanks. Minor dyke-like NNW-SSE magnetic trends are also visible.

The relationships between the EM and magnetic signatures are highlighted in our dBz/dt EM decay constant (TAU_{sf}) map with magnetic CVG contour (Appendix B) and the RDI resistivity-depth image sections with profiles.

Electromagnetically, the block hosts a variety of conductive signatures, ranging from a large (>5x1.5 km), central, EW-elongated, thick plate/tabular type (single-peak) mid-late channel (>ch35-45), lithologic like body that coincides with the central magnetic high mentioned above; and shorter strike length/discrete (<1 km), steeply dipping, thin-plate (double-peak), conductive signature that subparallel the main intrusion-like body and also coincide with magnetic highs. Electromagnetically, conductive anomalies feature EM dBz/dt time constants are in the ~0.14-4.02 ms range, which indicates a mix of weak to high conductivities. Negative EM decays, related to AIP effects (airborne inductive induced polarization) are present inside the large tabular EM conductor but are uncommon. According to the RDI imaging results, apparent resistivities range from lows of approx. 0.3-60 ohm-m and reach highs of >4000 ohm-m. Based on RDI's, the estimated depths of burial of conductive units vary from within the 50m of surface to >250

m depths. Maximum depths of depths of investigation (DOI) range from ~300m in conductive regions to >700m depths in resistive rocks.

The Midlothian Project is understood to be prospective for magmatic peridotite-dunnite hosted nickel mineralization (www.canadanickel.com). Based on the geologic model, it is quite likely that both the EM and magnetic results will be of exploration interest. We recommend that, in addition to EM anomaly picking, Maxwell 3D EM plate modeling be performed over anomalies of interest, prior to ground follow up and drill testing. 3D MVI magnetic inversions will be useful for mapping structure, alteration, and lithology in 2D-3D space across the property. We recommend that more advanced, integrated interpretation be performed, such as AI-assisted SOM (self-organizing maps) analysis be performed to better correlate EM and magnetic features in 3D and these results be further evaluated against the known geology for future targeting.

The synthesis of overlapping geophysical signatures combined with the compilation and interpretation of both surface prospecting and diamond drill hole surveys; has proven the Midlothian Project is a potentially valuable brownfields site that could host a bulk tonnage magmatic nickel sulphide deposit.

Future work should include but not be limited to:

1. A 10-hole, 4,000 m diamond drill program consisting of widely spaced (~200 m apart) drill holes perpendicular to strike with the target of crossing stratigraphy and testing resource definition to a true depth of ~350m.
2. Surface prospecting and ground truthing to further refine the lithological and structural characteristics of the property geology.

8.0 REFERENCES

- Ausenco Engineering Canada Inc. (2021). *Crawford Nickel Sulphide Project NI 43-101 Technical Report & Preliminary Economic Assessment*.
- Ayer, J., Amelin, Y., Corfu, F., Kamo, S., Ketchum, J., Kwok, K., & Trowell, N. (2002). Evolution of the southern Abitibi greenstone belt based on U-Pb geochronology: Autochthonous volcanic construction followed by plutonism, regional deformation and sedimentation. *Precambrian Research*, 115(1–4). [https://doi.org/10.1016/S0301-9268\(02\)00006-2](https://doi.org/10.1016/S0301-9268(02)00006-2)
- Ayer, J., Thurston, P. C., Bateman, R., Dubé, B., Gibson, H. L., Hamilton, M. A., Hathway, B., Hocker, S. M., Houlié, M., Hudak, G. J., Ispolatov, V., Lafrance, B., Leshner, C. M., MacDonald, P. J., Péroquin, A. S., Piercey, S. J., Reed, L. E., & Thompson, P. H. (2005). Overview of results from the Greenstone Architecture Project: Discover Abitibi Initiative. In *Ontario Geological Survey: Vol. OFR 6154*.
- BRIGHT EG. (1970). GEOLOGY OF HALLIDAY AND MIDLOTHIAN TOWNSHIPS, DISTRICTS OF SUDBURY AND TIMISKAMING. *Ont, Dept Mines, Geol Rep 79*.
- Houlié, M. G., & Leshner, C. M. (2019). Komatiite-Associated Ni-Cu-(PGE) Deposits, Abitibi Greenstone Belt, Superior Province, Canada. In *Magmatic Ni-Cu and PGE Deposits_{title>Geology, Geochemistry, and Genesis}*. <https://doi.org/10.5382/rev.17.03>
- Monecke, T., Mercier-Langevin, P., & Dubé, B. (2017). Archean Base and Precious Metal Deposits, Southern Abitibi Greenstone Belt, Canada. In *Archean Base and Precious Metal Deposits, Southern Abitibi Greenstone Belt, Canada*. <https://doi.org/10.5382/rev.19>
- Monecke, T., Mercier-Langevin, P., Dubé, B., & Frieman, B. M. (2019). Geology of the Abitibi Greenstone Belt. In *Archean Base and Precious Metal Deposits, Southern Abitibi Greenstone Belt, Canada*. <https://doi.org/10.5382/rev.19.01>
- Sciortino, M., Mungall, J. E., & Muinonen, J. (2015). Generation of High-Ni sulfide and alloy phases during serpentinization of dunite in the dumont sill, Quebec. *Economic Geology*, 110(3). <https://doi.org/10.2113/econgeo.110.3.733>
- Thurston, P. C., Ayer, J. A., Goutier, J., & Hamilton, M. A. (2008). Depositional gaps in abitibi greenstone belt stratigraphy: A key to exploration for syngenetic mineralization. *Economic Geology*, 103(6). <https://doi.org/10.2113/gsecongeo.103.6.1097>
- Xcalibur MPH (Canada) Ltd. (2022). *FALCON® Airborne Gravity Gradiometer and Magnetometer Survey The Eminem Project, Midlothian Block 2, Ontario Logistics and Processing Report*.

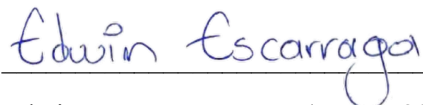
9.0 CERTIFICATE OF QUALIFICATIONS

STATEMENT OF QUALIFICATIONS

I, Edwin Escarraga, P.Ge., do hereby certify that:

- 1) I am a Senior Project geologist, Director of Exploration employed by Canada Nickel Company., with a business address at 130 King Street West, Suite 1900, Toronto ON, M5X 1E3.
- 2) I graduated with a degree of Bachelor of Science Honours, Geology from the Universidad Nacional de Colombia in 2007 and a M. Sc Geology from Acadia University, NS, Canada, in 2010.
- 3) I am a Professional Geoscientist (P.Ge.) registered with the Professional Geoscientists of Ontario (PGO No. 2859) and I am a member of the Prospectors and Developers Association of Canada.
- 4) I am responsible for the preparation of this report.
- 5) I have no prior involvement with the property that is the subject of this Report.
- 6) I own directly or indirectly shares of Canada Nickel which I hold for investment purposes.
- 7) I have no direct interest in the Midlothian Property.
- 8) I reviewed the data contained within this report based on my general experience and my involvement with planning the survey and reviewing the data, and I am responsible for its contents.

Dated this 21st day of December 2022.



Edwin Escarraga, P.Ge. (PGO # 2859)

APPENDIX A – MINING CLAIMS DATA

The following is a summary table of mining claims contained within the Midlothian Project boundary.

Tenure Number	Title Type	Issue Date	Anniversary	Extension
680182	Single Cell Mining Claim	2021-10-04	2023-10-04	
680183	Single Cell Mining Claim	2021-10-04	2023-10-04	
680184	Single Cell Mining Claim	2021-10-04	2023-10-04	
680185	Single Cell Mining Claim	2021-10-04	2023-10-04	
680186	Single Cell Mining Claim	2021-10-04	2023-10-04	
680187	Single Cell Mining Claim	2021-10-04	2023-10-04	
680188	Single Cell Mining Claim	2021-10-04	2023-10-04	
680189	Single Cell Mining Claim	2021-10-04	2023-10-04	
680190	Single Cell Mining Claim	2021-10-04	2023-10-04	
680191	Single Cell Mining Claim	2021-10-04	2023-10-04	
339951	Boundary Cell Mining Claim	2018-04-10	2027-03-10	
339953	Single Cell Mining Claim	2018-04-10	2022-12-24	
339954	Single Cell Mining Claim	2018-04-10	2022-12-24	
101320	Single Cell Mining Claim	2018-04-10	2022-12-24	
104002	Single Cell Mining Claim	2018-04-10	2023-07-09	
104003	Boundary Cell Mining Claim	2018-04-10	2023-07-09	
101319	Single Cell Mining Claim	2018-04-10	2022-12-24	
108106	Boundary Cell Mining Claim	2018-04-10	2023-12-24	
108957	Single Cell Mining Claim	2018-04-10	2022-07-09	2023-07-09
108975	Single Cell Mining Claim	2018-04-10	2022-07-09	2023-07-09
108976	Single Cell Mining Claim	2018-04-10	2022-07-09	2023-07-09

112502	Single Cell Mining Claim	2018-04-10	2022-12-24	
113075	Single Cell Mining Claim	2018-04-10	2022-07-09	2023-07-09
112937	Boundary Cell Mining Claim	2018-04-10	2022-12-24	
112836	Boundary Cell Mining Claim	2018-04-10	2022-12-24	
111833	Single Cell Mining Claim	2018-04-10	2022-12-24	
111834	Boundary Cell Mining Claim	2018-04-10	2022-12-24	
116653	Boundary Cell Mining Claim	2018-04-10	2022-12-24	
119973	Boundary Cell Mining Claim	2018-04-10	2019-12-05	
120634	Single Cell Mining Claim	2018-04-10	2023-07-09	
120423	Single Cell Mining Claim	2018-04-10	2022-12-24	
120424	Boundary Cell Mining Claim	2018-04-10	2022-12-24	
121470	Boundary Cell Mining Claim	2018-04-10	2022-12-24	
126048	Single Cell Mining Claim	2018-04-10	2023-12-24	
131568	Single Cell Mining Claim	2018-04-10	2022-07-09	2023-07-09
131738	Boundary Cell Mining Claim	2018-04-10	2022-12-24	
131600	Single Cell Mining Claim	2018-04-10	2022-07-09	2023-07-09
131632	Single Cell Mining Claim	2018-04-10	2023-07-09	
131633	Single Cell Mining Claim	2018-04-10	2022-07-09	2023-07-09
133863	Single Cell Mining Claim	2018-04-10	2022-07-09	2023-07-09
680162	Single Cell Mining Claim	2021-10-04	2023-10-04	
680163	Single Cell Mining Claim	2021-10-04	2023-10-04	
680164	Single Cell Mining Claim	2021-10-04	2023-10-04	
680165	Single Cell Mining Claim	2021-10-04	2023-10-04	

680166	Single Cell Mining Claim	2021-10-04	2023-10-04	
680167	Single Cell Mining Claim	2021-10-04	2023-10-04	
680168	Single Cell Mining Claim	2021-10-04	2023-10-04	
680169	Single Cell Mining Claim	2021-10-04	2023-10-04	
680170	Single Cell Mining Claim	2021-10-04	2023-10-04	
680171	Single Cell Mining Claim	2021-10-04	2023-10-04	
680172	Single Cell Mining Claim	2021-10-04	2023-10-04	
680173	Single Cell Mining Claim	2021-10-04	2023-10-04	
680175	Single Cell Mining Claim	2021-10-04	2023-10-04	
680174	Single Cell Mining Claim	2021-10-04	2023-10-04	
680176	Single Cell Mining Claim	2021-10-04	2023-10-04	
680177	Single Cell Mining Claim	2021-10-04	2023-10-04	
680178	Single Cell Mining Claim	2021-10-04	2023-10-04	
680179	Single Cell Mining Claim	2021-10-04	2023-10-04	
680180	Single Cell Mining Claim	2021-10-04	2023-10-04	
133869	Single Cell Mining Claim	2018-04-10	2022-07-09	2023-07-09
133511	Single Cell Mining Claim	2018-04-10	2022-12-24	
133512	Single Cell Mining Claim	2018-04-10	2022-12-24	
133513	Single Cell Mining Claim	2018-04-10	2022-12-24	
135903	Single Cell Mining Claim	2018-04-10	2022-07-09	2023-07-09
135181	Boundary Cell Mining Claim	2018-04-10	2022-12-24	
134930	Single Cell Mining Claim	2018-04-10	2022-07-09	2023-07-09
134931	Single Cell Mining Claim	2018-04-10	2022-07-09	2023-07-09

138454	Boundary Cell Mining Claim	2018-04-10	2022-12-24	
136579	Single Cell Mining Claim	2018-04-10	2022-12-24	
136580	Single Cell Mining Claim	2018-04-10	2022-12-24	
141948	Boundary Cell Mining Claim	2018-04-10	2022-07-09	2023-07-09
142557	Single Cell Mining Claim	2018-04-10	2022-12-24	
142567	Boundary Cell Mining Claim	2018-04-10	2022-07-09	2023-07-09
141865	Single Cell Mining Claim	2018-04-10	2023-07-09	
143905	Single Cell Mining Claim	2018-04-10	2022-12-24	
150291	Boundary Cell Mining Claim	2018-04-10	2023-07-09	
148432	Single Cell Mining Claim	2018-04-10	2022-12-24	
150476	Single Cell Mining Claim	2018-04-10	2022-07-09	2023-07-09
149184	Boundary Cell Mining Claim	2018-04-10	2023-07-09	
151934	Single Cell Mining Claim	2018-04-10	2022-12-24	
153949	Boundary Cell Mining Claim	2018-04-10	2022-07-09	2023-07-09
153950	Single Cell Mining Claim	2018-04-10	2022-07-09	2023-07-09
153990	Boundary Cell Mining Claim	2018-04-10	2019-12-05	
156634	Single Cell Mining Claim	2018-04-10	2022-12-24	
156635	Boundary Cell Mining Claim	2018-04-10	2022-12-24	
155374	Single Cell Mining Claim	2018-04-10	2022-07-09	2023-07-09
157444	Boundary Cell Mining Claim	2018-04-10	2027-03-10	
157445	Boundary Cell Mining Claim	2018-04-10	2027-03-10	
196436	Single Cell Mining Claim	2018-04-10	2022-07-09	2023-07-09
301632	Single Cell Mining Claim	2018-04-10	2022-07-09	2023-07-09

196437	Single Cell Mining Claim	2018-04-10	2022-07-09	2023-07-09
198410	Single Cell Mining Claim	2018-04-10	2023-07-09	2020-02-09
244494	Single Cell Mining Claim	2018-04-10	2023-07-09	2020-02-09
251064	Single Cell Mining Claim	2018-04-10	2022-07-09	2023-07-09
253080	Single Cell Mining Claim	2018-04-10	2022-07-09	2023-07-09
280081	Single Cell Mining Claim	2018-04-10	2023-07-09	2020-02-09
159095	Boundary Cell Mining Claim	2018-04-10	2022-07-09	2023-07-09
159096	Single Cell Mining Claim	2018-04-10	2022-07-09	2023-07-09
157974	Single Cell Mining Claim	2018-04-10	2022-12-24	
161431	Boundary Cell Mining Claim	2018-04-10	2027-03-10	
165590	Single Cell Mining Claim	2018-04-10	2022-12-24	
165591	Boundary Cell Mining Claim	2018-04-10	2022-12-24	
165592	Single Cell Mining Claim	2018-04-10	2022-12-24	
165718	Boundary Cell Mining Claim	2018-04-10	2022-07-09	2023-07-09
168610	Single Cell Mining Claim	2018-04-10	2022-07-09	2023-07-09
168645	Single Cell Mining Claim	2018-04-10	2022-07-09	2023-07-09
168646	Single Cell Mining Claim	2018-04-10	2022-07-09	2023-07-09
168659	Boundary Cell Mining Claim	2018-04-10	2019-12-05	
168597	Single Cell Mining Claim	2018-04-10	2022-07-09	2023-07-09
171307	Boundary Cell Mining Claim	2018-04-10	2022-07-09	2023-07-09
175691	Single Cell Mining Claim	2018-04-10	2022-12-24	
178149	Single Cell Mining Claim	2018-04-10	2022-12-24	
176916	Single Cell Mining Claim	2018-04-10	2023-07-09	

177097	Single Cell Mining Claim	2018-04-10	2022-12-24	
178434	Single Cell Mining Claim	2018-04-10	2022-12-24	
179599	Single Cell Mining Claim	2018-04-10	2022-07-09	2023-07-09
178706	Boundary Cell Mining Claim	2018-04-10	2022-12-24	
184517	Single Cell Mining Claim	2018-04-10	2022-12-24	
184274	Single Cell Mining Claim	2018-04-10	2023-07-09	
183446	Boundary Cell Mining Claim	2018-04-10	2019-12-05	
186435	Single Cell Mining Claim	2018-04-10	2023-07-09	
185736	Single Cell Mining Claim	2018-04-10	2022-07-09	2023-07-09
187047	Single Cell Mining Claim	2018-04-10	2022-07-09	2023-07-09
185492	Boundary Cell Mining Claim	2018-04-10	2022-12-24	
187840	Single Cell Mining Claim	2018-04-10	2022-12-24	
187841	Boundary Cell Mining Claim	2018-04-10	2022-12-24	
196402	Single Cell Mining Claim	2018-04-10	2022-07-09	2023-07-09
196559	Single Cell Mining Claim	2018-04-10	2022-12-24	
196438	Single Cell Mining Claim	2018-04-10	2022-07-09	2023-07-09
196439	Single Cell Mining Claim	2018-04-10	2023-07-09	
196440	Single Cell Mining Claim	2018-04-10	2023-07-09	
196441	Single Cell Mining Claim	2018-04-10	2022-07-09	2023-07-09
194860	Boundary Cell Mining Claim	2018-04-10	2022-12-24	
194861	Single Cell Mining Claim	2018-04-10	2022-12-24	
194862	Single Cell Mining Claim	2018-04-10	2022-12-24	
198575	Boundary Cell Mining Claim	2018-04-10	2022-07-09	2023-07-09

198596	Boundary Cell Mining Claim	2018-04-10	2019-12-05	
199340	Boundary Cell Mining Claim	2018-04-10	2019-12-05	
200667	Single Cell Mining Claim	2018-04-10	2022-07-09	2023-07-09
200668	Boundary Cell Mining Claim	2018-04-10	2022-07-09	2023-07-09
200004	Single Cell Mining Claim	2018-04-10	2022-07-09	2023-07-09
199748	Single Cell Mining Claim	2018-04-10	2022-07-09	2023-07-09
205753	Boundary Cell Mining Claim	2018-04-10	2023-07-09	
208029	Single Cell Mining Claim	2018-04-10	2022-07-09	2023-07-09
206595	Single Cell Mining Claim	2018-04-10	2022-07-09	2023-07-09
206609	Boundary Cell Mining Claim	2018-04-10	2019-12-05	
206047	Single Cell Mining Claim	2018-04-10	2022-07-09	2023-07-09
206048	Boundary Cell Mining Claim	2018-04-10	2022-07-09	2023-07-09
209603	Boundary Cell Mining Claim	2018-04-10	2019-12-05	
208594	Single Cell Mining Claim	2018-04-10	2022-07-09	2023-07-09
208595	Single Cell Mining Claim	2018-04-10	2022-07-09	2023-07-09
209280	Single Cell Mining Claim	2018-04-10	2022-12-24	
210630	Single Cell Mining Claim	2018-04-10	2022-12-24	
210631	Single Cell Mining Claim	2018-04-10	2022-12-24	
340441	Single Cell Mining Claim	2018-04-10	2022-07-09	2023-07-09
318504	Single Cell Mining Claim	2018-04-10	2022-07-09	2023-07-09
213499	Single Cell Mining Claim	2018-04-10	2022-12-24	
213500	Single Cell Mining Claim	2018-04-10	2022-12-24	
213596	Single Cell Mining Claim	2018-04-10	2022-07-09	2023-07-09

214472	Boundary Cell Mining Claim	2018-04-10	2023-12-24	
213616	Single Cell Mining Claim	2018-04-10	2022-07-09	2023-07-09
219436	Single Cell Mining Claim	2018-04-10	2023-12-24	
219437	Boundary Cell Mining Claim	2018-04-10	2023-12-24	
220165	Single Cell Mining Claim	2018-04-10	2023-07-09	
220100	Single Cell Mining Claim	2018-04-10	2022-07-09	2023-07-09
223263	Boundary Cell Mining Claim	2018-04-10	2019-12-05	
224489	Single Cell Mining Claim	2018-04-10	2023-07-09	
225000	Single Cell Mining Claim	2018-04-10	2022-12-24	
225001	Single Cell Mining Claim	2018-04-10	2022-12-24	
225277	Boundary Cell Mining Claim	2018-04-10	2022-12-24	
227499	Boundary Cell Mining Claim	2018-04-10	2019-12-05	
232302	Single Cell Mining Claim	2018-04-10	2022-12-24	
229642	Boundary Cell Mining Claim	2018-04-10	2027-03-10	
233283	Boundary Cell Mining Claim	2018-04-10	2022-12-24	
232475	Single Cell Mining Claim	2018-04-10	2022-07-09	2023-07-09
237884	Boundary Cell Mining Claim	2018-04-10	2022-07-09	2023-07-09
237765	Single Cell Mining Claim	2018-04-10	2022-07-09	2023-07-09
237766	Single Cell Mining Claim	2018-04-10	2022-07-09	2023-07-09
237875	Single Cell Mining Claim	2018-04-10	2022-12-24	
237876	Boundary Cell Mining Claim	2018-04-10	2022-12-24	
243755	Boundary Cell Mining Claim	2018-04-10	2022-12-24	
243756	Boundary Cell Mining Claim	2018-04-10	2022-12-24	

242988	Single Cell Mining Claim	2018-04-10	2022-07-09	2023-07-09
242989	Single Cell Mining Claim	2018-04-10	2022-07-09	2023-07-09
242990	Single Cell Mining Claim	2018-04-10	2022-07-09	2023-07-09
243138	Single Cell Mining Claim	2018-04-10	2022-12-24	
243428	Boundary Cell Mining Claim	2018-04-10	2019-12-05	
244495	Single Cell Mining Claim	2018-04-10	2023-07-09	
244496	Single Cell Mining Claim	2018-04-10	2023-07-09	
246311	Single Cell Mining Claim	2018-04-10	2022-07-09	2023-07-09
245459	Single Cell Mining Claim	2018-04-10	2022-12-24	
245460	Boundary Cell Mining Claim	2018-04-10	2022-12-24	
245186	Boundary Cell Mining Claim	2018-04-10	2023-07-09	
245809	Single Cell Mining Claim	2018-04-10	2022-07-09	2023-07-09
252795	Boundary Cell Mining Claim	2018-04-10	2022-12-24	
253800	Single Cell Mining Claim	2018-04-10	2022-07-09	2023-07-09
255916	Single Cell Mining Claim	2018-04-10	2022-12-24	
253783	Single Cell Mining Claim	2018-04-10	2022-07-09	2023-07-09
253784	Single Cell Mining Claim	2018-04-10	2022-07-09	2023-07-09
253785	Boundary Cell Mining Claim	2018-04-10	2022-07-09	2023-07-09
253927	Boundary Cell Mining Claim	2018-04-10	2022-12-24	
255820	Boundary Cell Mining Claim	2018-04-10	2022-07-09	2023-07-09
254379	Boundary Cell Mining Claim	2018-04-10	2022-07-09	2023-07-09
254441	Boundary Cell Mining Claim	2018-04-10	2023-12-24	
255167	Single Cell Mining Claim	2018-04-10	2022-07-09	2023-07-09

257261	Boundary Cell Mining Claim	2018-04-10	2022-12-24	
257306	Boundary Cell Mining Claim	2018-04-10	2022-12-24	
257309	Single Cell Mining Claim	2018-04-10	2022-07-09	2023-07-09
258634	Single Cell Mining Claim	2018-04-10	2022-12-24	
260330	Single Cell Mining Claim	2018-04-10	2022-07-09	2023-07-09
260331	Single Cell Mining Claim	2018-04-10	2022-07-09	2023-07-09
261475	Single Cell Mining Claim	2018-04-10	2022-12-24	
261476	Single Cell Mining Claim	2018-04-10	2022-12-24	
262045	Boundary Cell Mining Claim	2018-04-10	2027-03-10	
264552	Single Cell Mining Claim	2018-04-10	2022-07-09	2023-07-09
265321	Single Cell Mining Claim	2018-04-10	2022-07-09	2023-07-09
265861	Single Cell Mining Claim	2018-04-10	2022-07-09	2023-07-09
269684	Boundary Cell Mining Claim	2018-04-10	2022-07-09	2023-07-09
265874	Boundary Cell Mining Claim	2018-04-10	2019-12-05	
265875	Boundary Cell Mining Claim	2018-04-10	2019-12-05	
268957	Boundary Cell Mining Claim	2018-04-10	2022-12-24	
268958	Single Cell Mining Claim	2018-04-10	2022-12-24	
272555	Single Cell Mining Claim	2018-04-10	2022-07-09	2023-07-09
272556	Single Cell Mining Claim	2018-04-10	2022-07-09	2023-07-09
272557	Single Cell Mining Claim	2018-04-10	2023-07-09	
272567	Single Cell Mining Claim	2018-04-10	2022-07-09	2023-07-09
272568	Boundary Cell Mining Claim	2018-04-10	2022-07-09	2023-07-09
272601	Single Cell Mining Claim	2018-04-10	2022-07-09	2023-07-09

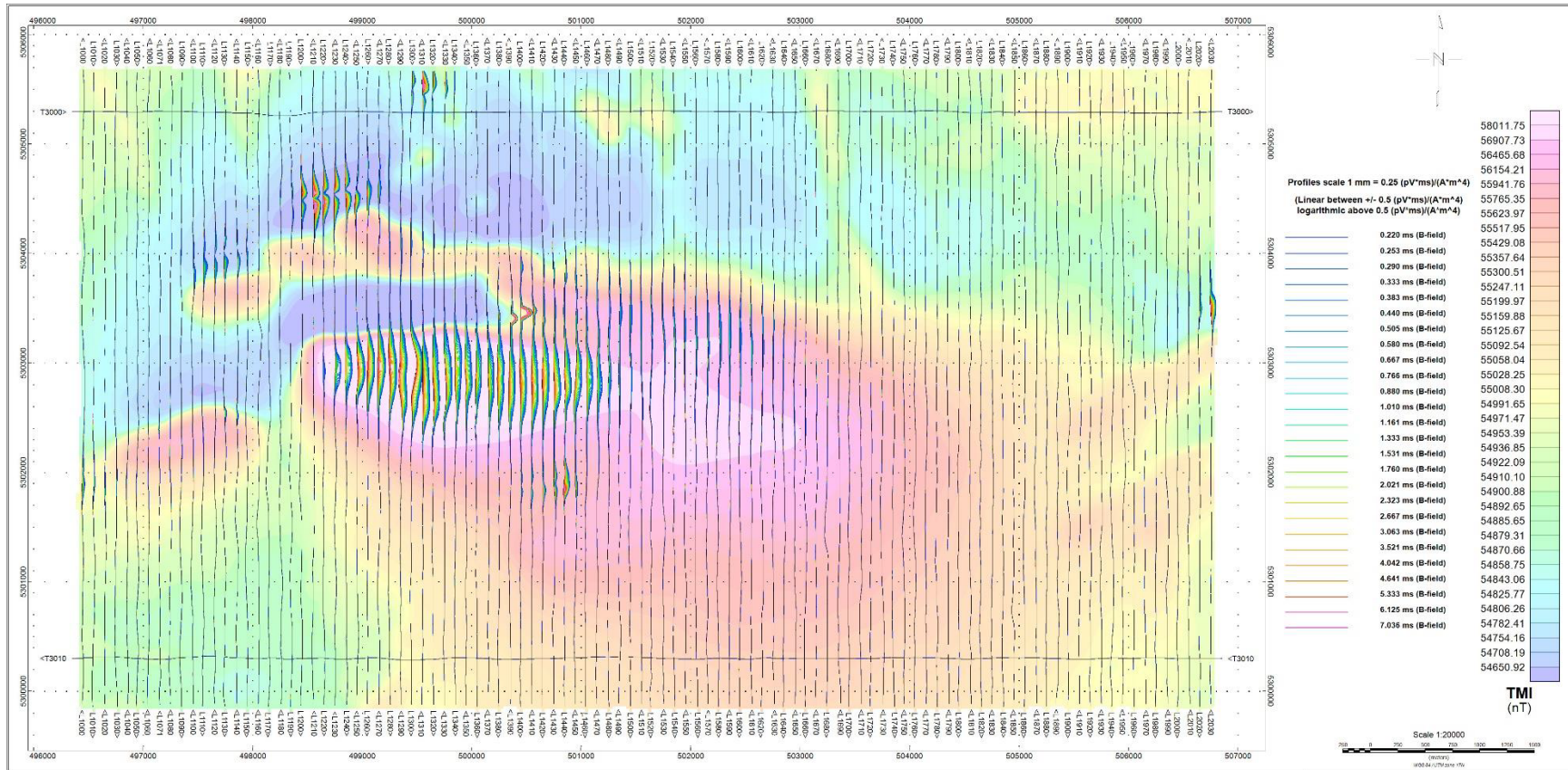
269908	Single Cell Mining Claim	2018-04-10	2022-12-24	
269909	Single Cell Mining Claim	2018-04-10	2022-12-24	
270526	Boundary Cell Mining Claim	2018-04-10	2022-12-24	
274670	Boundary Cell Mining Claim	2018-04-10	2022-07-09	2023-07-09
276593	Single Cell Mining Claim	2018-04-10	2022-12-24	
276594	Single Cell Mining Claim	2018-04-10	2022-12-24	
273343	Boundary Cell Mining Claim	2018-04-10	2019-12-05	
275258	Boundary Cell Mining Claim	2018-04-10	2022-07-09	2023-07-09
280049	Single Cell Mining Claim	2018-04-10	2022-07-09	2023-07-09
280080	Single Cell Mining Claim	2018-04-10	2022-07-09	2023-07-09
280462	Single Cell Mining Claim	2018-04-10	2022-07-09	2023-07-09
280843	Boundary Cell Mining Claim	2018-04-10	2022-12-24	
280844	Boundary Cell Mining Claim	2018-04-10	2022-12-24	
280845	Single Cell Mining Claim	2018-04-10	2022-12-24	
280846	Boundary Cell Mining Claim	2018-04-10	2022-12-24	
281022	Boundary Cell Mining Claim	2018-04-10	2022-12-24	
282758	Single Cell Mining Claim	2018-04-10	2023-07-09	
289565	Single Cell Mining Claim	2018-04-10	2022-07-09	2023-07-09
294520	Boundary Cell Mining Claim	2018-04-10	2019-12-05	
296201	Boundary Cell Mining Claim	2018-04-10	2027-03-10	
294130	Boundary Cell Mining Claim	2018-04-10	2019-12-05	
299139	Boundary Cell Mining Claim	2018-04-10	2022-07-09	2023-07-09
299140	Single Cell Mining Claim	2018-04-10	2023-07-09	

299591	Single Cell Mining Claim	2018-04-10	2022-07-09	2023-07-09
298123	Single Cell Mining Claim	2018-04-10	2022-07-09	2023-07-09
299620	Single Cell Mining Claim	2018-04-10	2022-07-09	2023-07-09
300453	Single Cell Mining Claim	2018-04-10	2022-12-24	
298160	Single Cell Mining Claim	2018-04-10	2022-07-09	2023-07-09
302413	Single Cell Mining Claim	2018-04-10	2022-07-09	2023-07-09
303870	Single Cell Mining Claim	2018-04-10	2022-07-09	2023-07-09
304469	Boundary Cell Mining Claim	2018-04-10	2019-12-05	
303215	Boundary Cell Mining Claim	2018-04-10	2022-12-24	
301631	Single Cell Mining Claim	2018-04-10	2022-07-09	2023-07-09
301633	Single Cell Mining Claim	2018-04-10	2022-07-09	2023-07-09
304575	Single Cell Mining Claim	2018-04-10	2022-12-24	
302939	Single Cell Mining Claim	2018-04-10	2022-07-09	2023-07-09
311269	Single Cell Mining Claim	2018-04-10	2022-07-09	2023-07-09
311870	Single Cell Mining Claim	2018-04-10	2022-12-24	
311871	Boundary Cell Mining Claim	2018-04-10	2022-12-24	
313208	Single Cell Mining Claim	2018-04-10	2022-12-24	
317147	Single Cell Mining Claim	2018-04-10	2022-12-24	
317148	Boundary Cell Mining Claim	2018-04-10	2022-12-24	
317603	Single Cell Mining Claim	2018-04-10	2022-07-09	2023-07-09
320357	Single Cell Mining Claim	2018-04-10	2022-07-09	2023-07-09
319814	Single Cell Mining Claim	2018-04-10	2022-07-09	2023-07-09
319815	Single Cell Mining Claim	2018-04-10	2022-07-09	2023-07-09

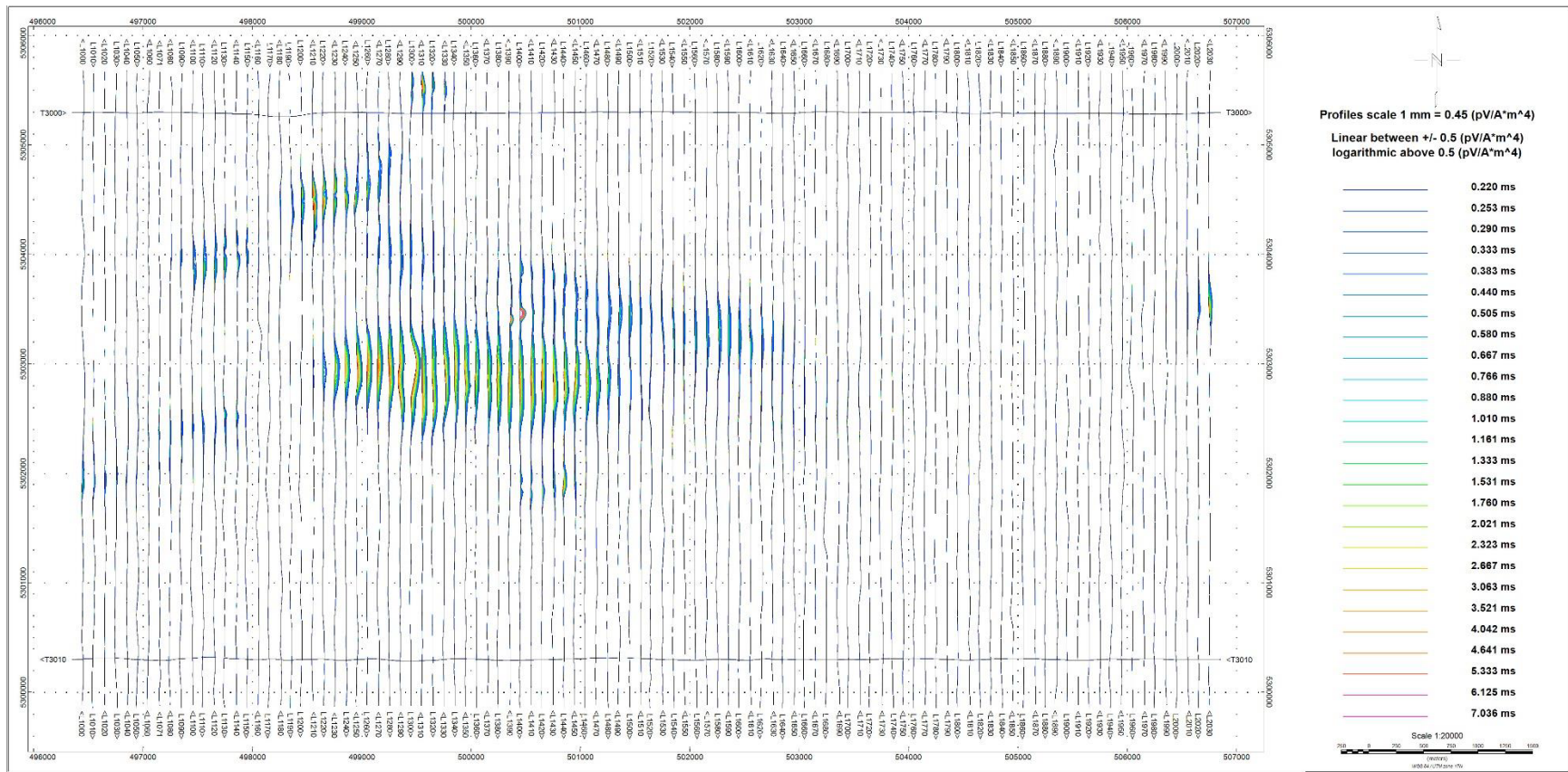
319822	Boundary Cell Mining Claim	2018-04-10	2019-12-05	
320538	Boundary Cell Mining Claim	2018-04-10	2019-12-05	
322628	Boundary Cell Mining Claim	2018-04-10	2022-12-24	
321922	Single Cell Mining Claim	2018-04-10	2023-07-09	
321923	Boundary Cell Mining Claim	2018-04-10	2023-07-09	
321942	Single Cell Mining Claim	2018-04-10	2022-07-09	2023-07-09
321943	Boundary Cell Mining Claim	2018-04-10	2022-07-09	2023-07-09
321944	Boundary Cell Mining Claim	2018-04-10	2022-07-09	2023-07-09
321975	Single Cell Mining Claim	2018-04-10	2022-07-09	2023-07-09
321982	Boundary Cell Mining Claim	2018-04-10	2019-12-05	
324597	Single Cell Mining Claim	2018-04-10	2022-12-24	
324598	Single Cell Mining Claim	2018-04-10	2022-12-24	
324608	Single Cell Mining Claim	2018-04-10	2022-07-09	2023-07-09
328119	Single Cell Mining Claim	2018-04-10	2022-12-24	
325938	Single Cell Mining Claim	2018-04-10	2022-12-24	
325939	Single Cell Mining Claim	2018-04-10	2022-12-24	
330481	Single Cell Mining Claim	2018-04-10	2022-12-24	
345030	Boundary Cell Mining Claim	2018-04-10	2019-12-05	
345052	Boundary Cell Mining Claim	2018-04-10	2019-12-05	
340271	Single Cell Mining Claim	2018-04-10	2022-12-24	
339755	Boundary Cell Mining Claim	2018-04-10	2022-12-24	
333323	Single Cell Mining Claim	2018-04-10	2022-07-09	2023-07-09
333331	Single Cell Mining Claim	2018-04-10	2022-07-09	2023-07-09

334508	Single Cell Mining Claim	2018-04-10	2022-07-09	2023-07-09
334509	Single Cell Mining Claim	2018-04-10	2022-07-09	2023-07-09
331220	Boundary Cell Mining Claim	2018-04-10	2022-07-09	2023-07-09
680181	Single Cell Mining Claim	2021-10-04	2023-10-04	

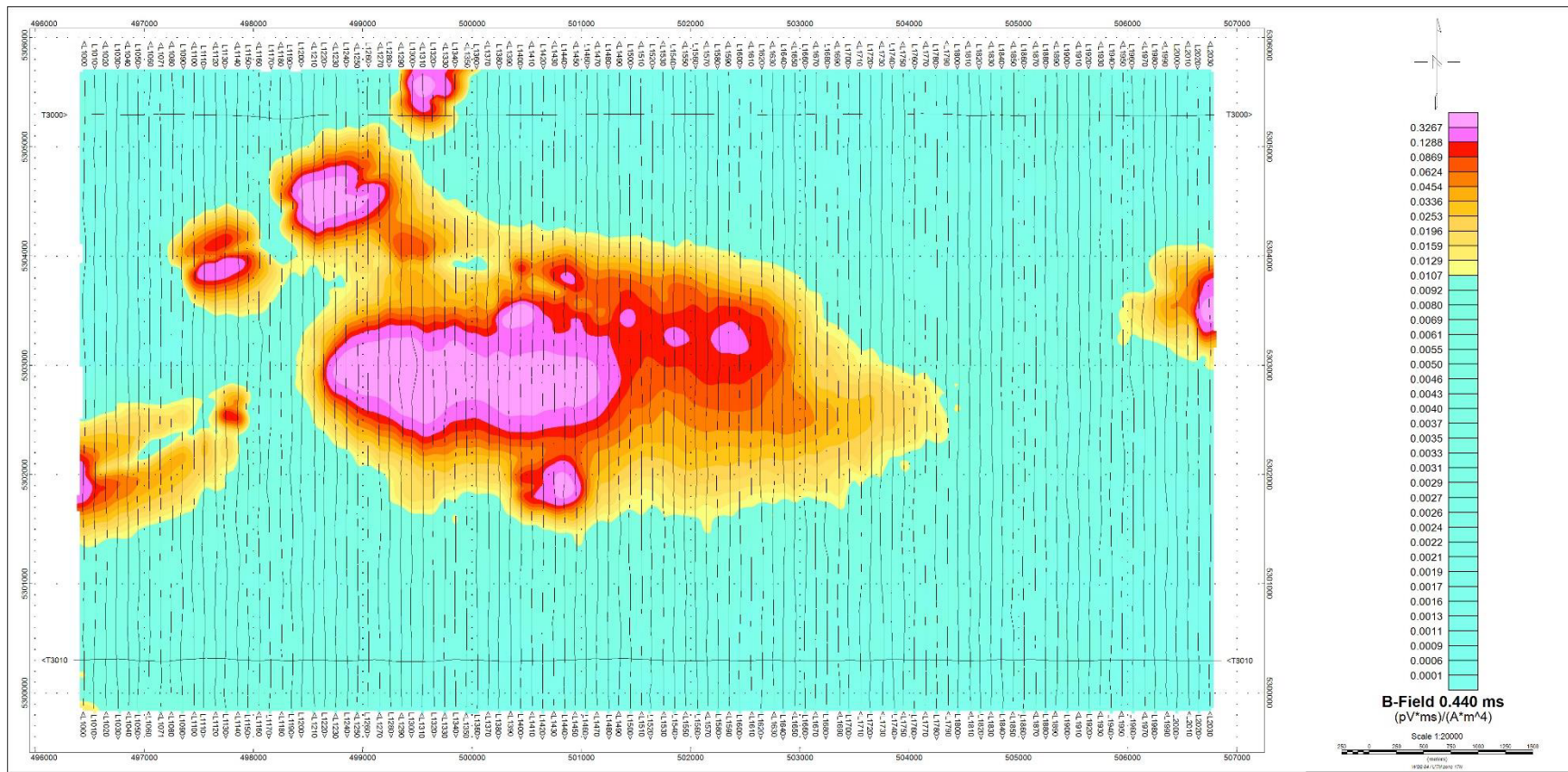
APPENDIX B – GEOPHYSICAL MAPS



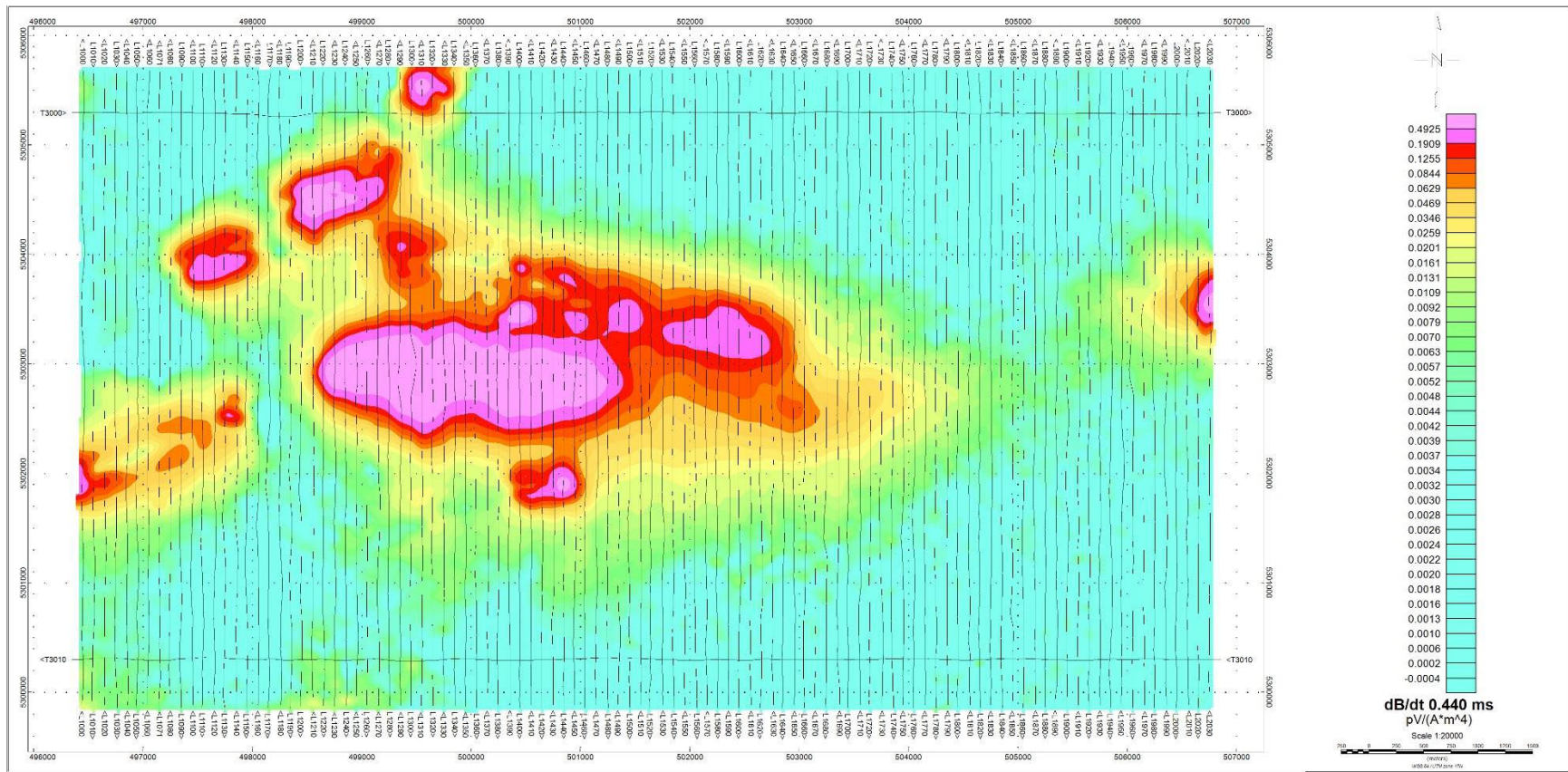
Z Component B-field profiles, Time Gates 0.220 – 7.036 ms over TMI colour image



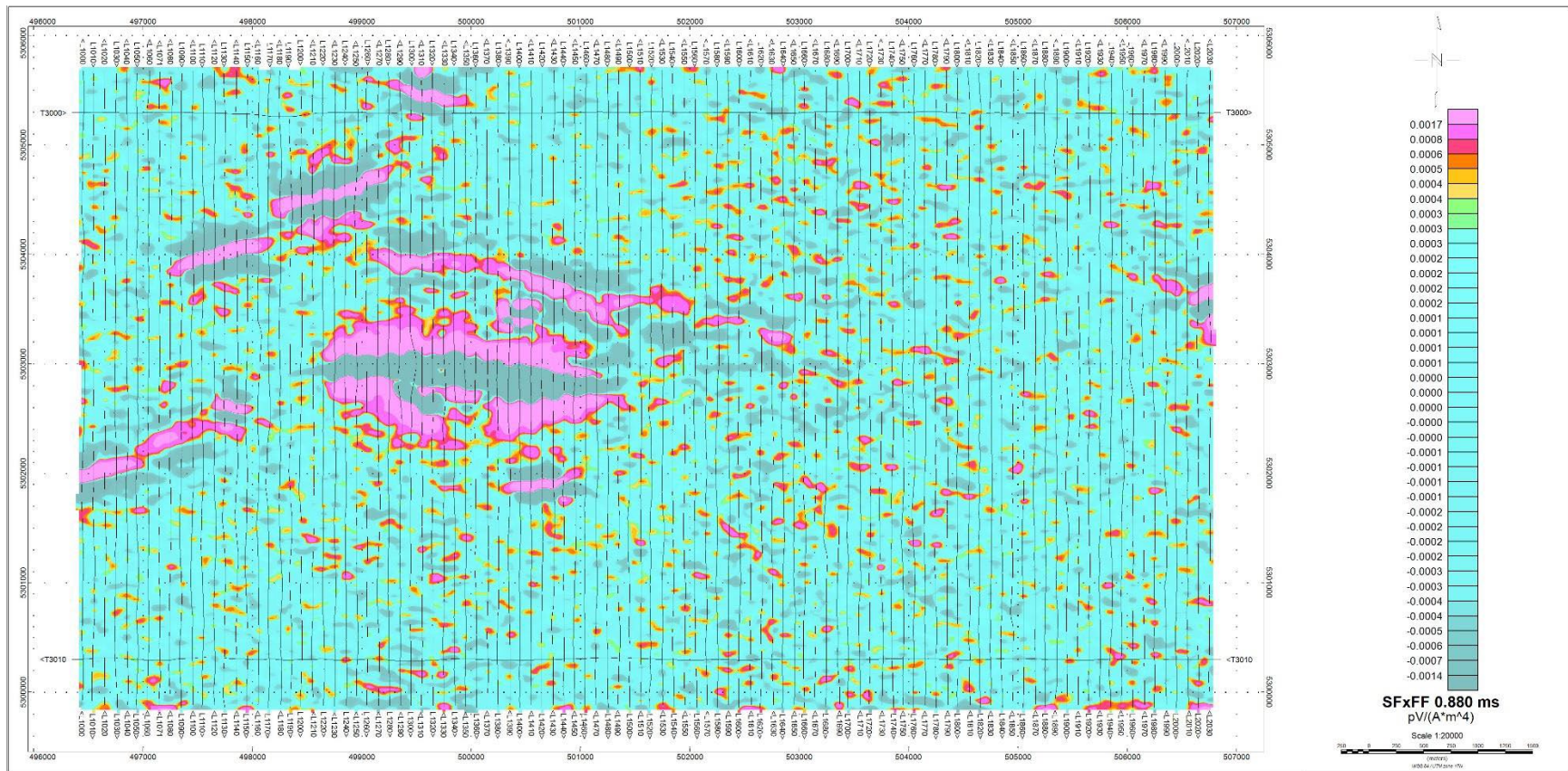
Z Component dB/dt profiles, Time Gates 0.220 – 7.036 ms



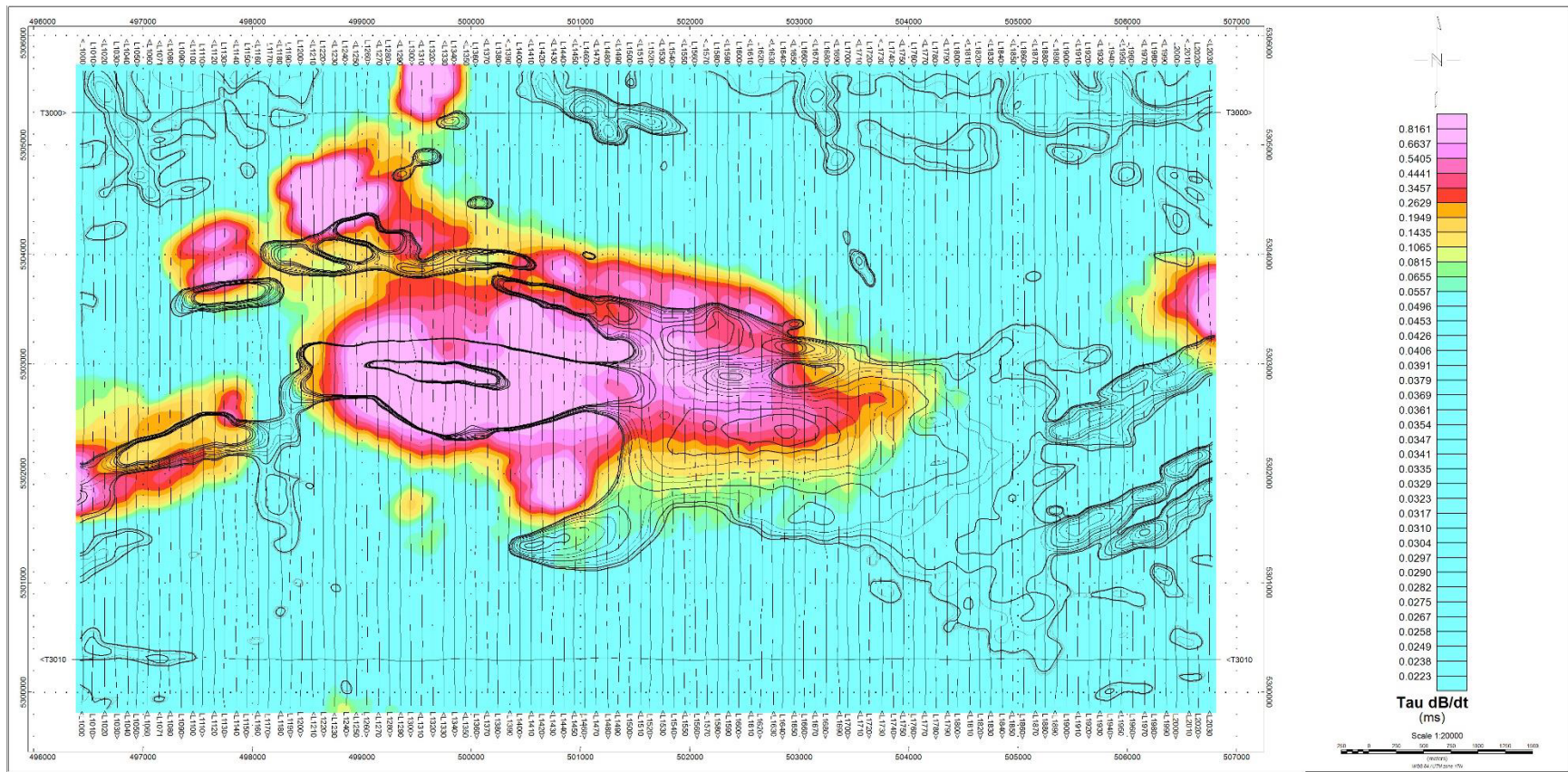
B-field Z Component Channel 25, Time Gate 0.440 ms colour image



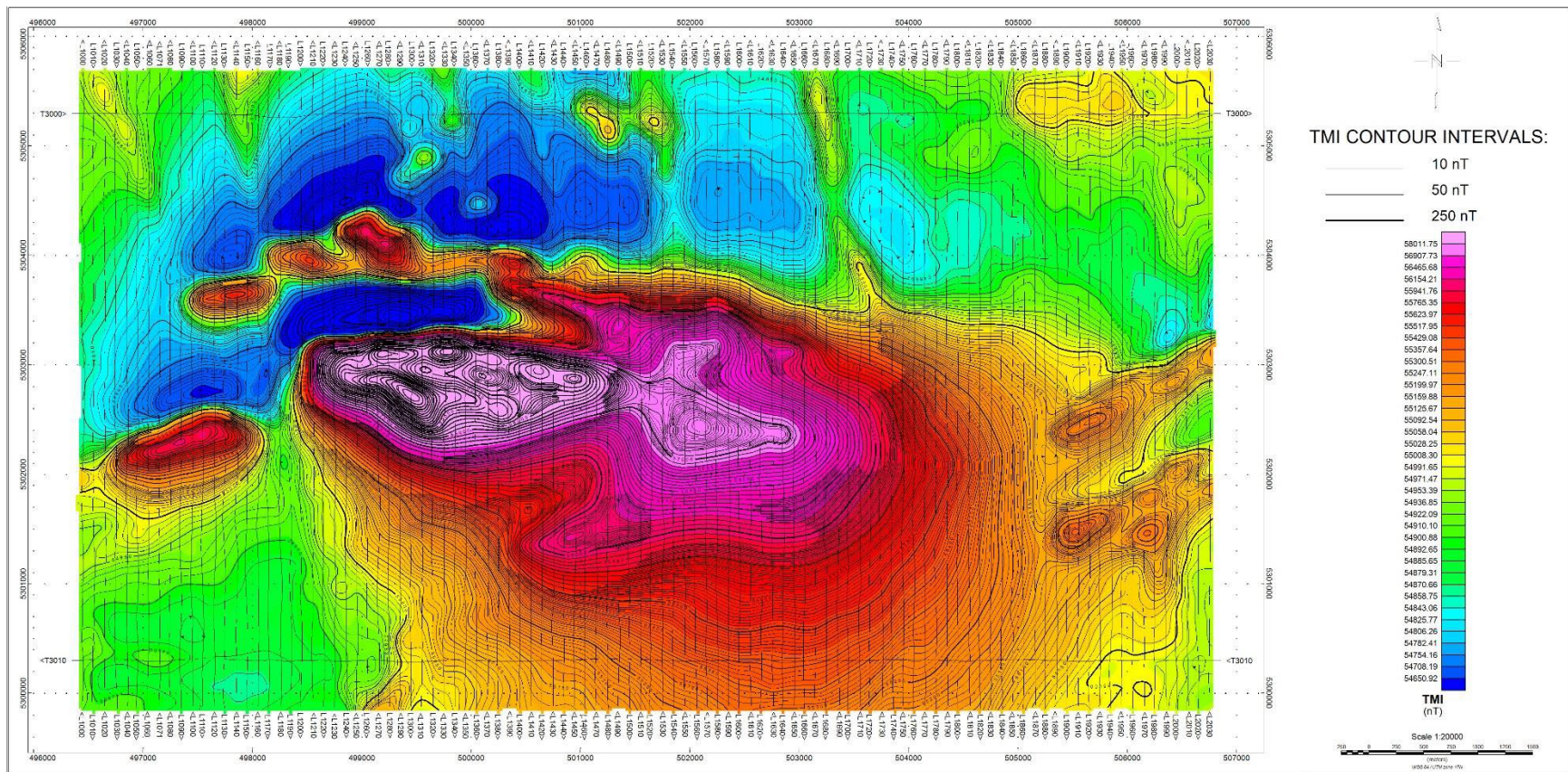
VTEM dB/dt Z Component Channel 25, Time Gate 0.440 ms colour image



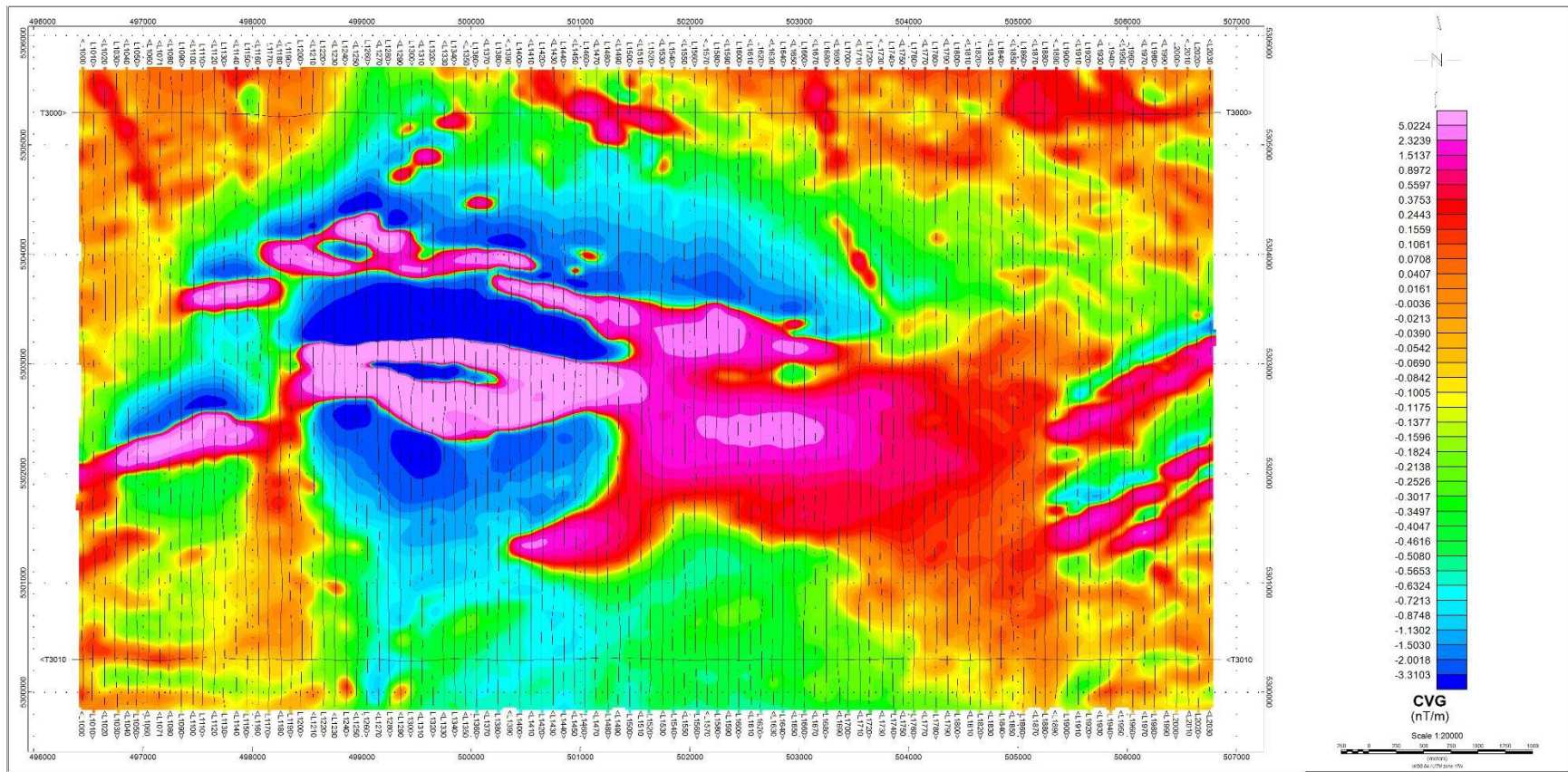
Fraser Filtered dB/dt X Component Channel 30, Time Gate 0.880 ms colour image



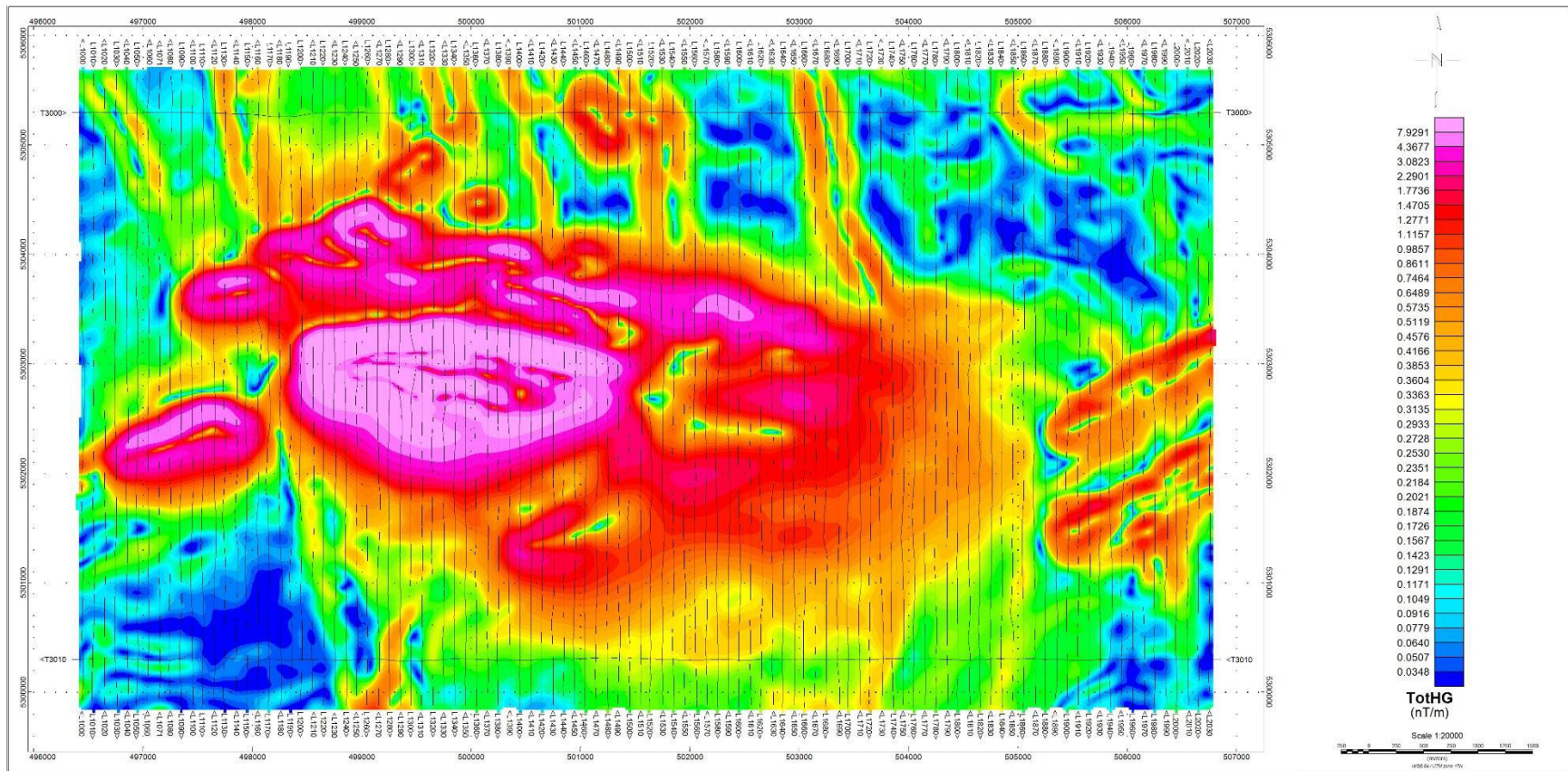
dB/dT Z-Component Calculated Time Constant (Tau) with Calculated Vertical Gradient (CVG) contours



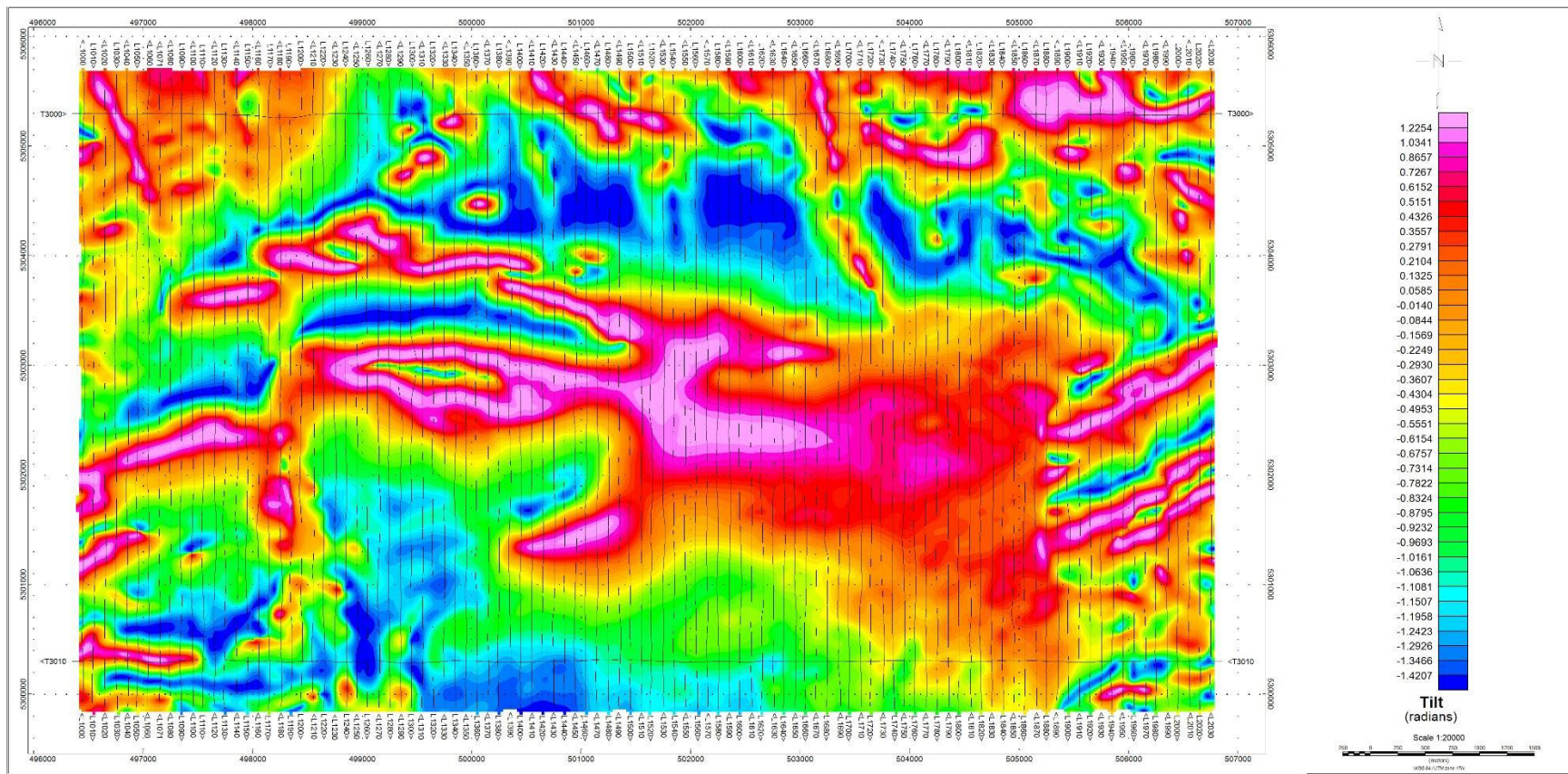
Total Magnetic Intensity (TMI) colour image and contours



Calculated Vertical Gradient (CVG)

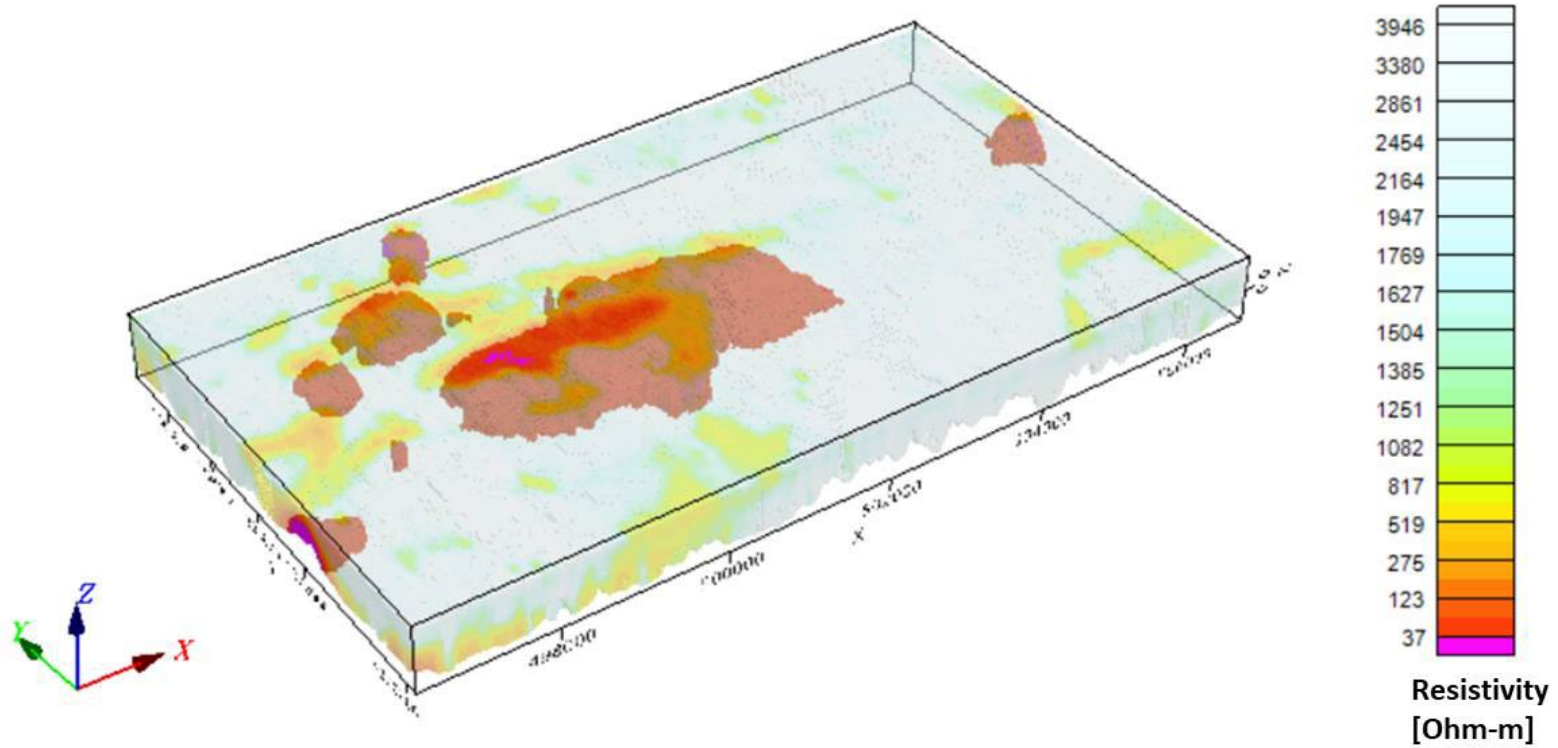


Magnetic Total Horizontal Gradient colour image



Magnetic Tilt Angle Derivative colour image

3D View of GL210350 Canada Nickel Midlothain Block



3D view of Resistivity-Depth-Image (RDI), Apparent Resistivity Voxel

APPENDIX C. GENERALIZED MODELING OF THE VTEM SYSTEM

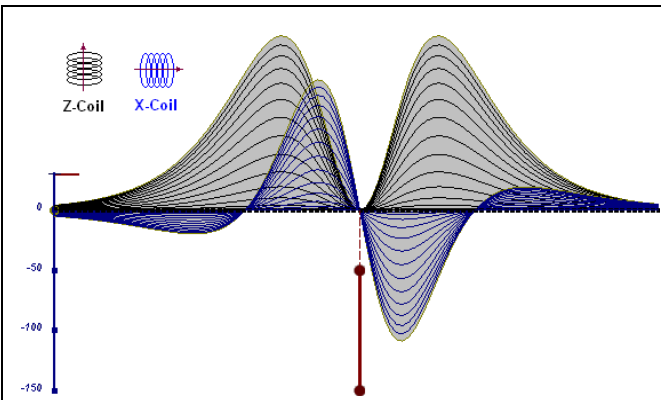


Figure C-1: vertical thin plate

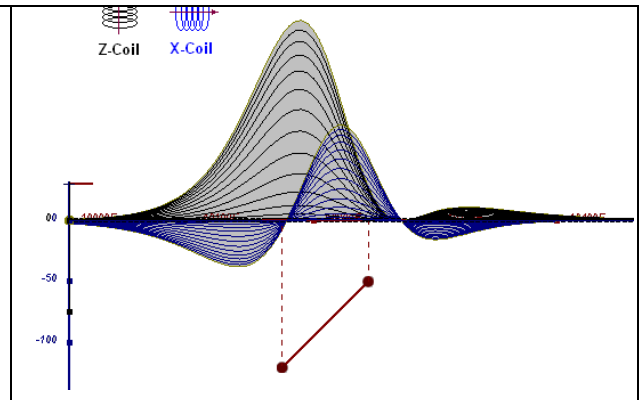


Figure C-2: inclined thin plate

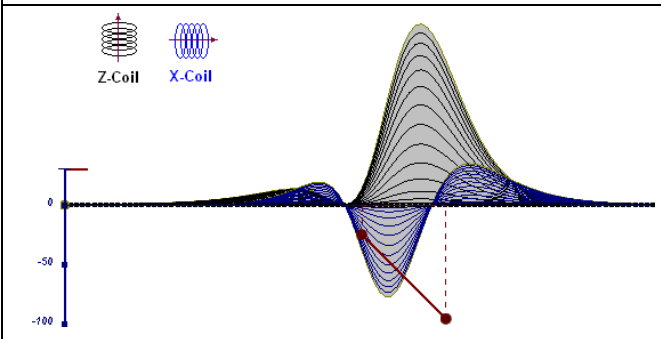


Figure C-3: inclined thin plate

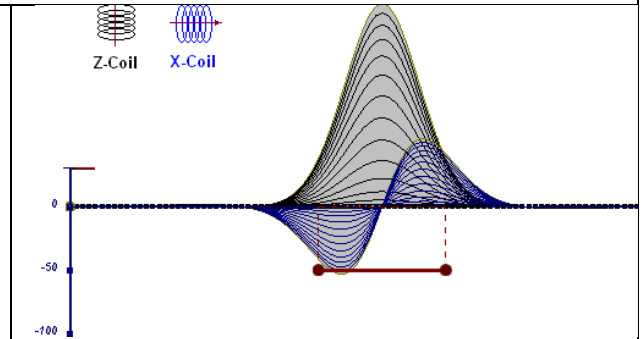


Figure C-4: horizontal thin plate

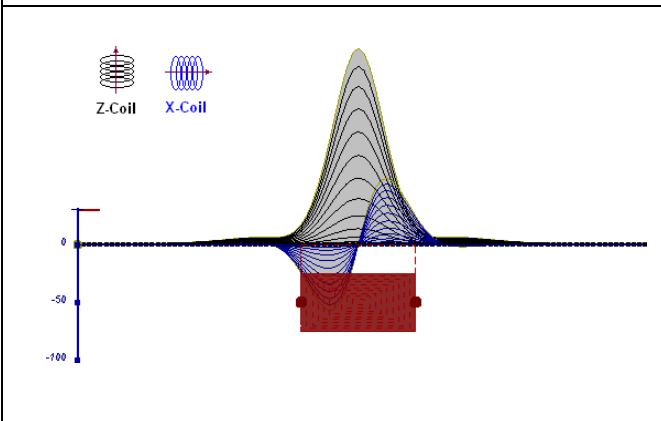


Figure C-5: horizontal thick plate (linear scale of the response)

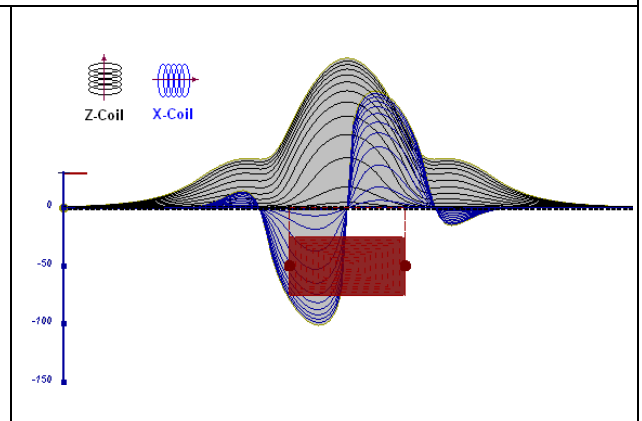


Figure C-6: horizontal thick plate (log scale of the response)

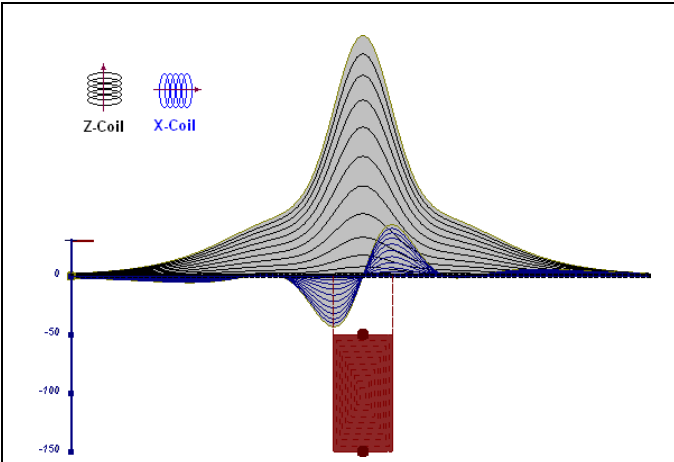


Figure C-7: vertical thick plate (linear scale of the response). 50 m depth

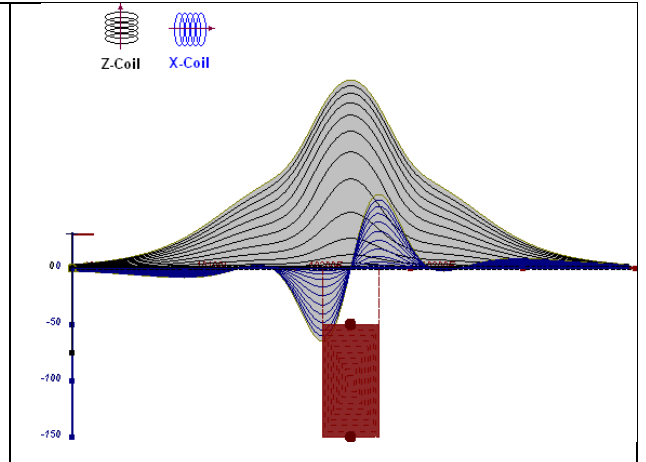


Figure C-8: vertical thick plate (log scale of the response). 50 m depth

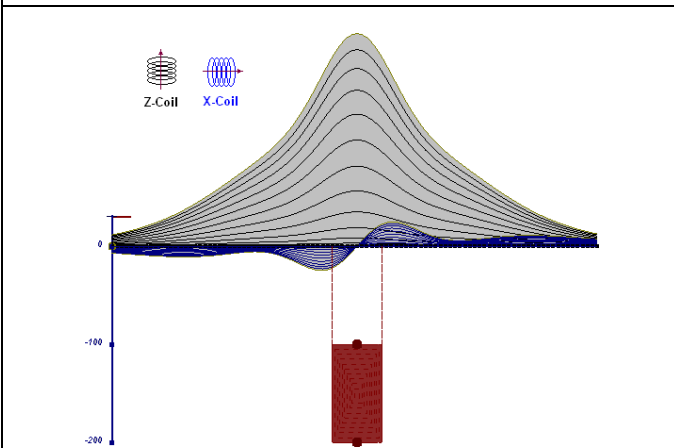


Figure C-9: vertical thick plate (linear scale of the response). 100 m depth

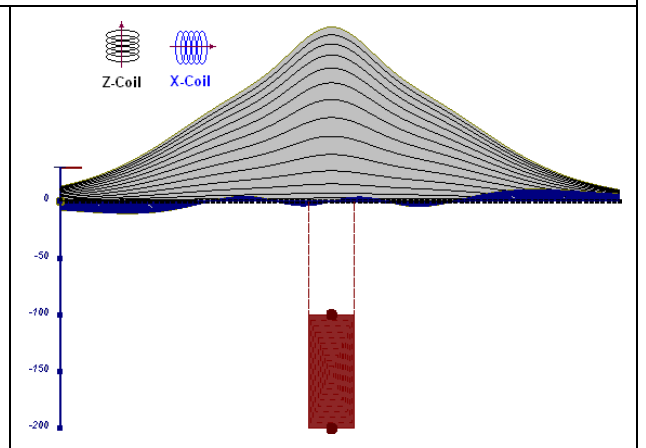


Figure C-10: vertical thick plate (linear scale of the response). Depth / horizontal thickness=2.5

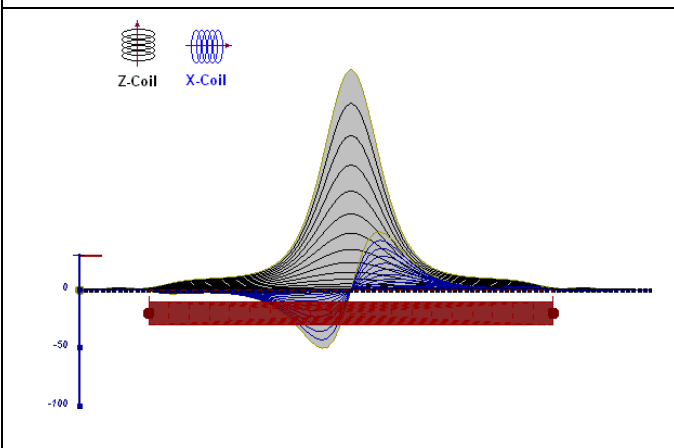


Figure C-11: horizontal thick plate (linear scale of the response)

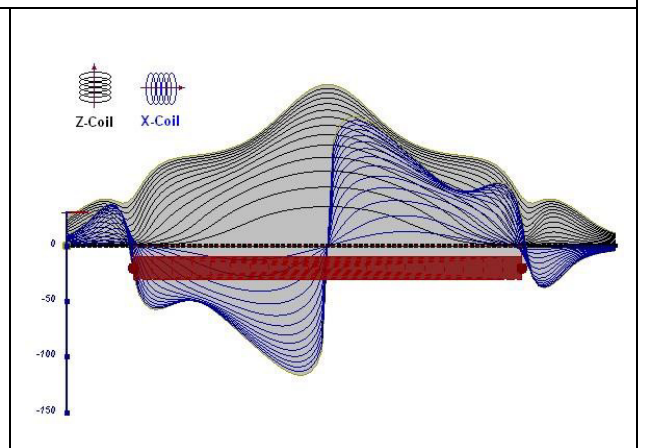


Figure C-12: horizontal thick plate (log scale of the response)

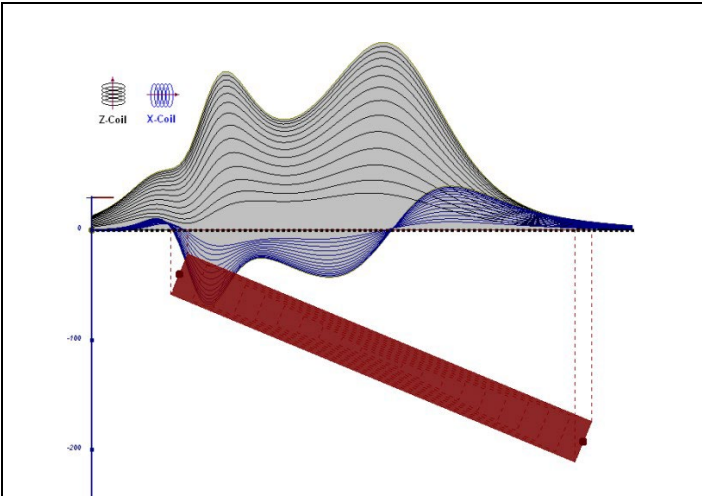


Figure C-13: inclined long thick plate

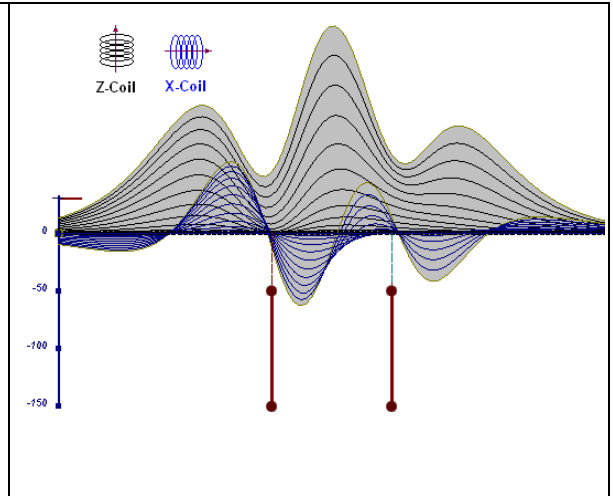


Figure C-14: two vertical thin plates

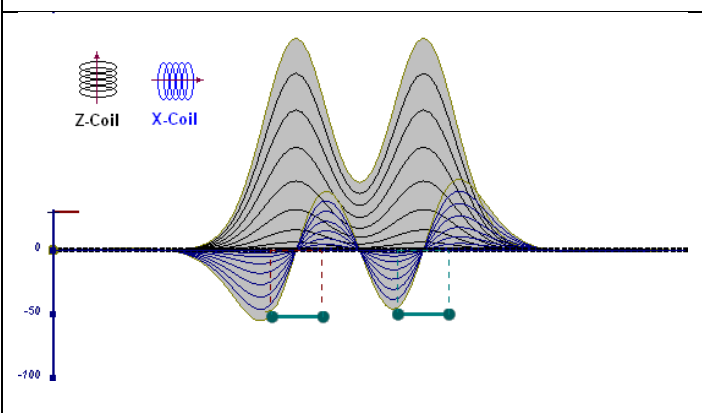


Figure C-15: two horizontal thin plates

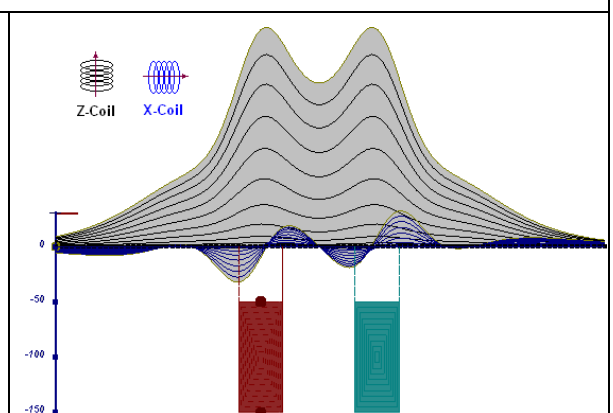


Figure C-16: two vertical thick plates

REPORT ON A FALCON® AIRBORNE GRAVITY
GRADIOMETER AND MAGNETOMETER SURVEY
MIDLOTHIAN PROJECT,
MIDLOTHIAN TOWNSHIP, ONTARIO, NTS 41P14 & 41P15



Project Name: Midlothian

Project Number: 2022-12-21

Client:  **CANADA NICKEL
COMPANY**

Contractor:  **Xcalibur**
MULTIPHYSICS

Date: December 21, 2022

Report Prepared by:

Steve Balch, P.Ge

And

Curtis Ferron, P.Ge

TABLE OF CONTENTS

EXECUTIVE SUMMARY	4
1.0 INTRODUCTION.....	5
1.1 CONTRACTOR	5
1.2 CLIENT	5
1.3 SURVEY OBJECTIVES.....	5
2.0 SURVEY AREA.....	5
2.1 LOCATION	5
2.2 ACCESS.....	5
2.3 INFRASTRUCTURE	5
2.4 CLIMATE	5
2.5 PHYSIOGRAPHY	7
2.6 MINERAL AND MINING CLAIMS.....	7
2.7 FLIGHT AND TIE LINES.....	7
2.8 DATUM AND PROJECTION	8
2.9 FIELD OPERATIONS	8
2.10 BASE STATIONS	8
2.10.1 GPS Base Station (Novatel OEM4)	8
2.10.2 Magnetometer Base station (CF1).....	8
2.11 FIELD PERSONNEL.....	8
3.0 EXPLORATION HISTORY	9
4.0 GEOLOGY	11
4.1 REGIONAL GEOLOGY	12
4.2 PROPERTY GEOLOGY	12
4.3 DEPOSIT GEOLOGY	12
5.0 DATA QUALITY CONTROL RESULTS.....	13
5.1 DATA RECORDING	13
5.2 DATA ACQUISITION.....	14
5.3 TURBULENCE	14
5.4 AGG SYSTEM NOISE.....	14
5.5 DIGITAL TERRAIN MODEL.....	15
5.6 DRAPE SURFACE DEVIATION	16
6.0 FALCON® AIRBORNE GRAVITY GRADIENT (AGG) RESULTS	16
6.1 PROCESSING SUMMARY	16
6.2 GRAVITY GRADIENT DATA	17
6.3 CONFORMED TO REGIONAL GRAVITY.....	20
7.0 AEROMAGNETIC RESULTS	21
7.1 PROCESSING SUMMARY	21
7.2 MAGNETIC DATA.....	21
8.0 INTERPRETATION AND CONCLUSIONS	24

9.0 REFERENCES	25
10.0 CERTIFICATE OF QUALIFICATIONS	26
STATEMENT OF QUALIFICATIONS	26
STATEMENT OF QUALIFICATIONS	27
APPENDIX I – SURVEY EQUIPMENT	28
SURVEY AIRCRAFT	28
FALCON AIRBORNE GRAVITY GRADIOMETER (AGG) SYSTEM (GALILEO)	28
DIGITAL ACQUISITION SYSTEM (FASDAS)	28
FALCON® AGG DATA ACQUISITION SYSTEM (ADAS)	28
AERIAL AND GROUND MAGNETOMETERS	28
REAL-TIME DIFFERENTIAL GPS	28
GPS BASE STATION RECEIVER	29
ALTIMETER.....	29
LASER SCANNER.....	29
DATA PROCESSING HARDWARE AND SOFTWARE	29
APPENDIX II – MINING CLAIMS DATA	30

FIGURES

Figure 1: Midlothian Project map showing location of geophysical survey area (blue) and property boundary (red).	6
Figure 2: Flight path map.	7
Figure 3: Midlothian Project bedrock geology map from: OGS report MRD 126 REV-1 1:250,000 Scale Bedrock Geology of Ontario.	11
Figure 4: Survey Turbulence (milli g where $g = 9.80665 \text{ m/sec}^2$).	13
Figure 5: System Noise NE Component (eotvos).	14
Figure 6: System Noise UV component (eotvos).	15
Figure 7: Final Digital Terrain Model (metres, referenced to the EGM96 geoid).	15
Figure 8: Deviation from drape surface (metres).	16
Figure 9: FALCON® AGG processing flowchart.	17
Figure 10: Enhanced Vertical Gravity Gradient (GDD) from Fourier processing (eotvos).	18
Figure 11: Enhanced Vertical Gravity (gD) from Fourier processing (milligal).	19
Figure 12: Enhanced Vertical Gravity (gD) from Fourier processing conformed to regional gravity data (milligal).	20
Figure 13: Aeromagnetic data processing flow chart.	21
Figure 14: Total Magnetic Intensity (TMI).	22
Figure 15: First Vertical Derivative of the Total Magnetic Intensity (nT/m).	23

TABLES

Table 1: Geophysical Survey Specifications	7
Table 2: Survey Field Personnel	8
Table 3: Ontario Assessment File Database (OAFD) Historical Exploration Work Completed at the Midlothian Project.	9
Table 4: List of mineral claims located on the Midlothian Project.	30

EXECUTIVE SUMMARY

Xcalibur Multiphysics was approached by Canada Nickel (the client) with the objective of conducting a gravity survey in order to gain information needed for detailed property scale targeting, with the ultimate goal of creating drill ready locations.

This report details the high-sensitivity aeromagnetic and FALCON[®] Airborne Gravity Gradiometer geophysical survey conducted, between July 31st and August 2nd, over the Midlothian Project located 23km WSW of Matachewan, Ontario.

The property consists of 272 contiguous mining claims centered around a potential bulk-tonnage magmatic nickel sulphide deposit. These Type II disseminated nickel sulphide deposits have unique geophysical characteristics due to the serpentinization process which liberates nickel from the mafic minerals, chiefly olivine found within ultramafic peridotite and dunite. This alteration process produces magnetite and an associated decrease in density which produces overlapping gravity lows with magnetic highs.

This survey was flown using the WGS-84 Datum. The projection is UTM, Zone 17 N. The survey successfully identified an approximately 3 km long by up to 800 m wide geophysical prospect that can now be confidently targeted due to the results of this study. The next steps for evaluating this target include but are not limited to a 10-hole ~4,000m diamond drill program with widely spaced holes, an airborne electromagnetic geophysical survey, and minor surface prospecting activities.

1.0 INTRODUCTION

This report details the high-sensitivity aeromagnetic and FALCON[®] Airborne Gravity Gradiometer (AGG) survey conducted over the Midlothian Project for Canada Nickel Company Inc. (“the Company” or “CNC”). The survey was completed by Xcalibur Multiphysics Ltd. (“Xcalibur”) between July 31st and August 2nd, 2022.

1.1 CONTRACTOR

The geophysical surveys were carried out by Xcalibur Multiphysics Ltd. (“Xcalibur”, the “Contractor”) having its head office at 2505 Meadowvale Boulevard, Mississauga, Ontario, Canada, L5N 5S2.

1.2 CLIENT

The client, Canada Nickel Company Inc., having its head office at 130 King Street West, Toronto, Ontario, Canada, M5X 1E3.

1.3 SURVEY OBJECTIVES

The objective of this survey is to delineate and evaluate ultramafic intrusions located on the property using the combination of density and magnetic properties of the survey area geology.

2.0 SURVEY AREA

2.1 LOCATION

The survey area centered at approximately 499750E, 5302990N (UTM Z 17N) contained within the NTS topographic sheet 041P, covered a 106 km² area approximately 23 km WSW of Matachewan, Ontario.

2.2 ACCESS

The property is accessible from Matachewan, Ontario by a series of logging roads. Follow Highway 566 west for 23 km’s then take a left (south) onto Wilson Lumber road. Follow Wilson for 14 km south until you reach the Asbestos Mine road, make a right and head west for 7 km until reaching the site.

2.3 INFRASTRUCTURE

Within the survey block there are few minor dirt roads and an abandoned open pit mine site at the approximate west-central portion of the survey area.

2.4 CLIMATE

The average daily temperature varies from a high of +24°C during July to a low of -10°C during January. Annual snowfall is approximately 41 cm and annual rainfall is 6 cm.

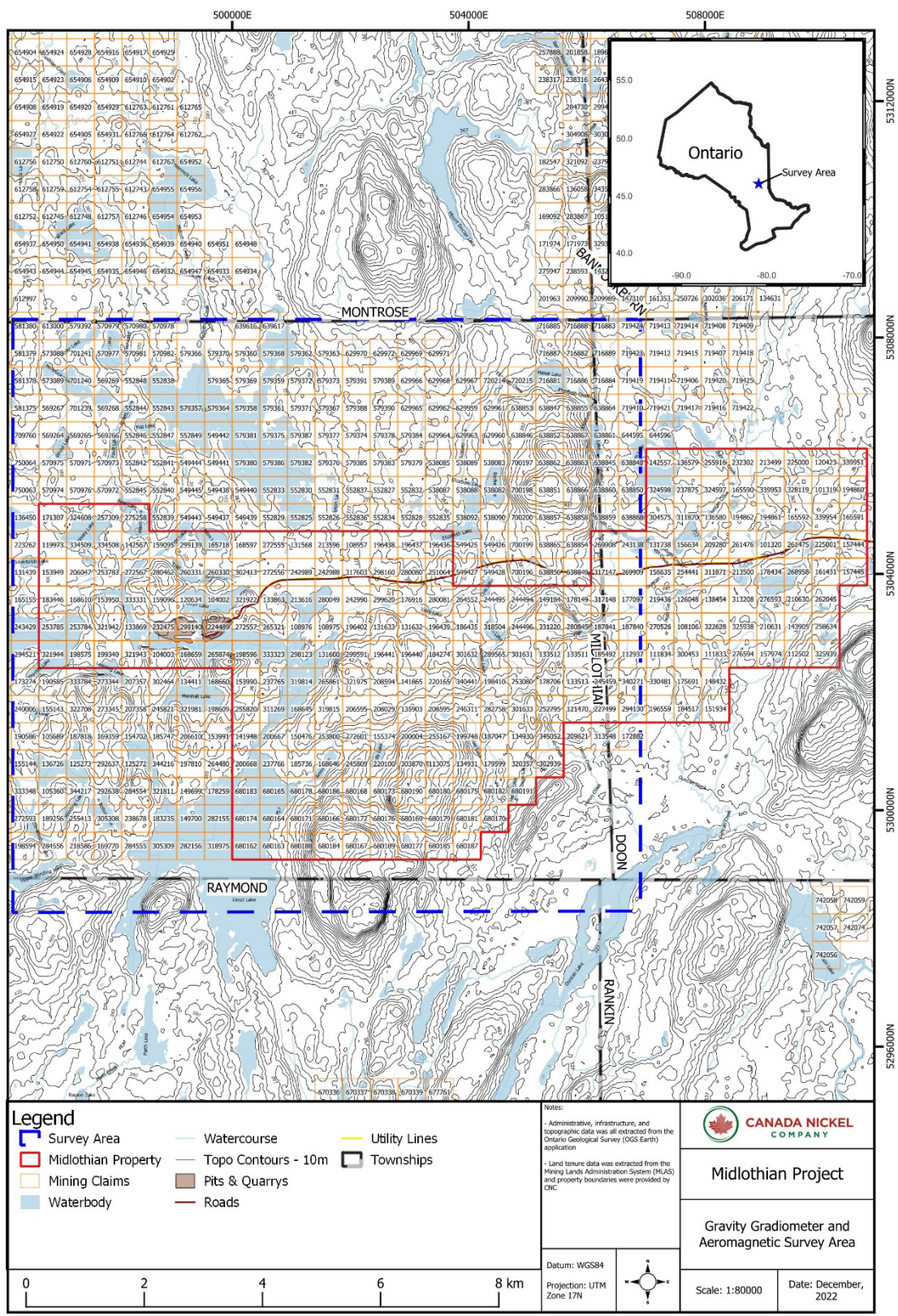


Figure 1: Midlothian Project map showing location of geophysical survey area (blue) and property boundary (red).

2.5 PHYSIOGRAPHY

The survey area physiography consists of rolling hills with some outcrop and a few lakes. Total topographic variation is ~162 m ranging from 336 m to 498 m for the ~106 square kilometer survey area.

2.6 MINERAL AND MINING CLAIMS

The property consists of 272 single cell mining claims (see Figure 1) optioned from Canadian Gold Miner Corp. (70% interest) and Laurion Mineral Exploration Inc. (30%) interest) to Canada Nickel Company (see CNC press release dated November 22, 2021).

2.7 FLIGHT AND TIE LINES

The survey consisted of a total of 1,166 total line km's, spaced 100m apart, oriented N-S, covering 106 km² with tie lines (E-W) every 1000m. The flight lines are shown in Figure 2 and summarized in Table 1.

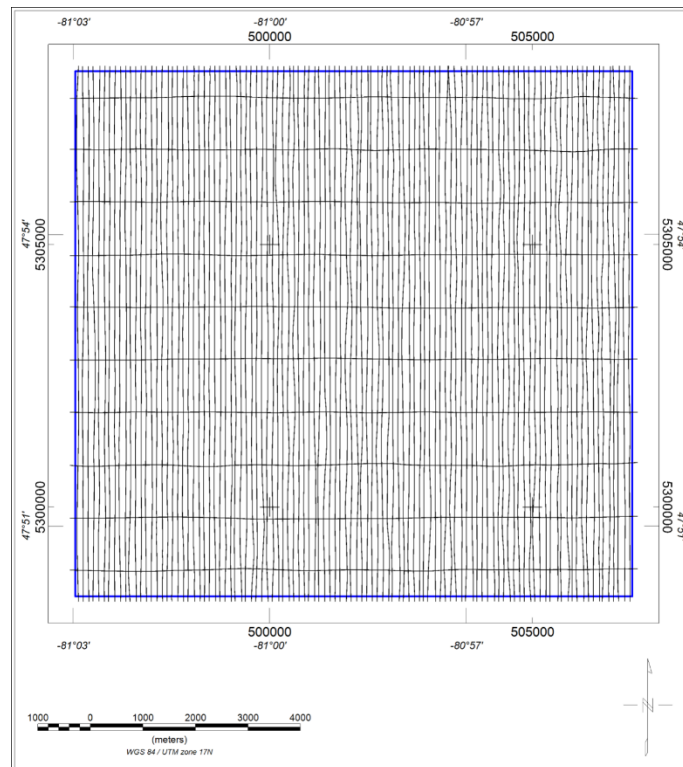


Figure 2: Flight path map.

Table 1: Geophysical Survey Specifications

Total Kilometres (km)	1,166
Clearance Method	Drape
Minimum Drape Height (m)	80
Traverse Line Direction (deg.)	000/180
Traverse Line Spacing (m)	100
Tie Line Direction (deg.)	090/270
Tie Line Spacing (m)	1000

2.8 DATUM AND PROJECTION

The survey was flown using the WGS-84 Datum. The Datum used to produce this report as well as the map products, grids and database is WGS-84. The projection is UTM, ZONE 17 N. All references to UTM coordinates in this report are based on the WGS-84 Datum.

2.9 FIELD OPERATIONS

The survey was based out of Timmins, Ontario. The survey aircraft was operated from Timmins Victor M. Power Airport using aviation fuel available on site. A temporary office was set up in Timmins where all survey operations were run, and the post-flight data verification was performed.

2.10 BASE STATIONS

A dual frequency GPS base station was set up to correct the raw GPS data collected in the aircraft. A secondary GPS base station was available but was not required.

2.10.1 GPS Base Station (Novatel OEM4)

Location: Timmins Victor M. Power Airport (ITRF 2014)

Date: July 25th, 2022

Latitude: 48° 34' 07.11379" N

Longitude: 81° 22' 09.30541" W

Height: 256.942 m ellipsoidal

2.10.2 Magnetometer Base station (CF1)

Location: Timmins Victor M. Power Airport

Date: July 25th, 2022

Used for flights: All

Base: 55,580 nT

2.11 FIELD PERSONNEL

The following technical personnel participated in field operations:

Table 2: Survey Field Personnel

Crew Leader:	D. Patzer
Pilots:	S. Parks, A. Gascoigne
AME:	D. Oystreck, P. van Schie
Technicians:	D. Patzer
Project Manager:	B. Robinson
QC and Processing:	J. Mohammed-Nour, P. Chambers

3.0 EXPLORATION HISTORY

Historical exploration activities completed at the Midlothian Project area are summarized in Table 3 below. The most recent exploration work was completed by Transition Metals Corp on behalf of Canadian Gold Miner (CGM) in 2017. The goal of this program was to test for the ‘Bjorkman Showing’ a precious metals occurrence near the northern contact of the main ultramafic body. Multiple short diamond drill holes were completed to test this mineral occurrence, and in the process, a better understanding of the property geology was gained. Refer to Table 3 for a summarized property exploration history acquired from the Ontario Assessment File Database (OAFD).

Table 3: Ontario Assessment File Database (OAFD) Historical Exploration Work Completed at the Midlothian Project.

Company	Year	File ID	Value of Work	Work Description
Transition Metals Corp	2017	20000015247	\$ 61,338.00	Diamond Drilling
Transition Metals Corp	2016	20000014020	\$ 85,836.00	Geological Survey / Mapping, Microscopic Studies, Overburden Stripping, Prospecting By Licence Holder, Rock Sampling
Kiska Metals Co.	2015	20000014242	\$ 52,924.00	Assaying and Analyses, Geochemical, Prospecting By Licence Holder
Laurion Mineral Exploration Inc	2014	20000008134	\$ 36,218.00	Assaying and Analyses, Prospecting By Licence Holder
Laurion Mineral Exploration Inc	2014	20000008134	\$ 36,218.00	Assaying and Analyses, Prospecting By Licence Holder
Laurion Mineral Exploration Inc	2009	20000003973	\$ 272,297.00	Assaying and Analyses, Diamond Drilling
Geoinformatics Expl Can Ltd, Laurion Mineral Expl Inc	2008	20000003994	\$ 72,833.00	Airborne Electromagnetic, Airborne Magnetometer
Falconbridge Ltd	2005	20000001787	\$ 30,764.00	Assaying and Analyses, Diamond Drilling
Falconbridge Ltd	2005	20000000908	\$ 7,600.00	Electromagnetic, Line cutting, Magnetic / Magnetometer Survey
Mustang Minerals Corp	2004	20000000463	\$ 50,406.00	Airborne Electromagnetic, Airborne Magnetometer
David V Mullen	1997	41P15NW2003	\$ 9,511.00	Electromagnetic Very Low Frequency, Geochemical
D R Pyke	1997	41P15NW0011	\$ 19,920.00	Assaying and Analyses, Geological Survey / Mapping, Microscopic Studies, Open Cutting, Other
D R Pyke	1997	41P15NW2006	\$ 7,352.00	Induced Polarization, Magnetic / Magnetometer Survey
United Asbestos Inc	1981	41P14SE8412	-	Geological Survey / Mapping
Scintrex Ltd	1981	41P14SE0001	-	Airborne Electromagnetic, Airborne Magnetometer

United Asbestos Inc	1981	41P14SE0002	-	Geological Survey / Mapping
Intl Trust Co	1976	41P14NE0112	-	Diamond Drilling
Intl Trust Co	1975	41P14NE0024	-	Compilation and Interpretation - Diamond Drilling, Magnetic / Magnetometer Survey
Intl Trust Co	1975	41P14NE0024	-	Compilation and Interpretation - Diamond Drilling, Magnetic / Magnetometer Survey
Northim Mines Inc	1975	41P14SE0013	-	Diamond Drilling
Northim Mines Inc	1975	41P14SE0003	-	Diamond Drilling
Northim Mines Inc	1975	41P14NE0115	-	Miscellaneous Compilation and Interpretation, Other
Hanna Mining Co Ltd	1974	41P14NE0027	-	Electromagnetic, Geological Survey / Mapping, Magnetic / Magnetometer Survey
Northim Mines Inc	1974	41P14SE0010	-	Compilation and Interpretation - Geology, Electromagnetic, Magnetic / Magnetometer Survey
Northim Mines Inc	1974	41P14SE0004	-	Electromagnetic, Geological Survey / Mapping
Hanna Mining Co Ltd	1973	41P14NE0026	-	Electromagnetic, Geological Survey / Mapping, Magnetic / Magnetometer Survey
Allied Mining Corp Ltd	1972	41P14SE0014	-	Diamond Drilling
Allied Mining Corp Ltd	1972	41P14SE0017	-	Diamond Drilling
J Hogan	1971	41P14SE0012	-	Diamond Drilling
J Hogan	1971	41P14SE0015	-	Diamond Drilling
Cdn Johns-Manville Co Ltd	1970	41P14SE0016	-	Diamond Drilling
Cdn Johns-Manville Co Ltd	1969	41P14NE0113	-	Airborne Magnetometer
Timiskaming Nickel Ltd	1968	41P14SE0018	-	Diamond Drilling
Timiskaming Nickel Ltd	1968	41P14NE0035	-	Airborne Electromagnetic, Airborne Magnetometer
Dominion Gulf Co	1956	41P14NE0038	-	Geological Survey / Mapping, Magnetic / Magnetometer Survey, Overburden Stripping, Prospecting By Licence Holder

4.0 GEOLOGY

The following descriptions of both regional and property geology are based on the key papers of (Ayer et al., 2002, 2005; BRIGHT EG, 1970; Houlé & Lesher, 2019; Monecke et al., 2017, 2019; Thurston et al.,

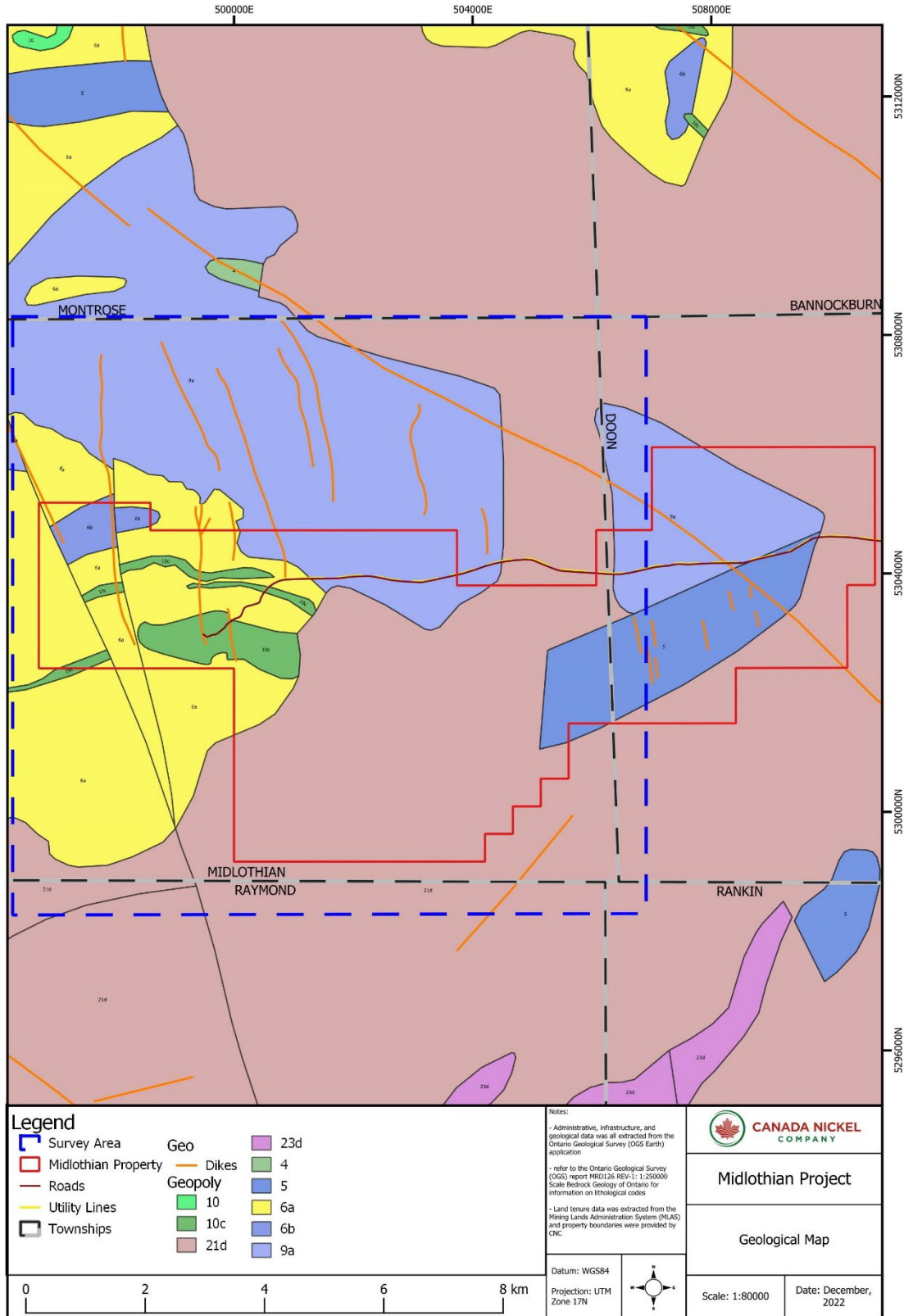


Figure 3: Midlothian Project bedrock geology map from: OGS report MRD 126 REV-1 1:250,000 Scale Bedrock Geology of Ontario.

2008). Deposit geology is based on the synthesis of historical exploration data by CNC staff geologists (see CNC press release dated November 22, 2021), key papers by (Ausenco Engineering Canada Inc., 2021; Sciortino et al., 2015) which includes the Preliminary Economic Assessment completed on the Crawford Project a possible analogue for the Midlothian Project.

4.1 REGIONAL GEOLOGY

The Midlothian Project is situated on the southern Abitibi Greenstone Belt ('AGB'), a Precambrian aged volcano-sedimentary belt cored by intervening domes of synvolcanic to syntectonic felsic plutonic rocks. Mafic to ultramafic sills and flows intrude volcanic stratigraphy, particularly around the flanks of regional volcanic domes. Younger Archean ultrabasic lamprophyre and minor carbonatite dikes variably cut stratigraphy. Regional east-west trending strike-slip faults such as the Porcupine-Destor and Cadillac-Larder deformation zones cross the AGB. These deformation zones are interpreted as Archean rifts, filled with clastic sediments, and later reactivated as strike-slip faults by compressional shortening that has tilted regional stratigraphy to near vertical dips. Multiple diabase dike swarms generally trending north-south occupy regional faults/structures in the AGB.

4.2 PROPERTY GEOLOGY

The property flanks the 'Holiday Dome' a major volcanic domal structure that is generally comprised of tuffs, breccias, volcanoclastics, and massive flows. A large east-west trending ultramafic sill consisting primarily of serpentized cumulate dunite/peridotite occurs in the center of the study area. The southeast portion of the study area is covered by Proterozoic Huronian Supergroup metasediments consisting primarily of wackes capped by conglomerates.

4.3 DEPOSIT GEOLOGY

Based on historic diamond drill logs, the interpreted overall structure of the main ultramafic unit from bottom-up is, a relatively sharp basal contact with a thick cumulate, variably serpentized dunitic core grading into a layered peridotite-pyroxenite-gabbro sequence with possible waning rhythmic layering to the top. These magmatic intrusions may contain disseminated primary blebs of predominantly pentlandite and nickeliferous pyrrhotite. Secondary greenschist alteration then liberates the Ni from the silicate olivine structure through the serpentization process, effectively adding to, and upgrading existing sulphides to the more nickeliferous heazlewoodite. Magnetite is produced as a byproduct of the serpentization process causing the deposits to have strong magnetic signatures. Additionally, during the serpentization process, the density of the dunite decreases from $\sim 3.2 \text{ g/cm}^3$ to $\sim 2.5\text{-}2.6 \text{ g/cm}^3$ producing a gravity low due to the contrast with surrounding volcanic sequences. The combined geophysical signatures of strong magnetic responses with overlapping low gravity anomalies are what is being targeted with this survey.

5.0 DATA QUALITY CONTROL RESULTS

Data quality control (QC) was provided by the contractor Xcalibur and reviewed by CNC. The QC results are summarised below.

5.1 DATA RECORDING

The following parameters were recorded during the survey:

- FALCON® AGG data: recorded at different intervals.
- Airborne total magnetic field: recorded with a 0.1 s sampling rate.
- Terrain clearance: provided by the radar altimeter at intervals of 0.1 s.
- Airborne GPS positional data (latitude, longitude, height, time and raw range from each satellite being tracked): recorded at intervals of 1 s.
- Time markers: in digital data.
- Ground total magnetic field: recorded with a 1 s sampling rate.
- Ground based GPS positional data (latitude, longitude, height, time and raw range from each satellite being tracked): recorded at intervals of 1 s.
- Ground surface below aircraft: mapped by the laser scanner system (when within range of the instrument and in the absence of thick vegetation), scanning at 36 times per second, recording 276 returns per scan.

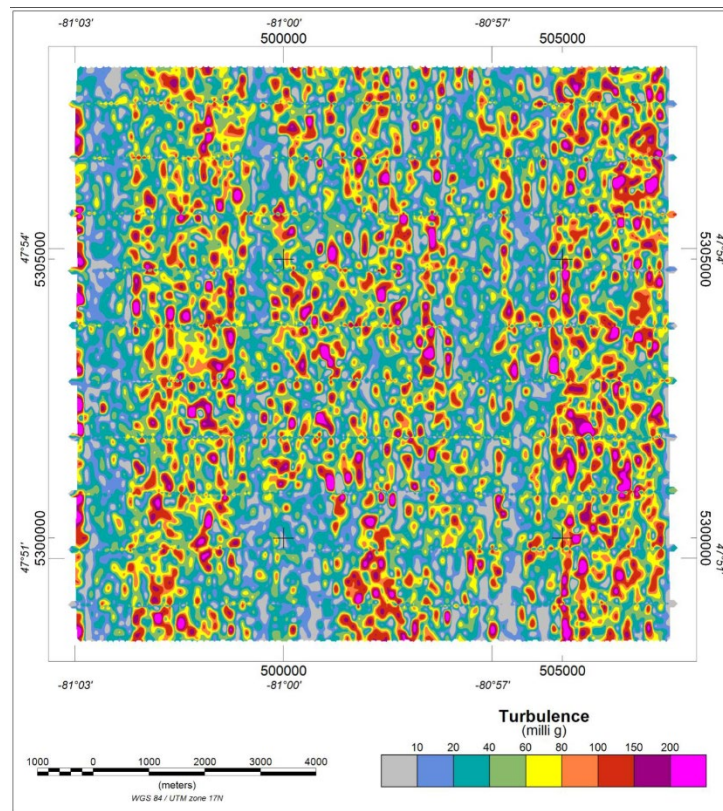


Figure 4: Survey Turbulence (milli g where $g = 9.80665 \text{ m/sec}^2$).

5.2 DATA ACQUISITION

During the course of the survey, there were no data quality issues with:

- AGG instrumentation
- Magnetic and GPS base stations
- Airborne magnetometer system
- Data acquisition systems
- Radar altimeter
- Laser scanner

5.3 TURBULENCE

The mean turbulence recorded was 53.2 milli g (where $g = 9.80665\text{m/sec/sec}$). Turbulence was variable (see Figure 4) but generally followed air temperature throughout the day.

5.4 AGG SYSTEM NOISE

The system noise for the AGG is the standard deviation of half the difference between the A & B components for each of the NE and UV components. The results of this survey were very good with values of 3.53 E and 3.31 E for NE and UV respectively (see Figures 5 & 6).

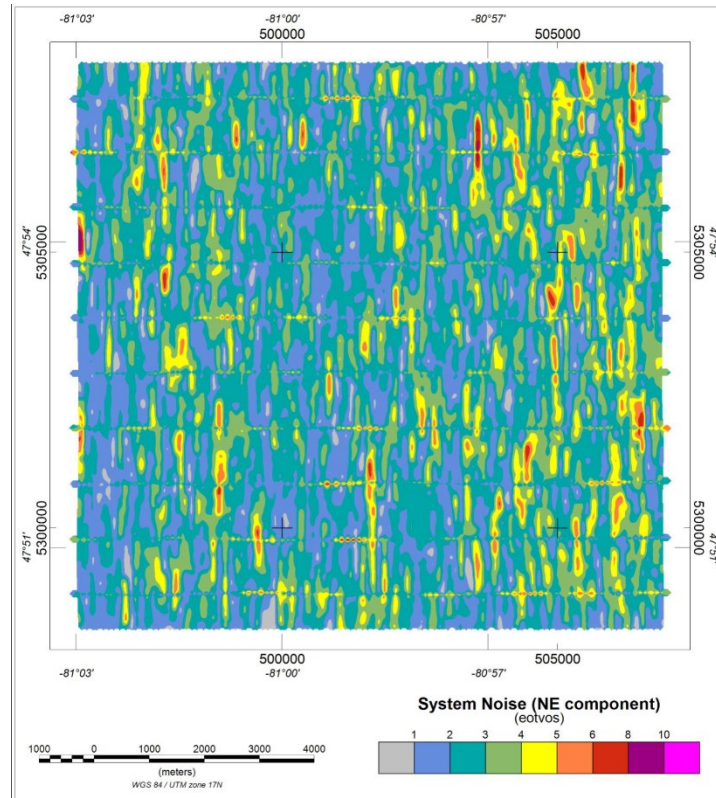


Figure 5: System Noise NE Component (eotvos).

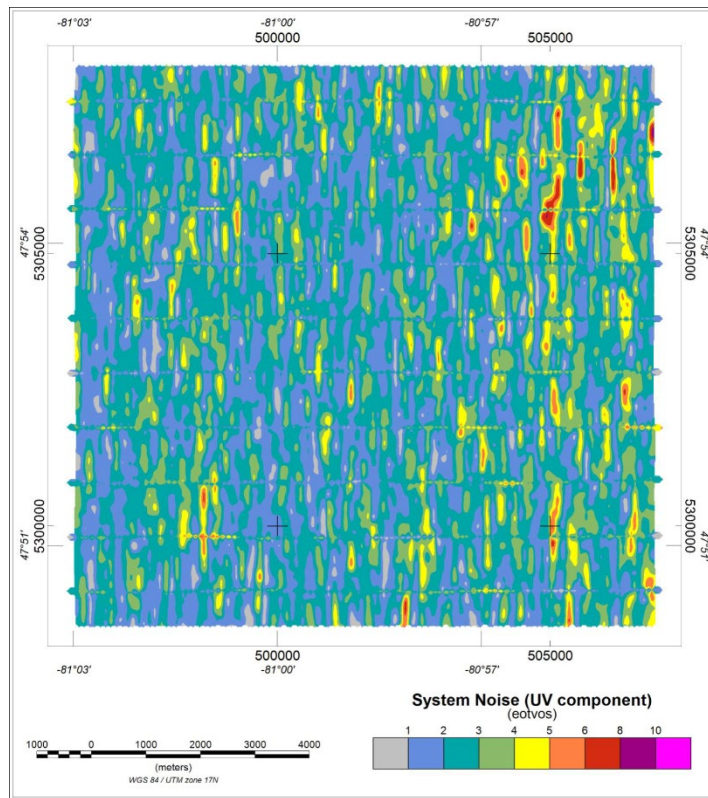


Figure 6: System Noise UV component (eotvos).

5.5 DIGITAL TERRAIN MODEL

Laser scanner range data were combined with GPS position and height data (adjusted from height above the WGS84 ellipsoid to height above the geoid by applying the Earth Gravitational Model 1996 (EGM96)).

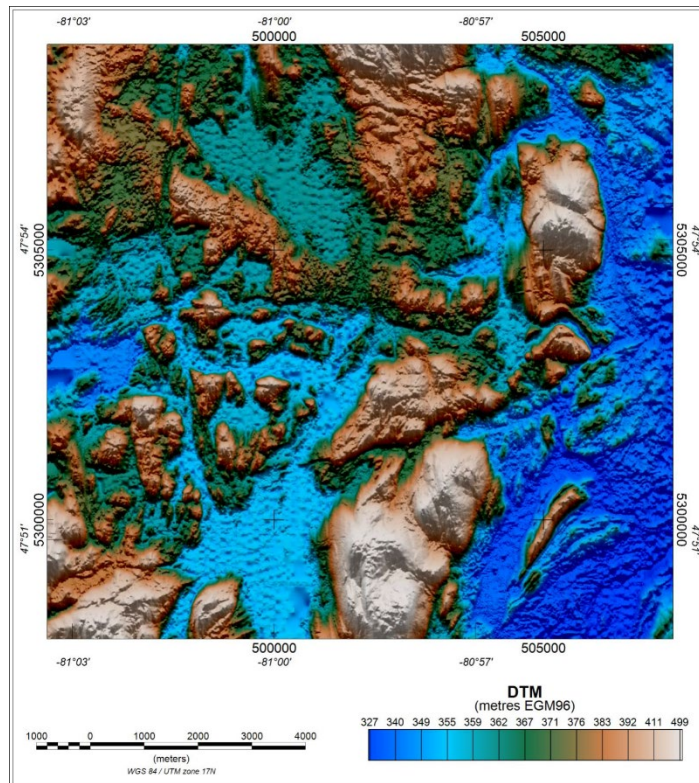


Figure 7: Final Digital Terrain Model (metres, referenced to the EGM96 geoid).

Terrain correction of AGG data requires knowledge of the terrain at distances up to at least 40 km from the data location, laser scanner data collected only along the survey line path must be supplemented by data from another source. Shuttle Radar Topography Mission (SRTM) v3 (one arc second resolution) data are used to supplement the laser scanner data.

Laser scanner data quality was good with scan density generally above 90%. Laser scanner data were gridded at 10 m with a 1 cell maximum extension beyond data limits. To fill gaps between lines and extend data coverage beyond the survey area, SRTM grid data were excised to an area 65 km beyond the planned survey area. The excised data were adjusted to the level of the laser scanner data using a Fourier domain wrapping method. The two grids were then combined into a single grid such that unmodified laser scanner data were used where defined and adjusted SRTM data were used to fill the gaps and extend the area.

5.6 DRAPE SURFACE DEVIATION

Flying height for the Midlothian survey was determined by a pre-computed “drape surface”; designed to create a smooth flight surface, maximising both acquisition quality and safety. The average deviation of actual flying height from this surface was 0.9 m across the survey area. The deviation is shown in Figure 8 below.

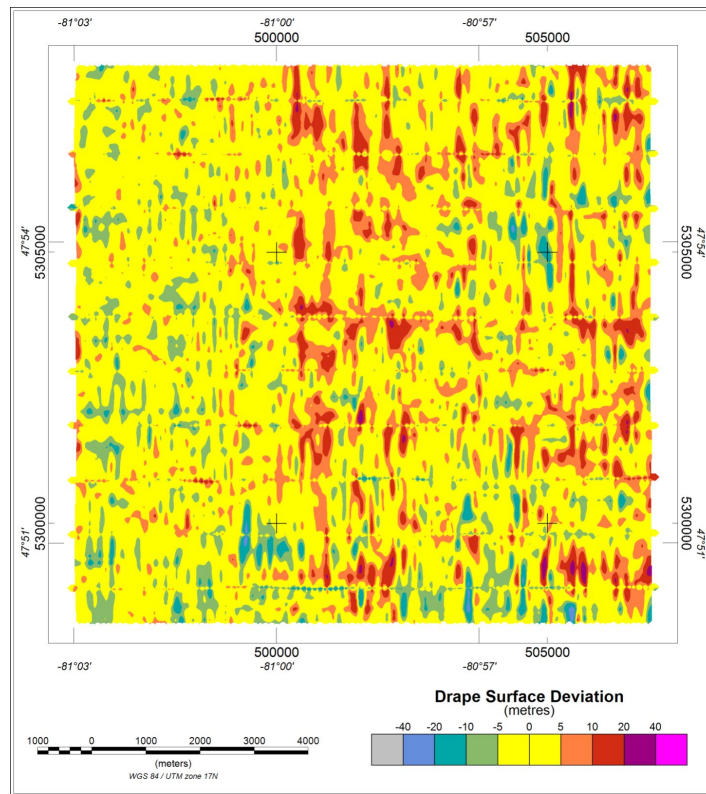


Figure 8: Deviation from drape surface (metres).

6.0 FALCON® AIRBORNE GRAVITY GRADIENT (AGG) RESULTS

6.1 PROCESSING SUMMARY

A summary of the processing steps for FALCON® AGG data as provided by the Contractor is shown in Figure 9.

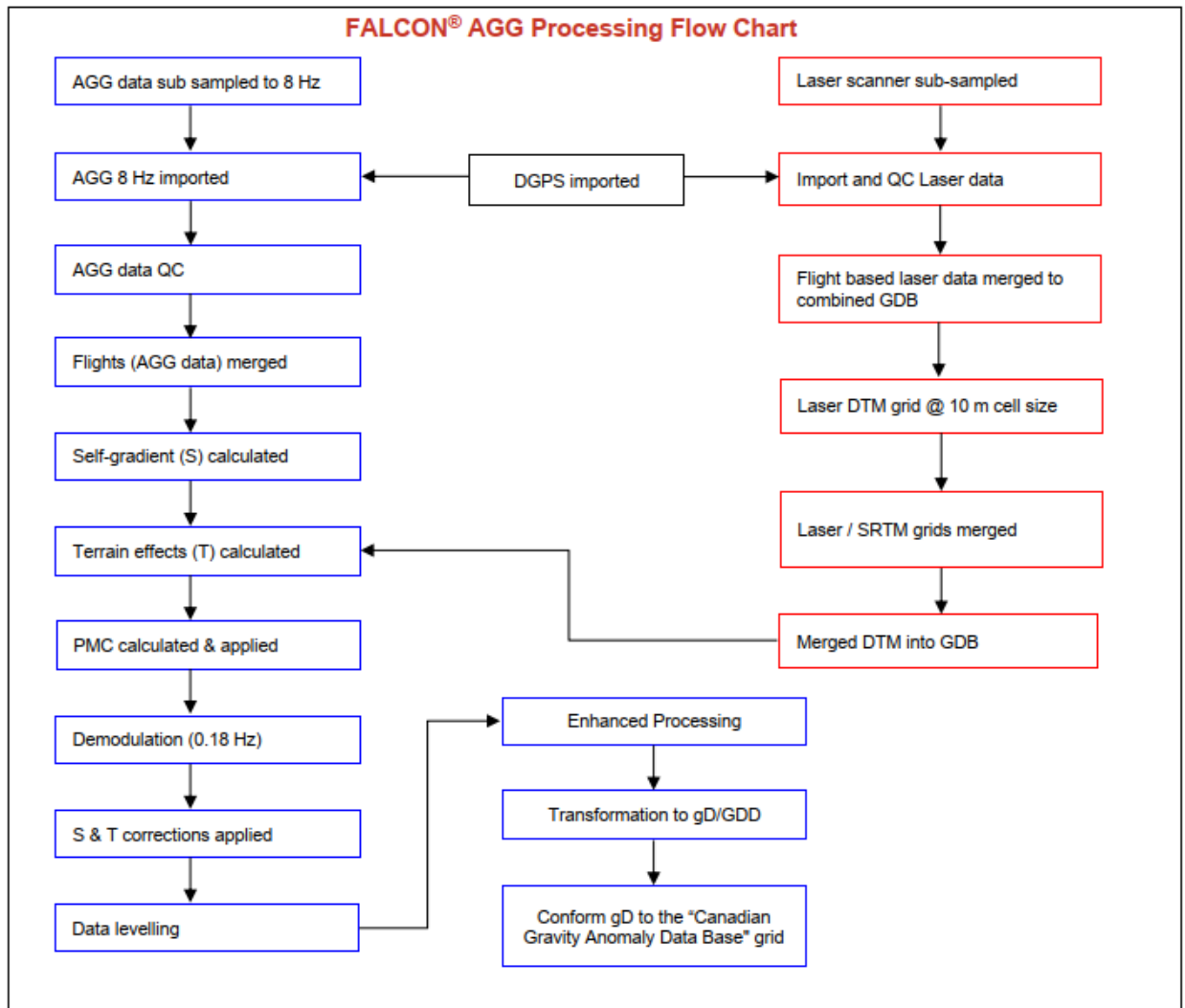


Figure 9: FALCON® AGG processing flowchart.

6.2 GRAVITY GRADIENT DATA

The transformation into G_{DD} and g_D was accomplished using a Fourier domain transformation method. The Fourier domain transformation method firstly calculates many flat surfaces at constant intervals between the lowest and highest-flying altitude. The transformation is performed on each of these surfaces and the result is a three-dimensional array for each tensor component where each level corresponds to a flat layer of a constant flying height. Using an approximation, the data is interpolated from this array back onto the processing drape surface. The transformation uses a smoothed surface onto which the output data are projected. This surface is a smoother equivalent of the actual flying surface. The Fourier (density 2.6 g/cm^3) G_{DD} map is shown in Figure 10. The Fourier vertical gravity (g_D), derived by integrating G_{DD} , (density 2.6 g/cm^3) result is presented in Figure 11.

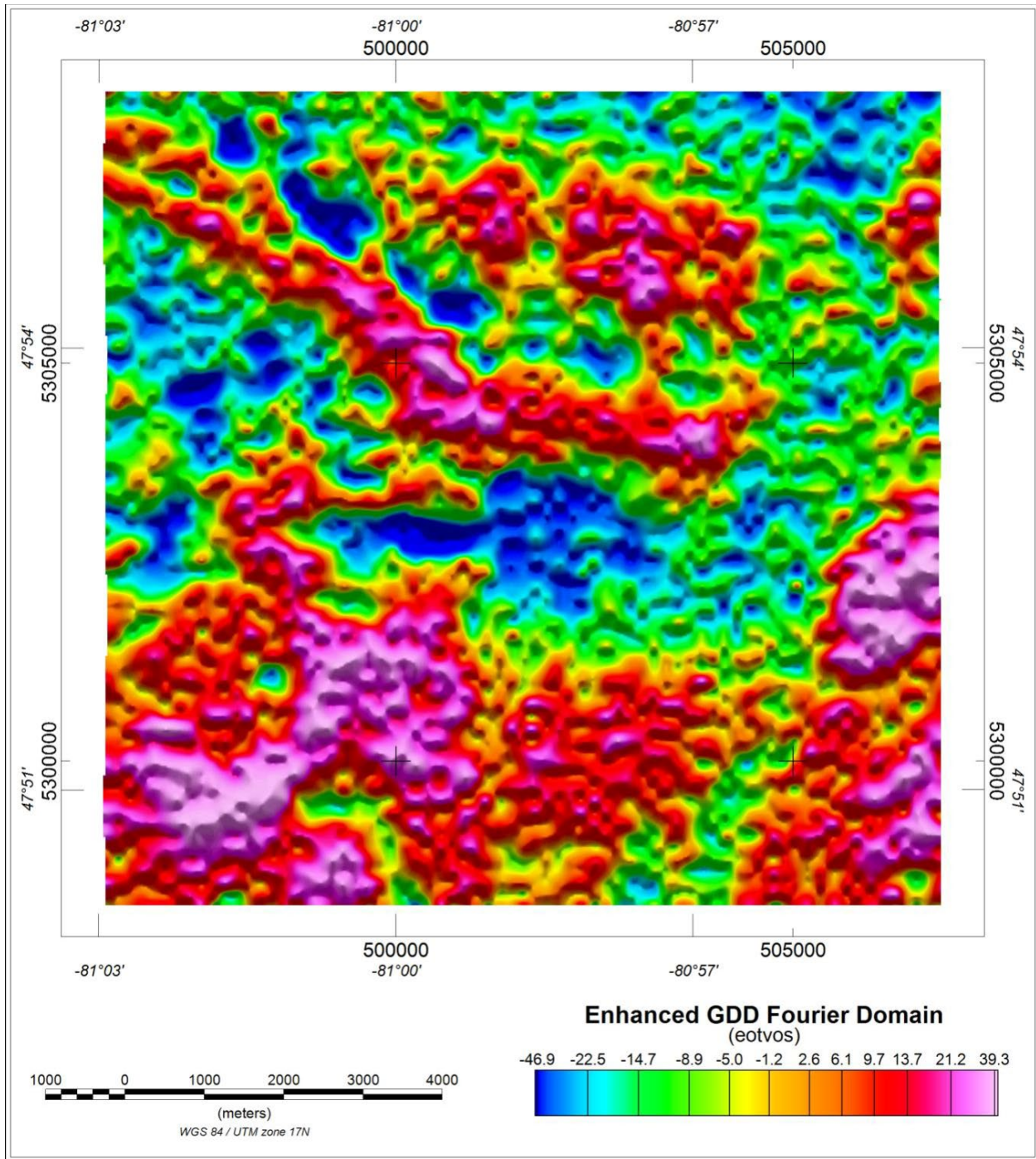


Figure 10: Enhanced Vertical Gravity Gradient (GDD) from Fourier processing (eotvos).

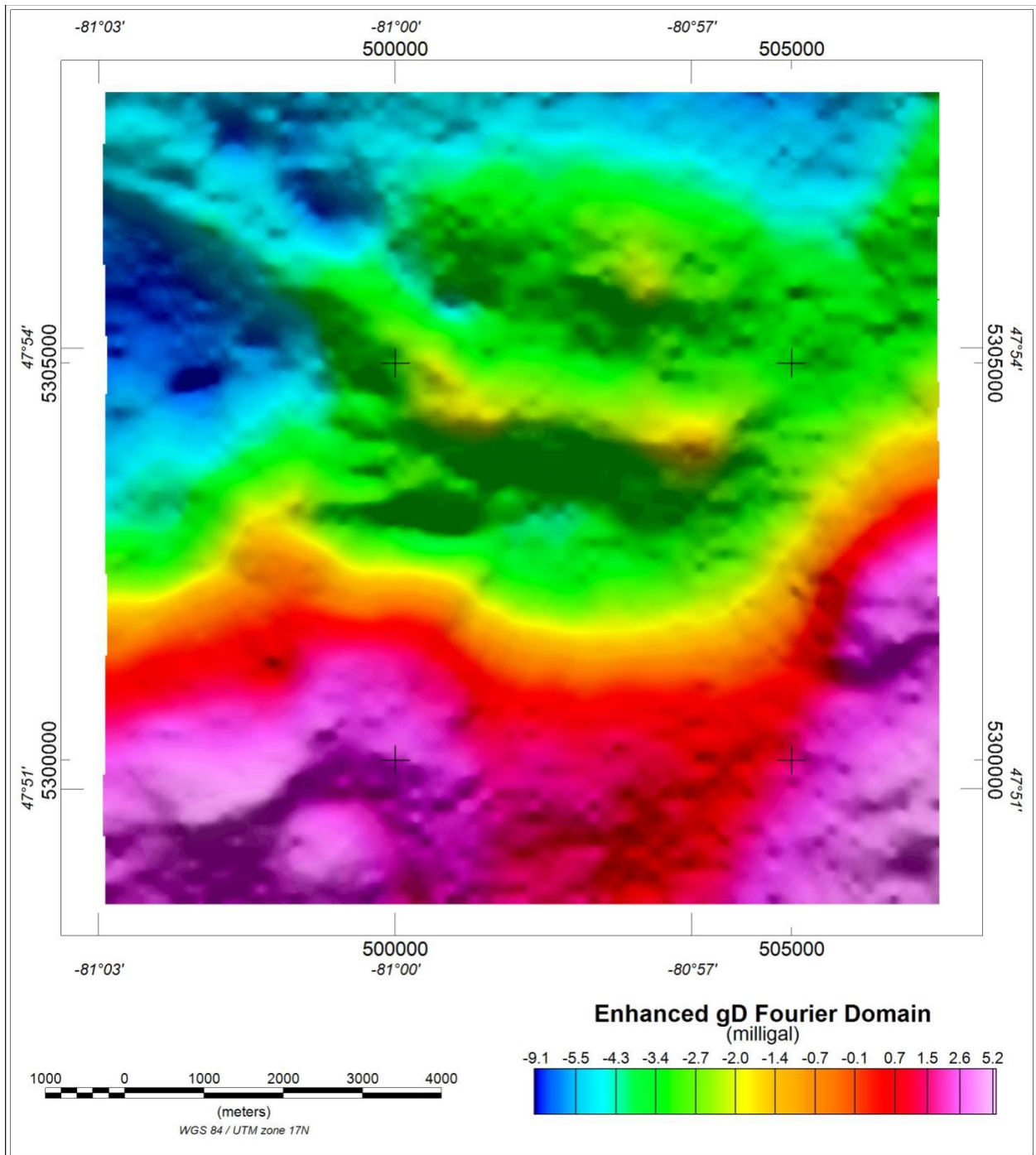


Figure 11: Enhanced Vertical Gravity (gD) from Fourier processing (milligal).

6.3 CONFORMED TO REGIONAL GRAVITY

The long wavelength information in g_D and G_{DD} can be improved by incorporating ancillary information such as the Canadian Gravity Anomaly Database. The Fourier g_D and G_{DD} grids were conformed to grids derived from a subset of the Canadian Gravity Anomaly Data Base.

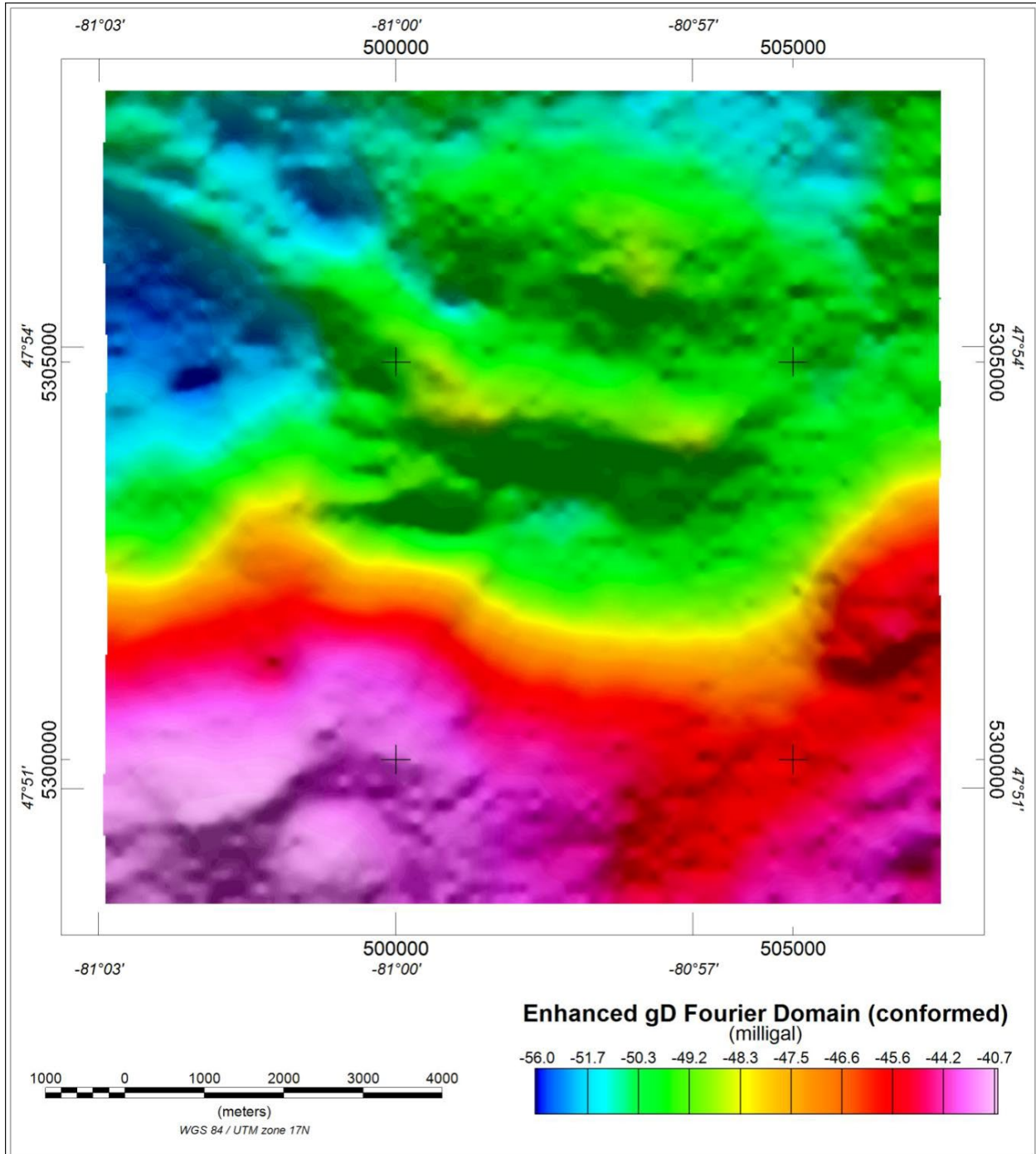


Figure 12: Enhanced Vertical Gravity (g_D) from Fourier processing conformed to regional gravity data (milligal).

7.0 AEROMAGNETIC RESULTS

7.1 PROCESSING SUMMARY

A summary flow chart of the processing steps for the aeromagnetic data is presented in Figure 13.

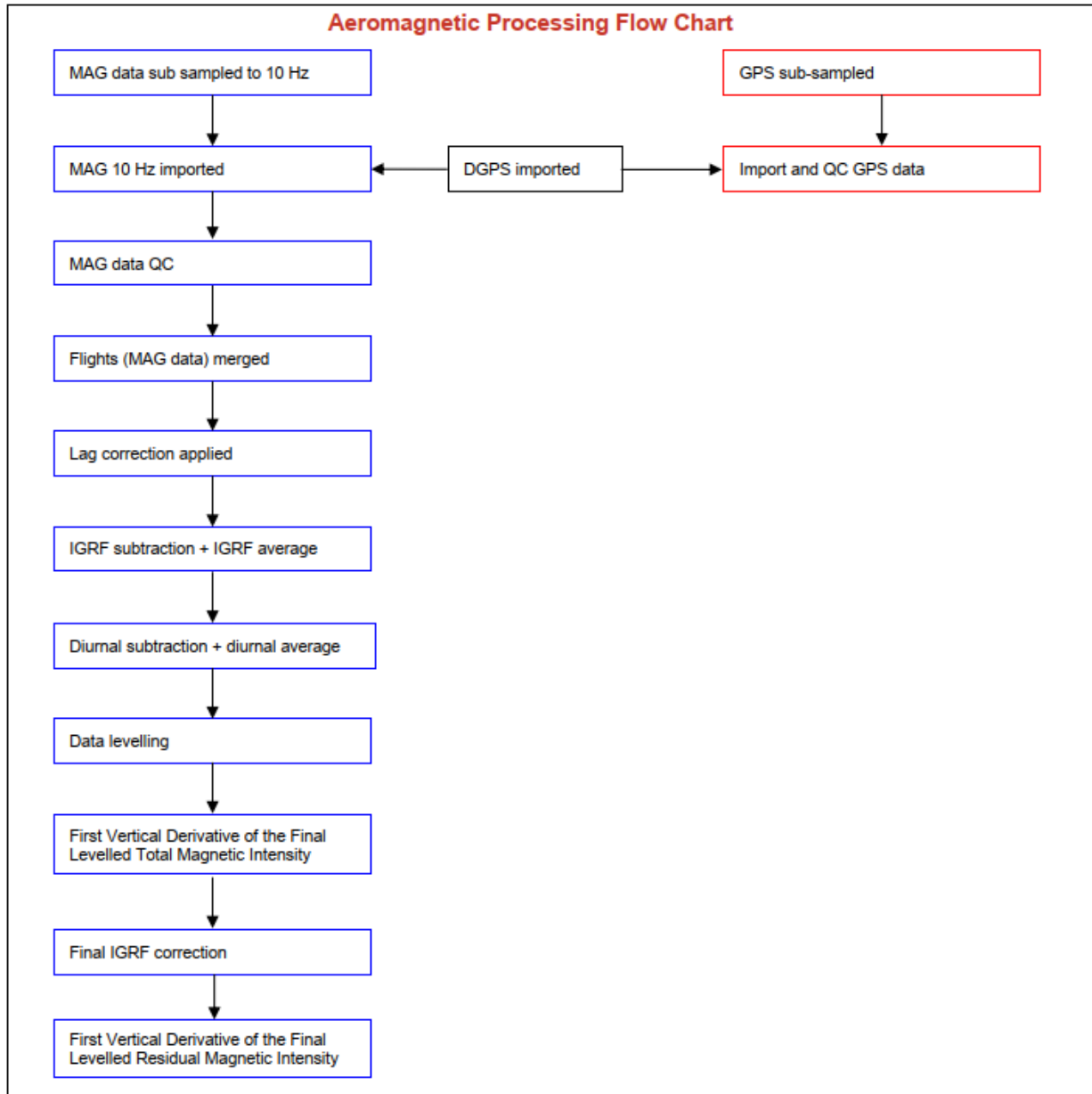


Figure 13: Aeromagnetic data processing flow chart.

7.2 MAGNETIC DATA

Figures 14 and 15 demonstrate the results of the Total Magnetic Intensity (TMI) measured in nanoteslas (nT) and the First Vertical Derivative of the TMI (nT/m), respectively.

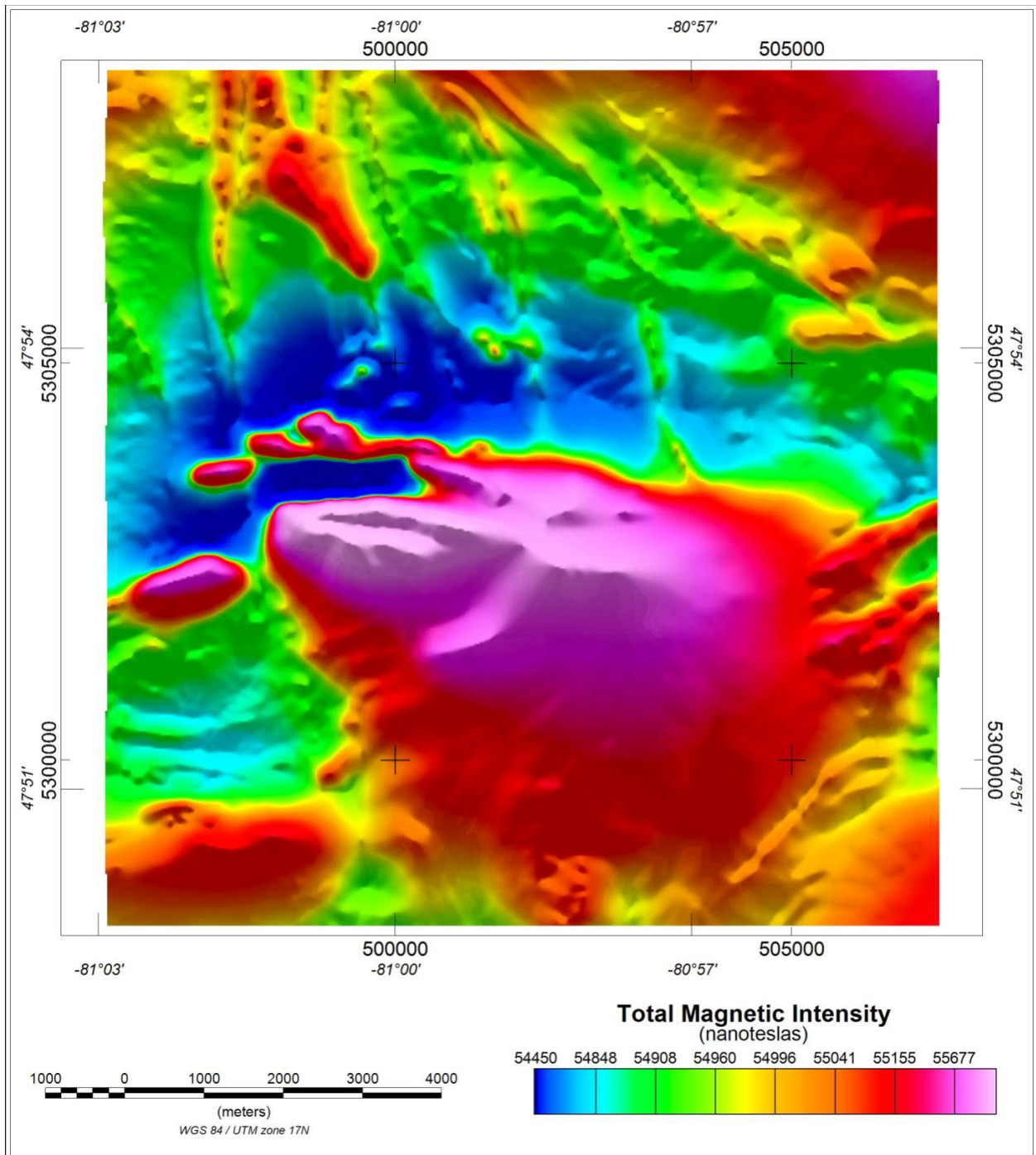


Figure 14: Total Magnetic Intensity (TMI).

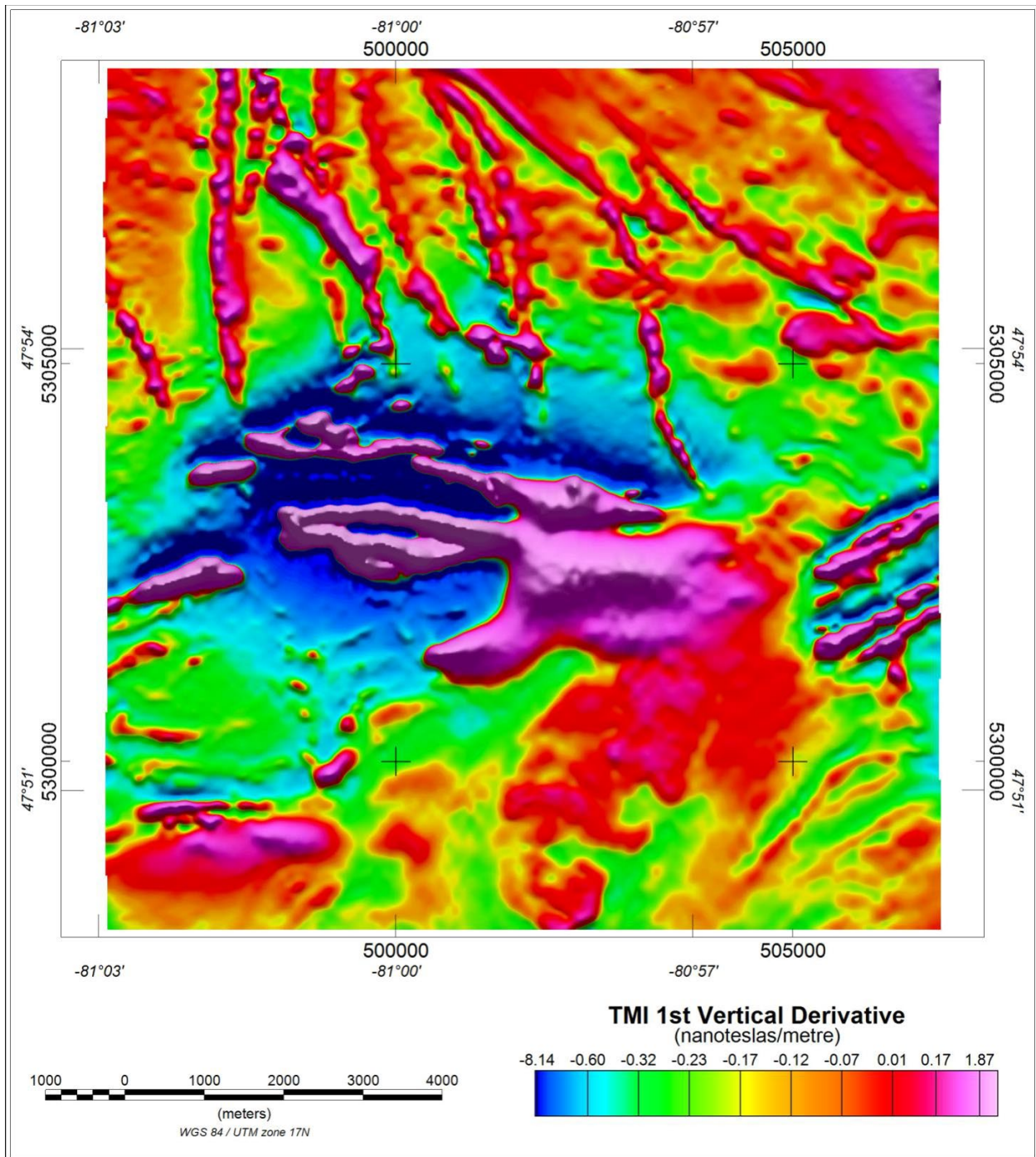


Figure 15: First Vertical Derivative of the Total Magnetic Intensity (nT/m).

8.0 INTERPRETATION AND CONCLUSIONS

The goal of this survey was to identify bulk-tonnage (Type II) disseminated magmatic nickel sulphide deposits. Geophysical signatures associated with the alteration and further endowment of these potentially substantial deposits produce overlapping low gravity anomalies with strong magnetic signatures.

The synthesis of overlapping geophysical signatures combined with the compilation and interpretation of both surface prospecting and diamond drill hole surveys; has proven the Midlothian Project is a potentially valuable brownfields site that could host a bulk tonnage magmatic nickel sulphide deposit.

Future work should include but not be limited to:

1. A 10-hole, 4,000 m diamond drill program consisting of widely spaced (~200 m apart) drill holes perpendicular to strike with the target of crossing stratigraphy and testing resource definition to a true depth of ~350m.
2. Airborne EM geophysical survey to locate potential primary sulphide accumulation or strongly disseminated bands within the mineralized envelope.
3. Surface prospecting and ground truthing to further refine the lithological and structural characteristics of the property geology.

9.0 REFERENCES

- Ausenco Engineering Canada Inc. (2021). *Crawford Nickel Sulphide Project NI 43-101 Technical Report & Preliminary Economic Assessment*.
- Ayer, J., Amelin, Y., Corfu, F., Kamo, S., Ketchum, J., Kwok, K., & Trowell, N. (2002). Evolution of the southern Abitibi greenstone belt based on U-Pb geochronology: Autochthonous volcanic construction followed by plutonism, regional deformation and sedimentation. *Precambrian Research*, 115(1–4). [https://doi.org/10.1016/S0301-9268\(02\)00006-2](https://doi.org/10.1016/S0301-9268(02)00006-2)
- Ayer, J., Thurston, P. C., Bateman, R., Dubé, B., Gibson, H. L., Hamilton, M. A., Hathway, B., Hocker, S. M., Houlié, M., Hudak, G. J., Ispolatov, V., Lafrance, B., Leshner, C. M., MacDonald, P. J., Péroquin, A. S., Piercey, S. J., Reed, L. E., & Thompson, P. H. (2005). Overview of results from the Greenstone Architecture Project: Discover Abitibi Initiative. In *Ontario Geological Survey: Vol. OFR 6154*.
- BRIGHT EG. (1970). GEOLOGY OF HALLIDAY AND MIDLOTHIAN TOWNSHIPS, DISTRICTS OF SUDBURY AND TIMISKAMING. *Ont, Dept Mines, Geol Rep 79*.
- Houlié, M. G., & Leshner, C. M. (2019). Komatiite-Associated Ni-Cu-(PGE) Deposits, Abitibi Greenstone Belt, Superior Province, Canada. In *Magmatic Ni-Cu and PGE Deposits_{title>Geology, Geochemistry, and Genesis}*. <https://doi.org/10.5382/rev.17.03>
- Monecke, T., Mercier-Langevin, P., & Dubé, B. (2017). Archean Base and Precious Metal Deposits, Southern Abitibi Greenstone Belt, Canada. In *Archean Base and Precious Metal Deposits, Southern Abitibi Greenstone Belt, Canada*. <https://doi.org/10.5382/rev.19>
- Monecke, T., Mercier-Langevin, P., Dubé, B., & Frieman, B. M. (2019). Geology of the Abitibi Greenstone Belt. In *Archean Base and Precious Metal Deposits, Southern Abitibi Greenstone Belt, Canada*. <https://doi.org/10.5382/rev.19.01>
- Sciortino, M., Mungall, J. E., & Muinonen, J. (2015). Generation of High-Ni sulfide and alloy phases during serpentinization of dunite in the dumont sill, Quebec. *Economic Geology*, 110(3). <https://doi.org/10.2113/econgeo.110.3.733>
- Thurston, P. C., Ayer, J. A., Goutier, J., & Hamilton, M. A. (2008). Depositional gaps in abitibi greenstone belt stratigraphy: A key to exploration for syngenetic mineralization. *Economic Geology*, 103(6). <https://doi.org/10.2113/gsecongeo.103.6.1097>
- Xcalibur MPH (Canada) Ltd. (2022). *FALCON® Airborne Gravity Gradiometer and Magnetometer Survey The Eminem Project, Midlothian Block 2, Ontario Logistics and Processing Report*.

10.0 CERTIFICATE OF QUALIFICATIONS

STATEMENT OF QUALIFICATIONS

I, Stephen Balch, do hereby state the following to be true:

1. I am a professional geoscientist (P.Ge.) in good standing, registered with the Association of Geoscientists of Ontario (#2250),
2. I am a graduate of University of Western Ontario with a degree in Honors Geophysics (1985),
3. I am a practicing exploration geophysicist with more than 37 years experience,
4. I reside at 11500 Fifth Line, Rockwood, Ontario, N0B 2K0,
5. I own directly or indirectly approximately 640,000 shares of Canada Nickel which I hold for investment purposes,
6. I have no direct interest in the Midlothian Property,
7. I reviewed the data contained within this report based on my general experience and my involvement with planning the survey and reviewing the data, and I am responsible for its contents.

Dated at Rockwood, Ontario on the 21st day of December 2022.



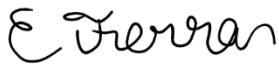
Stephen Balch, P.Ge.
Geophysicist
Balch Exploration Consulting Inc.

STATEMENT OF QUALIFICATIONS

I, Curtis Ferron, do hereby state the following to be true:

1. I am a professional geoscientist (P.Geo.) in good standing, registered with the Association of Geoscientists of Ontario (#3736),
2. I am a graduate of McMaster University with a BSc. degree in Honours Earth Sciences (2017),
3. I am a graduate of McMaster University with a MSc. Degree in Earth Sciences (2019),
4. I am currently employed as the Lead Geologist for Canada Nickel Company Inc.,
5. I have over 4 years of progressive experience in the mineral exploration industry,
6. I own directly or indirectly approximately 65,000 shares of Canada Nickel which I hold for investment purposes,
7. I have no direct interest in the Midlothian Property,
8. I reviewed the data contained within this report based on my general experience and my involvement with planning the survey and reviewing the data, and I am responsible for its contents.

Dated at Timmins, Ontario on the 21st day of December 2022.



Curtis Ferron, MSc., P.Ge.
Lead Geologist
Canada Nickel Company Inc.

APPENDIX I – SURVEY EQUIPMENT

The following survey equipment information is cited from the processing and logistics report provided by the Contractor Xcalibur Multiphysics (Xcalibur MPH (Canada) Ltd., 2022).

SURVEY AIRCRAFT

An Xcalibur Multiphysics Cessna C208B turbo prop, Canadian registration C-FXAG was used to fly the survey area.

FALCON AIRBORNE GRAVITY GRADIOMETER (AGG) SYSTEM (GALILEO)

The FALCON® AGG System is based on current state-of-the-art airborne gravity gradiometer technology and has been optimized for airborne broadband geophysical exploration. The system is capable of supporting surveying activities in areas ranging from 1,000 ft below sea level to 13,000 ft above sea level with aircraft speeds from 30 to 130 knots. The FALCON® AGG data streams were digitally recorded at different rates on removable drives installed in the FALCON® AGG electronics rack.

DIGITAL ACQUISITION SYSTEM (FASDAS)

The FASDAS is a data acquisition system executing propriety software for the acquisition and recording of location, magnetic and ancillary data. Data are presented both numerically and graphically in real time on the VGA display providing on-line quality control capability.

The FASDAS is also used for real time navigation. A pre-programmed flight plan, containing boundary coordinates, line start and end coordinates, altitude values calculated for a theoretical drape surface, line spacing and cross track definitions is loaded into the computer prior to each flight. The WGS84 latitude, longitude and altitude received from the real-time corrected, dual frequency Novatel positioning receiver, is transformed to the local coordinate system for cross track and distance to go values. This information, together with ground heading and speed, is displayed to the pilot numerically and graphically on a two-line LCD display. It is also presented on the operator LCD screen in conjunction with a pictorial representation of the survey area, survey lines and ongoing flight path.

FALCON® AGG DATA ACQUISITION SYSTEM (ADAS)

The ADAS provides control and data display for the FALCON® AGG system. Data are displayed in real time for the operator and warnings displayed should system parameters deviate from tolerance specifications. All FALCON® AGG and laser scanner data are recorded to a removable hard drive.

AERIAL AND GROUND MAGNETOMETERS

The airborne Caesium magnetometer was a Scintrex CS-3 having a noise envelope of 0.05 nT pk-pk, 0.1 Hz bandwidth. The ground magnetometer was a Scintrex CS-3 Caesium sensor sampling at 1 Hz.

REAL-TIME DIFFERENTIAL GPS

The Novatel OEMV-3G multi-frequency positioning receiver provides real-time differential GNSS for the on-board navigation system. The OEMV-3 is designed to track the GPS L1 and L2 signals, as well as GLONASS L1 and L2. The differential data set is relayed via a geo-synchronous satellite to the aircraft where the receiver optimized the corrections for the current location.

GPS BASE STATION RECEIVER

The Novatel OEMV-3 is a multi-channel, L1/L2 GNSS receiver. It provides raw range information of all satellites in view sampled every second and recorded on a computer laptop. These data are used to provide post-processed differential GNSS (DGNSS) corrections for the rover data flight path.

ALTIMETER

The King KRA405B Radar Altimeter has an accuracy of 3 ft or $\pm 3\%$ at 0-500 ft and $\pm 5\%$ at 500-2500 ft, a range of 0-2,500 ft and a measurement rate of 10 Hz.

LASER SCANNER

The Riegl LMS-Q240I-60 laser scanner is designed for high-speed line scanning applications. The system is based upon the principle of time-of-flight measurement of short laser pulses in the infrared wavelength region and the angular deflection of the laser beam is obtained by a rotating polygon mirror wheel. The measurement range is up to 650 m with a minimum range of 2 m and an accuracy of 20 mm. The laser beam is eye-safe, the laser wavelength is 0.9 μm , the scan angle range is $\pm 40^\circ$ and the scan speed is 36 scans/s.

DATA PROCESSING HARDWARE AND SOFTWARE

The following equipment and software were used:

Hardware

- One 2.0 GHz (or higher) laptop computer
- External USB hard drive reader for ADAS removable drives
- Two External USB hard drives for data backup
- All-In-One printer, copier, scanner

Software

- Oasis Montaj data processing and imaging software
- GrafNav Differential GPS processing software
- Xcalibur Multiphysics' Atlas data processing software
- Xcalibur Multiphysics' DiAGG processing software

APPENDIX II – MINING CLAIMS DATA

The following is a summary table of mining claims contained within the Midlothian Project boundary.

Table 4: List of mineral claims located on the Midlothian Project.

Tenure #	Title Type	Issue Date	Anniversary	Extension	Claim Due
680182	SCMC	2021-10-04	2023-10-04		2023-10-04
680183	SCMC	2021-10-04	2023-10-04		2023-10-04
680184	SCMC	2021-10-04	2023-10-04		2023-10-04
680185	SCMC	2021-10-04	2023-10-04		2023-10-04
680186	SCMC	2021-10-04	2023-10-04		2023-10-04
680187	SCMC	2021-10-04	2023-10-04		2023-10-04
680188	SCMC	2021-10-04	2023-10-04		2023-10-04
680189	SCMC	2021-10-04	2023-10-04		2023-10-04
680190	SCMC	2021-10-04	2023-10-04		2023-10-04
680191	SCMC	2021-10-04	2023-10-04		2023-10-04
339953	SCMC	2018-04-10	2022-12-24		2022-12-24
339954	SCMC	2018-04-10	2022-12-24		2022-12-24
101320	SCMC	2018-04-10	2022-12-24		2022-12-24
104002	SCMC	2018-04-10	2023-07-09		2023-07-09
104003	BCMC	2018-04-10	2023-07-09		2023-07-09
101319	SCMC	2018-04-10	2022-12-24		2022-12-24
108106	BCMC	2018-04-10	2023-12-24		2023-12-24
108957	SCMC	2018-04-10	2022-07-09	2023-07-09	2023-07-09
108975	SCMC	2018-04-10	2022-07-09	2023-07-09	2023-07-09
108976	SCMC	2018-04-10	2022-07-09	2023-07-09	2023-07-09
112502	SCMC	2018-04-10	2022-12-24		2022-12-24
113075	SCMC	2018-04-10	2022-07-09	2023-07-09	2023-07-09
112937	BCMC	2018-04-10	2022-12-24		2022-12-24
112836	BCMC	2018-04-10	2022-12-24		2022-12-24
111833	SCMC	2018-04-10	2022-12-24		2022-12-24
111834	BCMC	2018-04-10	2022-12-24		2022-12-24
116653	BCMC	2018-04-10	2022-12-24		2022-12-24
120634	SCMC	2018-04-10	2023-07-09		2023-07-09
120423	SCMC	2018-04-10	2022-12-24		2022-12-24
120424	BCMC	2018-04-10	2022-12-24		2022-12-24
121470	BCMC	2018-04-10	2022-12-24		2022-12-24
126048	SCMC	2018-04-10	2023-12-24		2023-12-24
131568	SCMC	2018-04-10	2022-07-09	2023-07-09	2023-07-09
131738	BCMC	2018-04-10	2022-12-24		2022-12-24
131600	SCMC	2018-04-10	2022-07-09	2023-07-09	2023-07-09
131632	SCMC	2018-04-10	2023-07-09		2023-07-09
131633	SCMC	2018-04-10	2022-07-09	2023-07-09	2023-07-09
133863	SCMC	2018-04-10	2022-07-09	2023-07-09	2023-07-09

680162	SCMC	2021-10-04	2023-10-04		2023-10-04
680163	SCMC	2021-10-04	2023-10-04		2023-10-04
680164	SCMC	2021-10-04	2023-10-04		2023-10-04
680165	SCMC	2021-10-04	2023-10-04		2023-10-04
680166	SCMC	2021-10-04	2023-10-04		2023-10-04
680167	SCMC	2021-10-04	2023-10-04		2023-10-04
680168	SCMC	2021-10-04	2023-10-04		2023-10-04
680169	SCMC	2021-10-04	2023-10-04		2023-10-04
680170	SCMC	2021-10-04	2023-10-04		2023-10-04
680171	SCMC	2021-10-04	2023-10-04		2023-10-04
680172	SCMC	2021-10-04	2023-10-04		2023-10-04
680173	SCMC	2021-10-04	2023-10-04		2023-10-04
680175	SCMC	2021-10-04	2023-10-04		2023-10-04
680174	SCMC	2021-10-04	2023-10-04		2023-10-04
680176	SCMC	2021-10-04	2023-10-04		2023-10-04
680177	SCMC	2021-10-04	2023-10-04		2023-10-04
680178	SCMC	2021-10-04	2023-10-04		2023-10-04
680179	SCMC	2021-10-04	2023-10-04		2023-10-04
680180	SCMC	2021-10-04	2023-10-04		2023-10-04
133869	SCMC	2018-04-10	2022-07-09	2023-07-09	2023-07-09
133511	SCMC	2018-04-10	2022-12-24		2022-12-24
133512	SCMC	2018-04-10	2022-12-24		2022-12-24
133513	SCMC	2018-04-10	2022-12-24		2022-12-24
135903	SCMC	2018-04-10	2022-07-09	2023-07-09	2023-07-09
135181	BCMC	2018-04-10	2022-12-24		2022-12-24
134930	SCMC	2018-04-10	2022-07-09	2023-07-09	2023-07-09
134931	SCMC	2018-04-10	2022-07-09	2023-07-09	2023-07-09
138454	BCMC	2018-04-10	2022-12-24		2022-12-24
136579	SCMC	2018-04-10	2022-12-24		2022-12-24
136580	SCMC	2018-04-10	2022-12-24		2022-12-24
141948	BCMC	2018-04-10	2022-07-09	2023-07-09	2023-07-09
142557	SCMC	2018-04-10	2022-12-24		2022-12-24
142567	BCMC	2018-04-10	2022-07-09	2023-07-09	2023-07-09
141865	SCMC	2018-04-10	2023-07-09		2023-07-09
143905	SCMC	2018-04-10	2022-12-24		2022-12-24
150291	BCMC	2018-04-10	2023-07-09		2023-07-09
148432	SCMC	2018-04-10	2022-12-24		2022-12-24
150476	SCMC	2018-04-10	2022-07-09	2023-07-09	2023-07-09
149184	BCMC	2018-04-10	2023-07-09		2023-07-09
151934	SCMC	2018-04-10	2022-12-24		2022-12-24
153949	BCMC	2018-04-10	2022-07-09	2023-07-09	2023-07-09
153950	SCMC	2018-04-10	2022-07-09	2023-07-09	2023-07-09
156634	SCMC	2018-04-10	2022-12-24		2022-12-24
156635	BCMC	2018-04-10	2022-12-24		2022-12-24

155374	SCMC	2018-04-10	2022-07-09	2023-07-09	2023-07-09
196436	SCMC	2018-04-10	2022-07-09	2023-07-09	2023-07-09
301632	SCMC	2018-04-10	2022-07-09	2023-07-09	2023-07-09
196437	SCMC	2018-04-10	2022-07-09	2023-07-09	2023-07-09
198410	SCMC	2018-04-10	2023-07-09	2020-02-09	2023-07-09
244494	SCMC	2018-04-10	2023-07-09	2020-02-09	2023-07-09
251064	SCMC	2018-04-10	2022-07-09	2023-07-09	2023-07-09
253080	SCMC	2018-04-10	2022-07-09	2023-07-09	2023-07-09
280081	SCMC	2018-04-10	2023-07-09	2020-02-09	2023-07-09
159095	BCMC	2018-04-10	2022-07-09	2023-07-09	2023-07-09
159096	SCMC	2018-04-10	2022-07-09	2023-07-09	2023-07-09
157974	SCMC	2018-04-10	2022-12-24		2022-12-24
165590	SCMC	2018-04-10	2022-12-24		2022-12-24
165591	BCMC	2018-04-10	2022-12-24		2022-12-24
165592	SCMC	2018-04-10	2022-12-24		2022-12-24
165718	BCMC	2018-04-10	2022-07-09	2023-07-09	2023-07-09
168610	SCMC	2018-04-10	2022-07-09	2023-07-09	2023-07-09
168645	SCMC	2018-04-10	2022-07-09	2023-07-09	2023-07-09
168646	SCMC	2018-04-10	2022-07-09	2023-07-09	2023-07-09
168597	SCMC	2018-04-10	2022-07-09	2023-07-09	2023-07-09
171307	BCMC	2018-04-10	2022-07-09	2023-07-09	2023-07-09
175691	SCMC	2018-04-10	2022-12-24		2022-12-24
178149	SCMC	2018-04-10	2022-12-24		2022-12-24
176916	SCMC	2018-04-10	2023-07-09		2023-07-09
177097	SCMC	2018-04-10	2022-12-24		2022-12-24
178434	SCMC	2018-04-10	2022-12-24		2022-12-24
179599	SCMC	2018-04-10	2022-07-09	2023-07-09	2023-07-09
178706	BCMC	2018-04-10	2022-12-24		2022-12-24
184517	SCMC	2018-04-10	2022-12-24		2022-12-24
184274	SCMC	2018-04-10	2023-07-09		2023-07-09
186435	SCMC	2018-04-10	2023-07-09		2023-07-09
185736	SCMC	2018-04-10	2022-07-09	2023-07-09	2023-07-09
187047	SCMC	2018-04-10	2022-07-09	2023-07-09	2023-07-09
185492	BCMC	2018-04-10	2022-12-24		2022-12-24
187840	SCMC	2018-04-10	2022-12-24		2022-12-24
187841	BCMC	2018-04-10	2022-12-24		2022-12-24
196402	SCMC	2018-04-10	2022-07-09	2023-07-09	2023-07-09
196559	SCMC	2018-04-10	2022-12-24		2022-12-24
196438	SCMC	2018-04-10	2022-07-09	2023-07-09	2023-07-09
196439	SCMC	2018-04-10	2023-07-09		2023-07-09
196440	SCMC	2018-04-10	2023-07-09		2023-07-09
196441	SCMC	2018-04-10	2022-07-09	2023-07-09	2023-07-09
194860	BCMC	2018-04-10	2022-12-24		2022-12-24
194861	SCMC	2018-04-10	2022-12-24		2022-12-24

194862	SCMC	2018-04-10	2022-12-24		2022-12-24
198575	BCMC	2018-04-10	2022-07-09	2023-07-09	2023-07-09
200667	SCMC	2018-04-10	2022-07-09	2023-07-09	2023-07-09
200668	BCMC	2018-04-10	2022-07-09	2023-07-09	2023-07-09
200004	SCMC	2018-04-10	2022-07-09	2023-07-09	2023-07-09
199748	SCMC	2018-04-10	2022-07-09	2023-07-09	2023-07-09
205753	BCMC	2018-04-10	2023-07-09		2023-07-09
208029	SCMC	2018-04-10	2022-07-09	2023-07-09	2023-07-09
206595	SCMC	2018-04-10	2022-07-09	2023-07-09	2023-07-09
206047	SCMC	2018-04-10	2022-07-09	2023-07-09	2023-07-09
206048	BCMC	2018-04-10	2022-07-09	2023-07-09	2023-07-09
208594	SCMC	2018-04-10	2022-07-09	2023-07-09	2023-07-09
208595	SCMC	2018-04-10	2022-07-09	2023-07-09	2023-07-09
209280	SCMC	2018-04-10	2022-12-24		2022-12-24
210630	SCMC	2018-04-10	2022-12-24		2022-12-24
210631	SCMC	2018-04-10	2022-12-24		2022-12-24
340441	SCMC	2018-04-10	2022-07-09	2023-07-09	2023-07-09
318504	SCMC	2018-04-10	2022-07-09	2023-07-09	2023-07-09
213499	SCMC	2018-04-10	2022-12-24		2022-12-24
213500	SCMC	2018-04-10	2022-12-24		2022-12-24
213596	SCMC	2018-04-10	2022-07-09	2023-07-09	2023-07-09
214472	BCMC	2018-04-10	2023-12-24		2023-12-24
213616	SCMC	2018-04-10	2022-07-09	2023-07-09	2023-07-09
219436	SCMC	2018-04-10	2023-12-24		2023-12-24
219437	BCMC	2018-04-10	2023-12-24		2023-12-24
220165	SCMC	2018-04-10	2023-07-09		2023-07-09
220100	SCMC	2018-04-10	2022-07-09	2023-07-09	2023-07-09
224489	SCMC	2018-04-10	2023-07-09		2023-07-09
225000	SCMC	2018-04-10	2022-12-24		2022-12-24
225001	SCMC	2018-04-10	2022-12-24		2022-12-24
225277	BCMC	2018-04-10	2022-12-24		2022-12-24
232302	SCMC	2018-04-10	2022-12-24		2022-12-24
233283	BCMC	2018-04-10	2022-12-24		2022-12-24
232475	SCMC	2018-04-10	2022-07-09	2023-07-09	2023-07-09
237884	BCMC	2018-04-10	2022-07-09	2023-07-09	2023-07-09
237765	SCMC	2018-04-10	2022-07-09	2023-07-09	2023-07-09
237766	SCMC	2018-04-10	2022-07-09	2023-07-09	2023-07-09
237875	SCMC	2018-04-10	2022-12-24		2022-12-24
237876	BCMC	2018-04-10	2022-12-24		2022-12-24
243755	BCMC	2018-04-10	2022-12-24		2022-12-24
243756	BCMC	2018-04-10	2022-12-24		2022-12-24
242988	SCMC	2018-04-10	2022-07-09	2023-07-09	2023-07-09
242989	SCMC	2018-04-10	2022-07-09	2023-07-09	2023-07-09
242990	SCMC	2018-04-10	2022-07-09	2023-07-09	2023-07-09

243138	SCMC	2018-04-10	2022-12-24		2022-12-24
244495	SCMC	2018-04-10	2023-07-09		2023-07-09
244496	SCMC	2018-04-10	2023-07-09		2023-07-09
246311	SCMC	2018-04-10	2022-07-09	2023-07-09	2023-07-09
245459	SCMC	2018-04-10	2022-12-24		2022-12-24
245460	BCMC	2018-04-10	2022-12-24		2022-12-24
245186	BCMC	2018-04-10	2023-07-09		2023-07-09
245809	SCMC	2018-04-10	2022-07-09	2023-07-09	2023-07-09
252795	BCMC	2018-04-10	2022-12-24		2022-12-24
253800	SCMC	2018-04-10	2022-07-09	2023-07-09	2023-07-09
255916	SCMC	2018-04-10	2022-12-24		2022-12-24
253783	SCMC	2018-04-10	2022-07-09	2023-07-09	2023-07-09
253784	SCMC	2018-04-10	2022-07-09	2023-07-09	2023-07-09
253785	BCMC	2018-04-10	2022-07-09	2023-07-09	2023-07-09
253927	BCMC	2018-04-10	2022-12-24		2022-12-24
255820	BCMC	2018-04-10	2022-07-09	2023-07-09	2023-07-09
254379	BCMC	2018-04-10	2022-07-09	2023-07-09	2023-07-09
254441	BCMC	2018-04-10	2023-12-24		2023-12-24
255167	SCMC	2018-04-10	2022-07-09	2023-07-09	2023-07-09
257261	BCMC	2018-04-10	2022-12-24		2022-12-24
257306	BCMC	2018-04-10	2022-12-24		2022-12-24
257309	SCMC	2018-04-10	2022-07-09	2023-07-09	2023-07-09
258634	SCMC	2018-04-10	2022-12-24		2022-12-24
260330	SCMC	2018-04-10	2022-07-09	2023-07-09	2023-07-09
260331	SCMC	2018-04-10	2022-07-09	2023-07-09	2023-07-09
261475	SCMC	2018-04-10	2022-12-24		2022-12-24
261476	SCMC	2018-04-10	2022-12-24		2022-12-24
264552	SCMC	2018-04-10	2022-07-09	2023-07-09	2023-07-09
265321	SCMC	2018-04-10	2022-07-09	2023-07-09	2023-07-09
265861	SCMC	2018-04-10	2022-07-09	2023-07-09	2023-07-09
269684	BCMC	2018-04-10	2022-07-09	2023-07-09	2023-07-09
268957	BCMC	2018-04-10	2022-12-24		2022-12-24
268958	SCMC	2018-04-10	2022-12-24		2022-12-24
272555	SCMC	2018-04-10	2022-07-09	2023-07-09	2023-07-09
272556	SCMC	2018-04-10	2022-07-09	2023-07-09	2023-07-09
272557	SCMC	2018-04-10	2023-07-09		2023-07-09
272567	SCMC	2018-04-10	2022-07-09	2023-07-09	2023-07-09
272568	BCMC	2018-04-10	2022-07-09	2023-07-09	2023-07-09
272601	SCMC	2018-04-10	2022-07-09	2023-07-09	2023-07-09
269908	SCMC	2018-04-10	2022-12-24		2022-12-24
269909	SCMC	2018-04-10	2022-12-24		2022-12-24
270526	BCMC	2018-04-10	2022-12-24		2022-12-24
274670	BCMC	2018-04-10	2022-07-09	2023-07-09	2023-07-09
276593	SCMC	2018-04-10	2022-12-24		2022-12-24

276594	SCMC	2018-04-10	2022-12-24		2022-12-24
275258	BCMC	2018-04-10	2022-07-09	2023-07-09	2023-07-09
280049	SCMC	2018-04-10	2022-07-09	2023-07-09	2023-07-09
280080	SCMC	2018-04-10	2022-07-09	2023-07-09	2023-07-09
280462	SCMC	2018-04-10	2022-07-09	2023-07-09	2023-07-09
280843	BCMC	2018-04-10	2022-12-24		2022-12-24
280844	BCMC	2018-04-10	2022-12-24		2022-12-24
280845	SCMC	2018-04-10	2022-12-24		2022-12-24
280846	BCMC	2018-04-10	2022-12-24		2022-12-24
281022	BCMC	2018-04-10	2022-12-24		2022-12-24
282758	SCMC	2018-04-10	2023-07-09		2023-07-09
289565	SCMC	2018-04-10	2022-07-09	2023-07-09	2023-07-09
299139	BCMC	2018-04-10	2022-07-09	2023-07-09	2023-07-09
299140	SCMC	2018-04-10	2023-07-09		2023-07-09
299591	SCMC	2018-04-10	2022-07-09	2023-07-09	2023-07-09
298123	SCMC	2018-04-10	2022-07-09	2023-07-09	2023-07-09
299620	SCMC	2018-04-10	2022-07-09	2023-07-09	2023-07-09
300453	SCMC	2018-04-10	2022-12-24		2022-12-24
298160	SCMC	2018-04-10	2022-07-09	2023-07-09	2023-07-09
302413	SCMC	2018-04-10	2022-07-09	2023-07-09	2023-07-09
303870	SCMC	2018-04-10	2022-07-09	2023-07-09	2023-07-09
303215	BCMC	2018-04-10	2022-12-24		2022-12-24
301631	SCMC	2018-04-10	2022-07-09	2023-07-09	2023-07-09
301633	SCMC	2018-04-10	2022-07-09	2023-07-09	2023-07-09
304575	SCMC	2018-04-10	2022-12-24		2022-12-24
302939	SCMC	2018-04-10	2022-07-09	2023-07-09	2023-07-09
311269	SCMC	2018-04-10	2022-07-09	2023-07-09	2023-07-09
311870	SCMC	2018-04-10	2022-12-24		2022-12-24
311871	BCMC	2018-04-10	2022-12-24		2022-12-24
313208	SCMC	2018-04-10	2022-12-24		2022-12-24
317147	SCMC	2018-04-10	2022-12-24		2022-12-24
317148	BCMC	2018-04-10	2022-12-24		2022-12-24
317603	SCMC	2018-04-10	2022-07-09	2023-07-09	2023-07-09
320357	SCMC	2018-04-10	2022-07-09	2023-07-09	2023-07-09
319814	SCMC	2018-04-10	2022-07-09	2023-07-09	2023-07-09
319815	SCMC	2018-04-10	2022-07-09	2023-07-09	2023-07-09
322628	BCMC	2018-04-10	2022-12-24		2022-12-24
321922	SCMC	2018-04-10	2023-07-09		2023-07-09
321923	BCMC	2018-04-10	2023-07-09		2023-07-09
321942	SCMC	2018-04-10	2022-07-09	2023-07-09	2023-07-09
321943	BCMC	2018-04-10	2022-07-09	2023-07-09	2023-07-09
321944	BCMC	2018-04-10	2022-07-09	2023-07-09	2023-07-09
321975	SCMC	2018-04-10	2022-07-09	2023-07-09	2023-07-09
324597	SCMC	2018-04-10	2022-12-24		2022-12-24

324598	SCMC	2018-04-10	2022-12-24		2022-12-24
324608	SCMC	2018-04-10	2022-07-09	2023-07-09	2023-07-09
328119	SCMC	2018-04-10	2022-12-24		2022-12-24
325938	SCMC	2018-04-10	2022-12-24		2022-12-24
325939	SCMC	2018-04-10	2022-12-24		2022-12-24
330481	SCMC	2018-04-10	2022-12-24		2022-12-24
340271	SCMC	2018-04-10	2022-12-24		2022-12-24
339755	BCMC	2018-04-10	2022-12-24		2022-12-24
333323	SCMC	2018-04-10	2022-07-09	2023-07-09	2023-07-09
333331	SCMC	2018-04-10	2022-07-09	2023-07-09	2023-07-09
334508	SCMC	2018-04-10	2022-07-09	2023-07-09	2023-07-09
334509	SCMC	2018-04-10	2022-07-09	2023-07-09	2023-07-09
331220	BCMC	2018-04-10	2022-07-09	2023-07-09	2023-07-09
680181	SCMC	2021-10-04	2023-10-04		2023-10-04

Category	Date	Invoice #	Subtotal (before taxes)	Description
Consultant	2022-10-05	221001	\$ 214,653.58	Xcalibur Airborne Gravity and Gradiometer Survey (Millothian Project only)
Consultant	2022-10-12	997043	\$ 132,598.49	Geotech Heli-borne VTEM and H. Magnetic Gradiometer Survey

VTEM 613 line kms Flown
 Airborne Gravity 1,166 line kms Flown
 Invoice is for 2,894 kms. Only 1,166 km claimed here for Midlothian Project

TOTAL COST	\$ 347,252.07
-------------------	----------------------

Flown Inside Property

VTEM	70% line kms inside property	\$	92,818.94
Airborne Gravity*	65% line kms inside property	\$	139,524.83

TOTAL TO USE FOR CREDIT	\$ 232,343.77
--------------------------------	----------------------

*Due to flying of gravity requiring to be at least 10 km long, even though our property is not that length, we request to be able to apply 65% of total cost

# of Claims flown	187
--------------------------	------------